SEXUAL DEVELOPMENT AND ASCOSPORE DISCHARGE IN FUSARIUM GRAMINEARUM: THE ROLE OF CALCIUM AND MYOSIN 2

By

Brad Lee Cavinder

A DISSERTATION

Submitted to
Michigan State University
in partial fulfillment of the requirements
for the degree of

DOCTOR OF PHILOSOPHY

Genetics

2011

ABSTRACT

By

Brad Lee Cavinder

The plant pathogen *Fusarium graminearum* is a cosmopolitan filamentous ascomycete fungus and the primary etiological species of Fusarium Head Blight (FHB) of wheat in North America, infecting the heads of the plants and contaminating the grain with mycotoxins. Direct infection of the heads is needed for development of FHB. An important source of inoculum for FHB is the aerial dispersal of forcibly discharged ascospores (sexual spores). Previous Trail lab results indicated that calcium signaling was involved in ascospores discharge, stimulating the examination of the role calcium channels and possible targets of calcium signaling play in the growth and development of *F. graminearum*.

In fungi, the high affinity calcium uptake system (HACS), consisting of the calcium channel Cch1 and the calcium channel/regulatory protein Mid1, and the low affinity calcium uptake system (LACS), for which only the transmembrane protein Fig1 is a known component, have been characterized. Previously, deletion of *CCH1* resulted in significantly reduced vegetative growth with a more fluffy appearance than wild-type, macroconidia (asexual spores) production, and ascospore discharge, and a few abnormally developed ascospores. Here, deletion of *MID1* resulted in phenotypes similar to the Δ*cch1* mutant but with a much higher rate of abnormal ascospore development. Results were similar but slightly more severe in a Δ*mid1* Δ*cch1* double mutant. Exogenous calcium partially rescued the phenotypes of all strains, suggesting an alternate route for calcium entry. As *FIG1* is involved in low affinity calcium uptake in other fungi, the role of Fig1 in the calcium uptake was explored. As with the HACS mutants, loss of Fig1 resulted in significantly slowed vegetative growth rate, but with mycelium

appressed to the surface of the medium rather than fluffy, and reduced conidiation. Following induction of sexual development, Δ*fig1* mutants did not produce perithecia, and a microscopic examination led to the finding that sexual development halted after the production of perithecium initials. The LACS and HACS double and triple mutants' phenotypes were similar but more severe than the Δ*fig1* mutants and included reduced pathogenicity on wheat. Addition of calcium did not lead to any detectable phenotypic rescue. As perithecia did not develop, the function of *FIG1* during ascus and ascospore development could not be determined.

To facilitate the examination of genes essential for sexual development, such as *FIG1*, a doxycycline inducible RNA interference (RNAi) system was adopted for use in *F. graminearum*. Vectors were constructed targeting a *PKS3*, a polyketide synthase gene needed to make a dark perithecium pigment, and *MYO2*, a myosin gene. Myosins are calcium regulated molecular motors that move along actin filaments, transporting membranous structures. Induction of RNAi during sexual development of strains with the *MYO2* construct resulted in severely slowed ascus growth and altered vesicle trafficking and ascospore delimitation. A transformant containing the *PKS3* construct was found to lack perithecium pigment without doxycycline induction, suggesting that either transcriptional read-through from upstream sequences or the influence of an enhancer drove expression of the RNAi construct.

These results indicate the importance of calcium uptake and signaling in the growth and development of *F. graminearum* and provide impetus for investigating the roles of other calcium signaling components. These results also show that doxycycline inducible RNAi can be effectively utilized in *F. graminearum* to investigate the function of genes involved in sexual development.

TABLE OF CONTENTS

LIST OF TABLES

LIST OF FIGURES

CHAPTER 1

LITERATURE REVIEW

Fusarium graminearum- a pathogenic fungus.

The filamentous ascomycete *Fusarium graminearum* is a cosmopolitan soil-associated haploid fungus living saprobically on plant debris, and is also a capable pathogen, infecting numerous plants worldwide (Burgess, 1981). The fungus is also known as *Gibberella zeae* due to long term use of early classification of the vegetative/asexual (anamorph: *F. graminearum*) and sexual (teleomorph: *Gibberella zeae*) stages of development as separate species. The taxonomy and nomenclature of *Fusarium* and *Gibberella* has undergone numerous changes since the first description of the anamorphic genus *Fusisporium* by Link (1809) from periods of lumping together or separating species from each other, resulting in as few as 9 to > 1,000 species over the years (Summerell and Leslie, 2011). The teleomorphs of *Fusarium* spp., when known, are mostly in but not limited to the genus *Gibberella* (Leslie and Summerell, 2006). Additionally, it has been known that many Fusaria are plant pathogens since the first description of the genus of *Fusarium* (Summerell and Leslie, 2011).

For *F. graminearum*, the current nomenclature comes from classifications of the anamorph and teleomorph, respectively, by Schwabe (1839) and Petch (1936). Previous designations include *Fusarium rosea* for the anamorph and *Sphaeria zeae* (1822) and *Dothidea zeae* (1832) by Schweinitz, *Gibbera saubinetii* (Montagne, 1856), and *Gibberella saubinetii* (Saccardo, 1879) for the teleomorph. *F. graminearum* became the

preferred binomial in the 1980s. Later phylogenetic studies support 13 lineages within *F. graminearum*, some that could interbreed and others that could not (O'Donnell et al., 2000; O'Donnell, 2004; Leslie and Summerell, 2006; Starkey, 2007), suggesting that even this classification may contain multiple species. The most economically significant hosts of *F. graminearum* are cereal crops such as wheat, barley, and corn though infection of rice, wild rice, and other crop and ornamental plants occurs (Chongo et al., 2001; Lee et al., 2009; Nyvall and Mirocha, 1999; Tomioka et al., 2008).

In North America, *F. graminearum* is the primary cause of Fusarium Head Blight of wheat and barley, with the earliest description on wheat occurring in the 1884 (Stack, 2003). Epidemics were documented at the turn of the twentieth century (Atanasoff, 1920; Pugh and Johann, 1933). By that time, the anamorph and teleomorph were recognized as a single species (Wollenweber, 1914). Infection of cereals by *F. graminearum* is variable in severity and distribution from year to year but has remained a concern through the 20th and into the 21st century. There was an increase in the distribution and severity of disease in the early 90s, possibly from the increased application of no-till practices for soil conservation that leave infected crop litter from harvest on the soil surface (Dill-Macky and Jones, 2000; Miller et al., 1998; Steinkellner and Langer, 2004; Yi et al., 2001). From 1998-2000 alone, the total loss to infection of crops by *F. graminearum* in nine Midwestern states was estimated to be $2.7 billion (Nganje et al., 2001). In addition to reducing grain size and yield, *F. graminearum* produces toxins, including zearalenone and deoxynivalenol, which render the grain inedible for humans and animals.

The United States Department of Agriculture screens harvested grains for both zearalenone and deoxynivalenol to reduce the levels of each that enter the food supply for

both human and animal consumption. Zearalenone is a nonsteroidal estrogenic mycotoxin that acts as an agonist to estrogen receptors, resulting in numerous effects on the reproductive systems of animals (Minervini and Dell'Aquila, 2008). Swine are particularly sensitive to the toxin, and zearalenone also has an immunomodulatory effect on swine cellular innate immunity response (Marin et al., 2010). Additionally, short-term exposure (21 d) of zebrafish to zearalenone at levels relevant to those found in North American and European rivers from field drainage resulted in reduced fecundity (Hartmann et al., 2008; Schwartz et al., 2010). Deoxynivalenol (DON) is a trichothecene mycotoxin that strongly inhibits protein synthesis at the ribosomal level both *in vivo* and *in vitro* and acts as a virulence factor during infection of wheat by *F. graminearum* (Desjardins et al., 1996). Consumption of sufficient quantities of DON by animals, including humans, can lead to digestive tract irritation and ulcers, feed refusal, vomiting, diarrhea, and weight loss (Bennett and Klich, 2003; Ramakrishna et al., 1989; Dänicke et al., 2006; Desjardins, 2006; Raghavender and Reddy, 2009; Robbana-Barnat et al., 1987; Stępień and Chełkowski, 2010; Ueno et al., 1968). As with zearalenone, DON has been found in environmental samples, including runoff water from fields and discharge from waste water treatment plants (Bucheli et al, 2008; Wettstein and Bucheli, 2010).

Screening programs certainly reduce the levels of *F. graminearum* mycotoxins entering the food supply, but do not address the issues of environmental contamination or the economic losses suffered by farmers with contaminated grain. Reduction of the incidence and severity of FHB would address all these issues. One route to accomplish FHB reduction is to develop our understanding of the biological processes governing the life cycle of *F. graminearum*. Of particular interest are the stages crucial for FHB

transmission in order to identify possible control methods, which may be applicable to other ascomycetous plant pathogens that also utilize forcible discharge to distribute the primary inoculum of ascospores, including *Sclerotinia sclerotiorum* and *Venturia inaequalis* (Clarkson et al., 2003; MacHardy, 1996).

The life cycle of *F. graminearum*

The life cycle of *F. graminearum* can be seen both in the field and in culture with only slight differences and consists of vegetative hyphae that colonize hosts or substrates and are capable of undergoing asexual and sexual development. Starting from germinating asexual (macroconidia) or sexual (ascospores) spores, vegetative hyphae grow and colonize a substrate or host. Behind the front of growing vegetative hyphae, older hyphae can generate differentiated phialide-bearing hyphae called conidiophores that are often but not exclusively aerial and produce macroconidia. The fungus can also form tightly packed clusters of conidiophores, arising from a hyphal stroma underneath, called sporodochia that produce copious amounts of macroconidia (Khonga and Sutton, 1988). Macroconidia are released and carried away by wind or water to new substrates or hosts to start vegetative growth again. *F. graminearum* also undergoes sexual development, producing flask shaped perithecia filled with asci containing eight multicelled ascospores.

The phenotypic course of sexual development of *F. graminearum* has been described thoroughly in culture (Trail and Common, 2000) and during colonization of wheat (Guenther and Trail, 2005). In culture, sexual development is easily induced and progresses rapidly. Perithecium initials and dikaryotic hyphae with lipid bodies are

present within 24 hours, growing and developing a central hollow cavity with croziers by three days post induction. Croziers are ascus precursor cells that maintain the dikaryotic state by an asymmetric and synchronous mitotic division of the two nuclei of the dikaryon, with septa formation blocking off one nucleus from each division and leaving the other two in the starting cell. Karyogamy follows and asci are present by the fourth day, growing upwards. Eight ascospores are produced by meiosis followed by a round of mitosis. Asci continue to grow towards an opening in the top of the perithecium called the ostiole and discharge their contents variably around day seven, one ascus at a time. Around three weeks post induction, fruiting bodies extrude undischarged ascospores and asci *en masse*, producing filaments called cirrhi.

Development on wheat proceeds similarly to that in culture, except the fungus can lie dormant after perithecium initial formation during unfavorable conditions (overwintering). Following initial colonization, the fungus enters the vascular tissue of the plant, develops wide binucleate hyphae, and begins storing lipids in numerous lipid bodies that likely serve as energy stores sexual development after overwintering (Guenther and Trail, 2005). An examination of gene expression during the course of sexual development found that lipid biosynthesis gene are upregulated early in development and that lipid degradation genes are upregulated later in development, supporting the role of lipid metabolism in sexual development (Guenther et al., 2009). Once favorable conditions are again present, development resumes and proceeds rapidly. Germination of ascospores on suitable hosts or substrates returns the fungus to the vegetative growth stage. Sexual development is associated with host infection and colonization in the field as perithecia develop on colonized crop debris left after grain

harvesting (Dill-Macky and Salas, 2002; Teich and Nelson, 1984; Windels and Kommedahl, 1984). There are no reports examining the ability of *F. graminearum* to sexually develop on already senesced plant material colonized only after contact with soil. However, this concept has been stated before (Sutton, 1982). Ascospores of *F. graminearum* are believed to be the primary inoculum of FHB, but there is some uncertainty to this presumption as both ascospores and macroconidia are capable of causing FHB when inoculated onto wheat spikelets (Sutton, 1982; Mitter et al., 2006).

Support for ascospores being the primary inoculum of FHB comes from several lines of research. While surveys of airborne fungal spores find both ascospores and macroconidia, they consistently find considerably more ascospores, though macroconidia levels are sometimes equivalent or greater than ascospore levels (Fernando et al., 2000; Inch et al., 2005; Markell and Francl, 2003). A number of phylogenetic studies from around the world characterizing field isolates each showed high genetic diversity among the isolates, little to no linkage disequilibrium between genetic markers, and almost as many haplotypes as isolates, suggesting a high rate of recombination and thus sexual reproduction in the field (Karugia et al., 2009; Tóth et al., 2005; Walker et al., 2001; Ward et al., 2008, Zeller et al., 2003). Those studies examining the same sites over numerous years found the allelic frequencies in the local populations are stable through the course of the studies, which was interpreted as the local population being part of a larger panmictic population. Desjardins et al (2006) found that ascospore non-producing strains of *F. graminearum* were significantly less able to cause FHB epidemics and DON accumulation in grain than wild-type ascospore producing strains with the source of inoculum being pieces of colonized corn placed on the ground. The ascospore non-

producing strains (hygromycin resistant) were isolated from ten-fold fewer infected kernels than complemented ascospore producing strains (hygromycin and geneticin resistant). Markell and Francl (2003) examined the adherence of both spore types to wheat by inoculating plants with known numbers of spores followed by washing them off with water from 30m to 24 hr post inoculation and found that significantly fewer ascospores than macroconidia were washed off at all time points. Considered together, these results provide good support for *F. graminearum* ascospores being the primary inoculum of FHB and suggest that developing ways to stop or reduced ascospore discharge could provide significant reduction of the incidence and severity of the disease. In order to do so, we need to understand the biological processes involved in sexual development and ascospore discharge.

Forcible spore dispersal and ascus development

The ability of fungi to discharge spores has been long associated with airborne spores of plant disease agents (Coons, 1918; Plowright, 1880). The buildup and release of turgor pressure had originally been hypothesized as driving ascospore discharge and the launching of zygomycete copriphilous fungus *Pilobolus* spp. sporangia. Pfeffer (1858) described a case of ascospore discharge in which one ascospore is discharged at a time through an apical pore in the ascus, another ascospore then blocks the pore, and turgor pressure builds until discharge occurs again. De Bary (1887) discusses the ascospore discharge of numerous species, integrating original research with the previous work of others, and emphasizes the swelling of asci as they mature, the buildup of turgor pressure within asci, and the likeliness that osmolytes within asci drive an influx of water to

generate the pressure needed for discharge. The simultaneous ascospore discharge of numerous asci caused by a physical disturbance, called puffing, by cup fungi in *Peziza* and the discharge of ascospores by *Ascobolus immersus*, a dung inhabiting fungus, was described by Buller (1909). Buller also discussed the physics involved in dividing the initial jet of discharged *Peziza* periplasmic fluid and ascospores into individual projectiles that can be carried away by wind and in allowing the large *Ascobolus* ascospores held together by mucilage to travel farther as a group than if they were separate and thus land on fresh plants for grazing herbivores to consume.

Through the 20th century, research consisted mainly of observational and descriptive studies of ascus development and ascospore discharge by numerous species and the environmental conditions that promote discharge (Chrismas, 1980; Gregory and Stedman, 1958; Jones, 1926; Lortie and Kuntz, 1963; Tschanz et al., 1976). However, a few studies by Ingold investigated the pressures obtained within asci for discharge. The osmotic pressure in mature asci of *Ascobolus stercorarius* (Ingold, 1939) and *Sordaria fimicola* (Ingold, 1966) were estimated to be between 1.0- 1.3 MPa and 1.0-3.0 mPA as assessed by incipient plasmolysis analysis and freezing point measurements of diluted ascus periplasmic fluid, respectively. Ingold (1939, 1966, 1971) offered that breakdown products of glycogen, sugars, and ions may serve as osmolytes in asci.

Although few researchers have tackled the ascospore discharge problem since Debary, the dramatic technical advances in biological research over the last forty years has facilitated other research into numerous biological processes in fungi, and the genes and proteins involved in them, that have shown connections to fungal growth and sexual development, influencing the initiation of more recent studies on ascospore discharge.

Measurement of the turgor pressure in *Ascobolus immersus* asci by pressure microprobe found an average pressure of 0.31 MPa and detected glycerol in ascus periplasmic fluid (Fischer et al., 2004). Pharmacological chemicals were screened for inhibition of *F. graminearum* ascospore discharge. Several K^+ channel blockers inhibited ascospore discharge up to 50%, and two L-type calcium channel blockers, verapamil and TMB8, showed almost complete inhibition of discharge (Trail et al., 2002). High calcium concentrations have been observed in the tips of cells undergoing polarized growth in fungi (Levina et al. 1995) and may be present in ascus tips as they elongate. A biomechanical study of *F. graminearum* ascospore discharge estimated that 1.54 MPa of pressure was needed to achieve the launch acceleration of 970,000 g and the trajectory characteristics observed. Analysis of periplasmic fluid from asci showed that $[K^+]$ and $[Cl^-]$ generated turgor pressure close to the estimate needed for discharge and that $[Ca^{2+}]$ was below detection, suggesting a role in signaling (Trail et al., 2005).

Calcium signaling

Calcium was well known to play a structural role in bones and teeth during the 18th century, but its role as a signaling messenger were not known until hinted at in a series of discoveries in the late 18th century. Ringer (1883a; 1883b) first noticed that frog hearts were able to continue beating when placed in tap water but stopped beating shortly after being placed in distilled water. Only when a calcium salt was added to the distilled water were the frog hearts able to keep beating. This was shortly followed by work showing that calcium was needed for frog hind leg muscle contraction, to prevent cells of

the brown alga *Laminaria* from bursting when placed in otherwise distilled water, for frog egg development, and for survival of the aquatic worm *Tubifex,* again in otherwise distilled water (Ringer, 1886, 1890; Ringer and Sainsbury, 1894). Although calcium signaling research did not progress until the 1950s, these initial results were rediscovered, and the known roles of calcium in cells have greatly expanded.

Calcium is a ubiquitous messenger in eukaryotic cells, acting both directly and indirectly to modulate protein activity, gene transcription, energy metabolism, endo- and exocytosis, and many other cellular processes (Berridge et al., 2003; Carafoli, 2005; Michalak et al., 2002). Calcium is normally abundant in many environments and shows a propensity for forming insoluble salts with inorganic and organic anions and also binds with complex macromolecules such as proteins (Carafoli, 2005; Carafoli, 2007; Williams, 2006). These properties likely made calcium toxic to early life and necessitated a system to maintain low cytosolic levels of calcium, setting up calcium to be an excellent messenger with the appearance of internally compartmentalized eukaryotes and the need for fast communication between compartments (Williams, 2006; 2007). The duality of calcium being integral to eukaryotic cell function yet also toxic is still seen today. Prolonged elevation of cytosolic calcium disrupts cellular processes often leading to cell death, and calcium is involved in both apoptotic and non-apoptotic programmed cell death and (Demaurex and Distelhorst, 2003; Dorn, 2009; Mattson and Chan, 2003).

Generally, low cytosolic calcium levels are maintained by the coordination of calcium influx and efflux through the plasma membrane and sequestration to and release from intracellular stores such as the endoplasmic reticulum (Berridge et al., 2003; Williams, 2007). Calcium diffusion in the cytosol is typically slow because proteins

quickly bind free calcium, some acting purely as calcium buffers and others as calcium signaling sensors (Allbritton et al., 1992; Biess et al., 2011). The buffering capacity of the cytosol is finite however. In response to stimuli, plasma membrane influx and intracellular stores release can generate local calcium gradients, or microdomains, that can be propagated as cytosol-wide or cytosol transversing calcium signals (Berridge et al., 2003; Laude and Simpson, 2009). Generally, calcium signals can be grouped into three classes: oscillations, sustained, and transient signals (Uhlén and Fritz, 2010). A number of calcium binding protein domains have evolved in eukaryotes, including the EF-hand, the annexin fold, and the C-2 domain. In particular, the EF-hand domain first found by Kretsinger and Nockolds (1973) in the protein parvalbumin from fish muscle is now known to be part of numerous proteins throughout eukaryotes (Carafoli, 2007). The binding of calcium by sensor proteins can elicit functional changes in the sensors and even interacting proteins. For example, calmodulin is a calcium sensor highly conserved in eukaryotes, containing four EF-hand domains, that undergoes a conformational change upon binding calcium. Calmodulin can then bind to and activate the protein phosphatase calcineurin by displacing an autoinhibitory domain from the calcineurin active site (Sagoo et al. 1996). The response of the cells to calcium signals is dependent on the spatial, temporal, and intensity qualities of the signal in addition to cell type and the current stage of the cell and life cycles (Berridge, 2007; Brenner et al., 2007).

While calcium signaling is used in many processes and can originate from both intra- and extracellular stimuli, there is a general scheme that occurs. A calcium signal starts with the detection of a stimulus often by receptor proteins that then interact either directly or indirectly with a calcium channel or pump (Hille, 1994). The interaction turns

on the calcium channel starting a calcium flux that generates the signal. The calcium ions are bound by sensor proteins that decode the signal by interaction with their target(s). Calmodulin is currently unique among calcium sensors in that it is known to interact with hundreds of proteins while other sensors interact with a few or even only one other protein (Carafoli et al., 2001). As the targets of calcium sensors perform their functions, creating the cellular response to the stimulus, the need for response to the stimulus is no longer necessary and feedback inhibition to the calcium channel stops the calcium flux (Armstrong, 1989). Finally, calcium is transported out of the cell or into internal stores to return the cytosolic calcium concentration back to its starting state.

Calcium signaling is ancient as evidenced by the fact that all eukaryotes utilize it. However, there is considerable evolutionary malleability to calcium signaling with only a few components highly conserved in all eukaryotes examined. More commonly, the conservation is scattered throughout the groups with each component displaying a different pattern. For instance, homologs to mammalian plasma membrane Ca^{2+}-ATPase efflux pumps (PMCA), including mammalian sarcoplasmic reticulum Ca^{2+}-ATPase pumps (SERCA), are found in all eukaryotes but in vascular land plants (gymnosperms and angiosperms) only an ortholog of the SERCA pump is present and the plasma membrane efflux pump is a non-homologous plant autoinhibited Ca^{2+}-ATPase pump (Connorton et al., 2011).

An important aspect of calcium signaling and homeostasis is the controlled importation of calcium into cells through the plasma membrane. In fungi, two types of calcium uptake are known – a high affinity calcium uptake system (HACS) and a low

affinity calcium uptake system. *FIG1* encodes a transmembrane protein of the low affinity calcium uptake system in *S. cerevisiae* (Muller et al., 2008) and another ascomycete yeast *Candida albicans* (Brand et al., 2007) but is lacking in the current assembly of the *F. graminearum* genome sequence. The HACS is composed of at least the calcium channels Cch1 and Mid1. In *S. cervisiae*, both *mid1* and *cch1* mutants died after exposure to mating pheromone (Iida et al., 1994; Fischer et al., 1997). Calcium uptake was significantly reduced in both single and double mutants. Growth in calcium-supplemented medium rescued the mutant phenotypes. Cch1 and Mid1 were found to coimmunoprecipitate, suggesting they form one complex, but mutants of the two channels differentially responded to some stimuli, suggesting both cooperative and individual function (Courchesne and Ozturk, 2003; Tokes-Fuzesi et al., 2002). HACS has been shown to respond to a number of stimuli such as exposure to mating pheromone, heat shock and cold stress, ionic stress, and mechanical stretching (Matsumoto et al., 2002; Peiter et al., 2005; Watts et al., 1998; Zhao et al., 1998).

In *F. graminearum*, Δ*cch1* mutants have been characterized (Hallen and Trail, 2008). These mutants displayed lower growth vigor, delayed sexual development, and significantly reduced ascospore discharge. The vegetative mycelium was distinctively fluffy and grew at ~50% the rate of the wild-type strain. Sexual development proceeded to completion but was delayed approximately 24 h. The Δ*cch1* mutants failed to grow on medium with low calcium availability. Addition of exogenous calcium restores the wild-type phenotype. These results suggest that Cch1 is needed for proper import of Ca^{2+} during all stages of growth, that calcium signaling may be involved in ascospore discharge, and that the other HACS component Mid1 may also be involved.

The *S. cerevisiae* Mid1 protein is an N-glycosylated stretch-activated calcium permeable ion channel (Iida et al., 1994; Maruoka et al., 2002). Parts of the C-terminus are required for proper localization and function (Ozeki-Miyawaki et al., 2005). Mid1 was found to localize to both the endoplasmic reticulum and cellular membranes, leading to the possibility of Mid1 having a function in both calcium entry into a cell and in intracellular sequestration and release of calcium. The presence of Mid1 homodimers, and computational structural analysis suggesting homotetramer formation, support earlier hypotheses that Mid1 may form its own channel (Yoshimura et al., 2003). When heterologously expressed in mammalian cells, Mid1 mediated a stretch-activated influx of calcium, but it was not determined whether Mid1 was modulating the activity of an endogenous channel or forming a channel itself (Kanzaki et al., 1999). In the non-pathogenic filamentous ascomycete *Neurospora crassa*, which also forcibly discharges ascospores, a *mid1* mutant displayed reduced vigor, reduced conidiation, lower hyphal turgor pressure, and lower membrane potential (Lew et al., 2008). Unlike *S. cerevisiae*, addition of calcium to culture medium did not restore the wild-type phenotype. The *mid1* mutants successfully mated and produced viable ascospores.

LACS is minimally composed of the Fig1 membrane protein, a PMP22_Claudin superfamily member, and is involved in calcium influx and membrane fusion during mating of *S. cerevisiae* and *Candida albicans* (Muller et al. 2003; Yang et al., 2011), mating projection development and cell wall degradation at the fusion site of appressed shmoos, haploid yeast cells with a mating projection, in *S. cerevisiae* (Erdman et al., 1998), and thigmotropism and repression of hyphal growth in *C. albicans* (Brand et al., 2007). Mammalian PMP22_Claudin superfamily members are involved in membrane-membrane interactions such as epithelial tight

junction formation and signal transduction such as ion flux (Matter and Balda, 2003; Tsukita et al., 1999). The fungal members show little overall sequence identity with the mammalian orthologs but most have similar secondary structure and topology including cytoplasmic N- and C- termini, four transmembrane domains, two extracellular and one intracellular loops, and a conserved GΦΦGXC(n)C motif (Φ = F, L, M, or Y hydrophobic residues, n = 8 > n > 20 amino acids) in the first extracellular loop (Brand et al., 2007; Erdman et al., 1998; Zhang et al., 2006). There have been no reports on the function of Fig1 in filamentous fungi.

Myosins

Myosins are eukaryotic molecular motors that can bind and move along actin filaments. Myosins are known to be involved in many motility processes, including amoeboid movement, the elongation of pollen germ tubes in plants, and muscle contraction (Franca-Koh et al., 2006; Krichevsky et al., 2007; Craig and Woodhead, 2006), and can be either activated or deactivated by calcium signaling (Krementsov et al., 2004). Myosins are a large and diverse family of proteins that has been expanded recently from 15 to 18 and then to 35 classes as scientists have found new classes. (Odronitz and Kollmar, 2007; Richards and Cavalier-Smith, 2005; Sellers, 200). Myosins consist of three domains: the head, neck, and tail (Bement and Mooseker, 1995). The head domain is conserved in all functional myosins and is the motor, containing an ATP modulated actin binding site and ATPase domain. The neck domain binds myosin light chains, regulatory proteins that increase myosin movement rates (Lowey et al., 1993; Watanabe et al., 2007). The tail domain is highly variable between myosin classes being composed of different combinations of domains, including dimerization, protein interaction and

membrane binding domains, though some myosins have no recognizable tail (Richards and Cavalier-Smith, 2005). Some myosins also bind actin in an ATP independent manner in the tail region, allowing the cross-linking of actin filaments (Fujisaki et al. 1985; Jung and Hammer, 1994; Rosenfeld and Renert, 1994). Some myosin tails are known to bind to membranes and are involved in endo- and exocytosis and vesicle transport (Desnos et al., 2007; Satoh et al., 2008) and sliding of plasma membranes across the cytoskeletal cortex (McConnell and Tyska, 2007).

In yeast and filamentous fungi, myosins were found to be required for polarized growth and secretion (McGoldrick et al., 1995; Woo et al., 2003; Schuchardt et al., 2005). Calmodulin was found to regulate both myosins and the actin cytoskeleton in *S. cerevisiae* (Cyert, 2001; Desrivières et al., 2002). Studies of ascus development in numerous species have described extensive actin cytoskeleton remodeling and membrane dynamics with actin and myosins being involved in the transition of croziers to asci, karyogamy and subsequent meiotic and mitotic divisions, migration and separation of spindle pole bodies, fungal equivalents of centrioles, and ascospore spore delimitation with a double-membrane layer derived from invaginations of a double membrane near the ascus plasma membrane, generating vesicles that migrate to the developing ascospores (Beckett and Crawford, 1973; Czymmek and Klomparens, 1992; Hackett and Chen, 1976; Healy, 2003; Raju, 2008; Read and Beckett, 1996; Thompson-Coffe and Zickler, 1993; Wu and Kimbrough, 2001).

Myosins may also be involved in the growth of asci by moving along actin polymers while attached to the ascus membrane, stretching the membrane, or while attached to transport vesicles carrying material and enzymes to the ascus tip. It is

conceivable that myosins may play roles in retention or firing mechanisms by generating tension along actin filaments anchored to the plasma membrane or other structures or by crosslinking actin filaments. There are three annotated myosins within the *F. graminearum* genome, *MYOI*, *MYOII*, and *MYO2*. Deletion of *F. graminearum MYOI*, a type I myosin, resulted in sickly mutants with severely reduced filamentous growth that failed to undergo sexual development, and deletion of *MYOII*, a type II myosin, was attempted several times but was not obtained, suggesting that *MYOII* is an essential gene (Trail, unpublished results). Deletion of *MYO2*, a type V myosin, has not been attempted.

Current research

In the following chapters, I present my investigations on the role of *MID1* and *FIG1* in the growth and sexual development of *F. graminearum* and the development of a doxycycline inducible RNAi system, and utilizing it to study the role of *MYO2*, a myosin, in ascus development. Given that deletion of *F. graminearum CCH1* resulted in reduced growth, conidiation, and ascospore discharge, that *MID1* is also a component of HACS, and that Δ*cch1* and Δ*mid1* mutants of *S. cerevisiae* have nearly identical phenotypes, it seemed likely that *MID1* would also play a role in the same processes. If *MID1* plays a role in calcium signaling, growth, and development of *F. graminearum*, then *MID1* deletion will result in phenotypes similar to the Δ*cch1* mutants. The results of the experiments designed to test that hypothesis showed that there was another route of calcium entry even in mutants lacking Mid1 and Cch1 as addition of exogenous calcium partially restored most of the observed phenotypes. Since LACS is the only other calcium

entry route in fungi, LACS is involved in sexual development of *S. cerevisiae* and *C. albicans*, and Fig1 is the only known component of LACS, Fig1 was hypothesized to mediate the calcium entry in the Δ*mid1* Δ*cch1* double mutants and play a role in sexual development. If Fig1 plays a role in *F. graminearum* sexual development and the importation of calcium seen in Δ*mid1* Δ*cch1* mutants, then deletion of *FIG1* will result in altered sexual development and the abolishment of the ability of calcium supplementation to rescue the Δ*mid1* Δ*cch1* double mutants in a Δ*fig1* Δ*mid1* Δ*cch1* triple mutant. Because the loss of essential genes is lethal and the loss of genes essential for sexual development prevent or halt sexual development, the adaptation of a doxycycline inducible RNAi system effective in another filamentous ascomycete for use in *F. graminearum* was thought to both feasible and a possible way to investigate genes essential for sexual development during sexual development. Because myosins are involved in sexual development, *MYO2* was targeting for doxycycline induced RNAi. If doxycycline induced RNAi is effective in *F. graminearum* and *MYO2* is involved in ascus development, then *MYO2* expression will be reduced when RNAi is induced and the normal development of asci and ascospores will be altered.

CHAPTER 2

MID1, A MECHANOSENSITIVE CALCIUM ION CHANNEL, AFFECTS GROWTH, DEVELOPMENT, AND ASCOSPORE DISCHARGE IN THE FILAMENTOUS FUNGUS *GIBBERELLA ZEAE*

Brad Cavinder,[1] Ahmed Hamam,[2] Roger R. Lew,[2] and Frances Trail[3,4]

Genetics Graduate Program, Michigan State University, East Lansing, Michigan, 48824-43201[1]; Department of Biology, York University, 4700 Keele Street, Toronto, Ontario M3J 1P3, Canada2; and Department of Plant Biology3 and Department of Plant Pathology,4 Michigan State University, East Lansing, Michigan 48824-1312

I performed all the work of this chapter in the Trail lab except the electrophysiology experiments that our collaborators Ahmed Hamam and Roger R. Lew carried out.

This chapter was published in Eukaryotic Cell Vol 10:832-842, 2011.

ABSTRACT

The role of Mid1, a stretch-activated calcium permeable ion channel, in ascospore development and forcible discharge from asci, was examined in the pathogenic fungus, *Gibberella zeae* (anamorph *Fusarium graminearum*). The Δ*mid1* mutants exhibited >12-fold reduction in ascospore discharge activity and produced predominately abnormal two-celled ascospores with constricted and fragile septa. The vegetative growth rate of the mutants was ~50% of the wild-type rate, and production of macroconidia was >10-fold lower than in wild-type. To better understand the role of calcium flux, Δ*mid1* Δ*cch1* double mutants were also examined, as Cch1, an L-type calcium ion channel, is associated with Mid1 in yeast. The phenotype of the Δ*mid1* Δ*cch1* double mutants was similar, but more severe than in the Δ*mid1* mutants for all categories. Potential and current voltage measurements were taken in the vegetative hyphae of the Δ*mid1* and Δ*cch1* mutants and wild-type, and both measurements were remarkably similar in all three strains, indicating that neither protein contributes significantly to the overall electrical properties of the plasma membrane. Pathogenicity of the Δ*mid1* and Δ*mid1*Δ*cch1* mutants on the host, wheat, was not affected by the mutations. Exogenous calcium supplementation partially restored the ascospore discharge and vegetative growth defects for all mutants, but abnormal ascospores were still produced. These results extend the known roles of Mid1 to ascospore development and forcible discharge. However, *Neurospora crassa* Δ*mid1* mutants were also examined and did not exhibit defects in ascospore development nor in ascospore discharge. In comparison to other ascomycetes, Mid1 shows remarkable adaptability of roles, particularly with regard to niche-specific adaptation.

Introduction

The majority of fungal spores are nonmotile, driving evolutionary creativity for other means of dispersal. In the Ascomycota, asci function predominantly as water cannons that forcibly discharge ascospores into the air. The buildup and release of turgor pressure within asci has long been hypothesized as driving ascospore discharge, with the first such reference by DeBary (1887), yet the mechanism of ascus function has never been elucidated in any fungus. In *Gibberella zeae,* pharmacological screens showed that K^+ channel and L-type calcium channel blockers inhibit discharge (Trail et al., 2002). Analysis of periplasmic fluid from discharging asci revealed that accumulation of K^+ and Cl^- would generate turgor pressure close to that necessary for discharge, with Ca^{2+} below detectable levels (Trail et al., 2005; Trail, unpublished results). These results suggest that potassium functions as the osmoticum and calcium plays an essential role in signaling ascospore discharge. Calcium signaling can result in rapid cellular responses such as cell motility and contractile events, or more paced responses, such as shifts in gene expression, and cell division (Berridge et al., 2003; Clapham, 2007).

In fungi, two types of calcium uptake are known – a high affinity calcium uptake system (HACS) and a low affinity calcium uptake system (LACS). Initially characterized in *Saccharomyces cerevisiae*, the HACS is composed minimally of Cch1, an L-type voltage gated calcium channel, and Mid1, a stretch-activated non-selective calcium permeable channel, acting as the major calcium entry route when calcium availability is low (Iida et al., 1994; Fischer et al., 1997; Paidhungat & Garrett, 1997); whereas, the LACS is composed minimally of Fig1, a transmembrane calcium channel or regulatory protein, and is the primary calcium entry route during high calcium availability (Muller et al., 2001; Muller et al., 2003). Mid1 and Cch1 have

been shown to be involved in calcium uptake from the environment for homeostasis and signaling. In calcium limited medium, calcium uptake was significantly reduced and death of *MAT***a** cells followed formation of shmoos upon exposure to α-factor in single mutants of each of these genes; double mutants behaved similarly. In mammalian cells, heterologous expression of *ScMid1* resulted in stretch-activated influx of Ca^{2+}. Whether the influx arose from direct formation of Mid1 channels or from regulatory modulation of an endogenous channel is still unclear as is whether Mid1 forms a channel, serves in a regulatory capacity, or both endogenously in fungi (Kanzaki et al., 1999; Locke et al., 2000; Tada et al., 2003).

In filamentous fungi, published investigations to date report only on *MID1* and *CCH1* of the HACS, with the LACS components uncharacterized. In the filamentous ascomycete *Neurospora crassa*, Δ*mid1* mutants displayed reduced vigor, reduced conidiation, lower hyphal turgor pressure, and lower membrane potential (Lew et al., 2008). Unlike Δ*mid1* mutants of *S. cerevisiae*, addition of calcium to culture medium does not restore the wild-type phenotype to *N. crassa* Δ*mid1* mutants. However, *N. crassa* Δ*mid1* mutants successfully mate and produce viable ascospores. In *G. zeae*, Δ*cch1* mutants displayed less vigorous hyphal growth, delayed sexual development, and significantly reduced ascospore discharge (Hallen and Trail, 2008). Application of exogenous calcium to Δ*cch1* mutants restored the wild-type phenotype. In particular, addition of calcium to cultures of Δ*cch1* mutants with mature perithecia rescued ascospore discharge, supporting a role for calcium signaling directly in the discharge mechanism. To further the understanding of the role of the HACS in growth and development of *G. zeae*, we report the generation Δ*mid1* and Δ*mid1* Δ*cch1* double mutants, and characterize the mutant phenotypes through a series of culture based assays, electrophysiology experiments, and a pathogenicity assay on the host, wheat. Additionally, the ability of *N. crassa* Δ*mid1* mutants to

forcibly discharge ascospores was not assessed in the Lew et al. (2008) study, so we also monitor the sexual development and ability to discharge ascospores in reciprocal crosses of these mutants to assess whether the role of HACS in forcible ascospore discharge is conserved between *G. zeae* and *N. crassa*.

Materials and Methods

Strains, culture conditions

All strains used in this study are listed in Table 1. *N. crassa* strains were obtained from the Fungal Genetics Stock Center (FGSC) and stored at -20°C. *G. zeae* strains were maintained on sterile soil at -20°C and as macroconidia stocks (10^6-10^8 conidia/ml) in 35% glycerol at -80°C. Macroconidia were produced in carboxymethylcellulose (CMC) liquid media as previously described (Cappellini and Peterson, 1965). For *G. zeae*, perithecia were induced in culture on carrot agar as previously detailed (Bowden and Leslie, 1999; Trail and Common, 2000). Briefly, strains were center inoculated on carrot agar, and cultures were incubated at room temperature (RT) under continuous fluorescent lighting. As mycelia reached the edge of the plates, it was gently removed from the surface, 1 ml of a 2.5% Tween 60 solution was spread across the surface, and the incubation was continued.

Sexual crosses

G. zeae is homothallic but can outcross. Crosses were initiated by the mycelial plug method. Along the interface between strains, cirrhi (masses of exuded ascospores) were isolated from individual perithecia and suspended in 200 µl of sterile deionized water (diH_2O) by vortexing.

Aliquots of the ascospore suspension (80 µl) were spread across the surface of minimal medium supplemented with tergitol and L(-)sorbose (MMTS) (Bowden and Leslie, 1999). Growth of non-nitrate-utilizing mutants (nit^-) is sparse on MMTS and easily distinguished from wild-type. As a result, recombinant cirrhi contained both wild-type nitrate-utilizing (nit^+) and nit^- mutant progeny and were easy to distinguish from cirrhi from homozygous perithecia. After 3-5 days of growth at RT, colonies from plates containing recombinant cirrhi were individually transferred to V8 agar to maintain the culture and also to Czapek-Dox agar (Thom and Church, 1926) for confirmation of nit phenotype before subsequent analysis. For the Δ*mid1* x PH-1 55 crosses, only nit^- colonies were harvested. Nit^+ colonies were selected from the mn-11 x Δ*cch1*-T14 crosses.

N. crassa crosses were performed by inoculating single strains of opposite mating type onto synthetic crossing medium (Davis and de Serres, 1970) and maintaining under continuous fluorescent lighting. Seven days post-inoculation, macro- and microconidia were washed from the medium and transferred to the culture of the opposite mating type where both conidial types function as spermatia to fertilize protoperithecia (Dodge, 1935; Bistis, 1981). Crosses were maintained under continuous fluorescent lighting at RT during perithecial development.

DNA constructs and genetic transformation

DNA was isolated from *G. zeae* and *N. crassa* mycelia using a hexadecyltrimethylammonium bromide (CTAB) method as previously described (Hallen and Trail 2008), modified by treatment with proteinase K (final concentration 2.0 mg/ml) for 1-2 hr at ≤ 65°C or overnight at 37°C following the RNase digestion after the first precipitation and resuspension.

TABLE 1. Strains used in this study

Strain	Genotype	Abbreviation used	Source
Gibberella zeae			
PH-1	wild-type (FGSC 9075; NRRL 31084)	wt	Trail and Common, 2000
PH-1 55	*nit1*	PH-1 55	H. C. Kistler[a]
M-Δ2	Δ*mid1*	Δ2	This Study
M-Δ12	Δ*mid1*	Δ12	This Study
M-E1	Ectopic insertion of *MID1* disruption construct	E1	This Study
M-C1	Δ*mid1* complement (M-Δ2)	C1	This Study
M-C2	Δ*mid1* complement (M-Δ2)	C2	This Study
Δ*cch 1*–T11	Δ*cch 1*	T11	Hallen and Trail, 2008
mn-11	Δ*mid1 nit1* (M-Δ2 x PH-1 55)	mn-11	This Study
MC-4	Δ*mid1* Δ*cch1* (mn-11 x Δ*cch1* -T11)	ΔmΔc	This Study
Neurospora crassa			
FGSC 2489	wild-type, A mating type		Colot et al., 2006[b]
FGSC 4200	wild-type, a mating type		Colot et al., 2006[b]
FGSC 11708	Δ*mid1* , A mating type		Colot et al., 2006[b]
FGSC 11709	Δ*mid1* , a mating type		Colot et al., 2006[b]

[a] USDA-ARS, University of Minnesota

[b] Directly received from the Fungal Genetics Stock Center

TABLE 2. Primers used in this study			
Name	Sequence (5'-3')	Contig	Coordinates
For replacement of the *G. zeaeMID1* locus			
Mid1 L5	CTTTGGAACGTCATGAGAACACGTTTCG	supercontig_3.4	3454860-3454833
Mid1 L3	TATTCAGGCGTAGCAACCAGGCGTGCTTAGTACGGCTTCGATCTAGC	supercontig_3.4	3454173-3454197
Mid1 R5	ATCTTTTACTTTCACCAGCGTTGGGATGTGCTTCTTGGGTATGTTTG	supercontig_3.4	3452227-3452202
Mid1 R3	CTGTAGTCTCAGTTCTATCGCACATTCAC	supercontig_3.4	3451691-3451719
Mid1 checkF	AACTTCCGTCGAGCAGAGTCTAAGAC	supercontig_3.4	3453746-3453721
Mid1 checkR	GTTGGCATACATCTTTCTGGCGTAGTC	supercontig_3.4	3452775-3452801
HygF for M1	GCCGTACTAAGCACGCCTGGTTGCTACGCCTGAATAAGTG	-	-
HygR for M1	CACATCCCAACGCTGGTGAAAGTAAAAGATGCTGAAGATC	-	-
3' 1/2 HygF	AGTACTTCTACACAGCCATCGGTCCAGACG	-	-
5' 1/2 HygR	CTGCTGCTTGGTGCACGATAACTTGGTGC	-	-
For complementation of *G. zeae* Δ*mid1* mutants			
Mid1 compF	ATGCTGCACGGTTTGAAGGTGGATGA	supercontig_3.4	3455042-3455017
Mid1 compR	AGGCCCTGTAAGTTAAATGGGTTGCTAAC	supercontig_3.4	3451300-3451328
Nit1 F	ATGGAACTGACGGGACGTTAAGGTACC	supercontig_3.1	6384100-6384074
Nit1 R	CTCACCTGTGTACGACAGGAGCAGA	supercontig_3.1	6379737-6379760
3' 1/2 Nit1F	CAGCAGTTGACCTATCCAGTTACATTCG	supercontig_3.1	6382391-6382418
5' 1/2 Nit1R	TTGACCAGCTGCACCAAAGATAGATG	supercontig_3.1	6381114-6381139
For probe generation			
Cch1 probeF	CTCAATCTCCTGCGAAGTGGAATGAG	supercontig_3.1	4488045-4488020
Cch1 probeR	GCAGACAAGGGACTAATAATCGCCAAC	supercontig_3.1	4487335-4487308
For confirmation of *N. crassa MID1* locus presence or absence			
NcM1-F	GTCCTTTATCGCATTATCTCTTCTCGTCG	contig 7.31	109555-109527

All *G. zeae* nucleotide data was obtained from http://mips.helmholtz-muenchen.de/genre/proj/FGDB/. Unless otherwise noted, PCR amplifications used PH-1 gDNA as the template. Primers used in this study are listed in Table 2. For targeted gene replacement constructs, a split marker protocol was performed (Catlett et al., 2003; Fairhead et al., 1996; Fairhead et al., 1998). Primers were designed to amplify a 687 bp (supercontig_3.4: 3454858-3454172) and a 536 bp (supercontig_3.4: 3452227-3451692) region upstream (L) and downstream (R), respectively, of the coding sequence of *MID1* using primers Mid1 L5 & L3 and Mid1 R5 & R3. Primers closest to *MID1* coding sequence, Mid1 L3 and R5, have 5' tails of 24 and 22 bases complementary to the 5' and 3' ends of the hygromycin resistance marker from pCB1004 (Carroll et al. 1994), which encodes hygromycin phosphotransferase (*hph*) and allows for selection of transformants with hygromycin B (HygB). For split *hph*, a 1.4 KB 5' fragment and a 1.2 KB 3' fragment of *hph* overlapping each other by 800 bp was amplified from using primers HygF for M1 & 5' 1/2 HygR and 3' 1/2 HygF & HygR for M1, respectively. Primers HygF for M1 and HygR for M1 contain 5' tails of 13 and 8 bases complementary to the 3' and 5' ends of the *MID1* L and R fragments, respectively. The 5' *hph* fragment was merged with the amplified L flank, and the 3' *hph* fragment was merged with the R flanking region by PCR. Both merged products were transformed into *G. zeae*. Thus, successful replacement of the *MID1* gene required two recombination events for each construct to integrate into the *MID1* locus and a third recombination between the constructs to create a functional *hph* marker.

For complementation of the *mid1* mutants, a 3741 bp fragment of the *MID1* locus, spanning 906 bp upstream to 927 bp downstream of the *MID1* coding sequence (supercontig_3.4: 3455040-3451301), was generated by PCR using primers Mid1 compF and compR. Split *NIT1* constructs were generated by PCR amplification of 2987 bp

(supercontig_3.1: 6383925-6380938) and 2478 bp (supercontig_3.1: 6382215-6379737) fragments that overlap by 1278 bp, using primers Nit1 F & 5' 1/2 Nit1R and 3' 1/2 Nit1F & Nit1 R, respectively. All three amplicons were used simultaneously to cotransform mn-11 protoplasts.

Genetic transformation of *G. zeae* protoplasts was polyethylene glycol-mediated as previously described (Gaffoor et al., 2005). Following transformation for gene replacement, protoplasts recovered on regeneration medium for 15 hr followed by an overlay of regeneration medium containing 150 μg/ml HygB. Putative transformants were selected for growth through the overlay and were transferred to V8 agar containing 450 μg/ml HygB. Following the complementation cotransformation, protoplasts recovered on Czapek-Dox agar adjusted to 0.79 M sucrose for 15 hr, and were then overlaid with standard Czapek-Dox agar. Colonies growing vigorously on the overlay were transferred individually to Czapek-Dox agar to confirm the nit^+ phenotype. All putative transformants were regenerated from single spores to obtain pure genetic cultures as previously described (Hallen and Trail, 2008) and were then transferred to V8 agar for subsequent phenotype analysis.

Southern hybridization was performed as previously described using standard molecular techniques (Gaffoor et al., 2005; Sambrook and Russell, 2001). Genomic DNA was digested to completion with PvuI and was resolved by electrophoresis in Tris-acetate-EDTA. DNA was transferred to Nytran Supercharge nylon membrane (Schleicher and Schuell Bioscience, Keene, New Hampshire). Three probes were generated by PCR. The *MID1* L (Left flank) fragment, a 1.2 kb *hph* fragment amplified using primers 3' 1/2 HygF and 5' 1/2 HygR, and a 738 bp internal *CCH1* fragment (supercontig_3.1: 4488045-4497308) using primers Cch1 probeF and Cch1 probeR. Probes were labeled with [α-^{32}P]dCTP using the Random Primer DNA Labeling System (Invitrogen, Carlsbad, California) as per the manufacturer's instructions with the addition of 0.5

µl of the 10mM primers used to generate each probe. After hybridization and washing, membranes were used to expose Hyperfilm MP (GE Healthcare, Chalfont St. Giles, United Kingdom).

The nucleotide sequence of the *N. crassa MID1* locus was obtained from http://mips.helmholtz-muenchen.de/genre/proj/ncrassa/. Analysis of PCR amplifications of an internal 808 bp sequence of *MID1* using primers NcM1-F & NcM1-R from gDNA of the wild-type and *mid1* mutant strains confirmed the presence or absence of *MID1*, respectively.

Characterization of *G. zeae* Δ*mid1* phenotypes

For characterization of vegetative growth and sexual development, carrot agar was center inoculated with a mycelial plug of the wild-type or individual mutants and incubated at RT under continuous light. Radial growth was measured at 24 h intervals until mycelia reached the edge of the Petri dish (approximately 4 d). The first and last day's growth were discounted. The growth rate was calculated by subtracting colony diameter at 24 h from the diameter at 48 h. Four biological replicates of each strain were performed, and the calculated growth rates of the replicates were averaged. Sexual development was monitored using squash mounts of perithecia at previously defined stages of development (Trail and Common, 2000). Samples were observed on a Zeiss Standard microscope or a Leica DMRA2 microscope.

The level of calcium available in growth medium was adjusted to determine the effect on the wild-type and mutants. The characterization of vegetative growth was repeated for growth on carrot agar amended with 80 mM $CaCl_2$ and with 80 mM Magnesium ($MgCl_2$). Significance between the strains growth on carrot agar compared to PH-1 and between the strains' growth on carrot agar versus carrot agar + 80 mM $CaCl_2$ was assessed. Because carrot agar is a rich,

undefined medium, Bilay's medium (Booth, 1971) was supplemented to 10 mM with the cell impermeable calcium chelator 1,2-bis(2-aminophenoxy)ethane-*N,N,N,N,*-tetraacetic acid tetrapotassium salt (BAPTA) to determine the ability of Δ*mid1* mutants to grow in limited calcium conditions, as previously described with Δ*cch1* mutants (Hallen and Trail, 2008) except that mycelia was used as inoculum instead of macroconidia. To determine the effect of increased intracellular calcium levels, some strains were center inoculated on V8 agar, and after 48 h growth, a point treatment of 10 µl of either a 9.5 mM solution of calcium ionophore A23187 (in ETOH) or 100% ETOH was applied to a point slightly ahead of the leading edge of mycelial growth. Images were taken of the cultures 72 h post treatment.

Ascospore discharge assays were performed as previously described (Trail et al, 2002) using 12 mm diameter discs of carrot agar removed from mature cultures, cut in half, and placed cut side down on glass microscope slides so spores were shot down the length of the slide. Slides were incubated in a humidity chamber for 24 h at RT to allow discharged spores to collect on the glass slides. Ascospore discharge assays were repeated for all strains grown on carrot agar + 79.6 mM $CaCl_2$ and for PH-1 grown and matured on carrot agar with the addition of BAPTA to 1 mM and 10 mM at the time of assay setup. To quantify ascospore discharge, after the 24 h incubation, the spores were washed off the slides and quantified. The results of the three replicates were averaged.

A qualitative assessment of ascospore viability for all strains was performed. Three cirrhi per strain were recovered and suspended in 200 µl of sterile diH_2O. For strains that lacked cirrhi, three perithecia were crushed on a glass slide with a glass rod in 30 µl of sterile diH_2O to release ascospores. The crushed perithecia and ascospores were rinsed off the glass slides with 170 µl of

sterile diH_2O. From these suspensions, 30 µl from each strain were spread on water agar. The plates were incubated at RT for 48 h and examined under a dissecting microscope for the presence and abundance of germ tubes.

To quantify conidiation, surface mycelia collected from 12 mm diameter circles of fully colonized V8 medium of each strain was used to inoculate 100 ml of CMC medium. The CMC cultures were incubated for 4 d at RT shaking at 250 rpm. The 4 d cultures were filtered through Miracloth (Calbiochem, La Jolla, CA) to separate macroconidia from mycelia. The macroconidia were pelleted by centrifugation, resuspended in 1 ml of sterile diH_2O and quantified. Total conidiation of the strains in 100 ml of CMC + 79.6 mM $CaCl_2$ was performed in the same manner.

Pathogenicity tests were performed with all strains on 7 greenhouse grown plants of *Triticum aestivum* L. cv. Norm. Plants near anthesis were inoculated with 10 µl of 10^5 conidia ml^{-1} to a single floret in the middle of the head as previously described (Guenther and Trail, 2005). Fourteen days after inoculation, plants were scored for the number of symptomatic and asymptomatic florets.

Characterization of *N. crassa* Δ*mid1* ascus and ascospore morphology and ascospore discharge phenotype

Reciprocal wild-type and reciprocal Δ*mid1* crosses were performed and cultured as detailed above. When discharged ascospores were observed on the covers of the Petri dishes containing the *N. crassa* wild-type or Δ*mid1* crosses, the lids were washed with 1 ml of diH_2O to

collect the spores, and ascospores were observed by light microscopy. Squash mounts of mature perithecia from the two wild-type and the two Δ*mid1* crosses were also examined by light microscopy.

Statistical Analysis

Analysis of variance (ANOVA) was performed to assess the significance of intragroup variation and of intergroup interaction and, if any were significant, was followed by the post hoc Tukey's Honestly Significant Difference (HSD) test to return associated p-values for all pairwise comparisons. ANOVA and Tukey's HSD were performed in the R language and environment for Windows (R Development Core Team, 2010). The electrophysiological data are shown as mean ± SD (sample size). Independent two-tail t-tests comparisons of the two mutant strains with the PH1 wild-type were performed in Excel (Microsoft).

Microscopy and Imaging

Samples were first observed on a Zeiss Standard microscope. To capture images, samples were observed on a Leica DMRA2 microscope using Q-Capture camera control software (Q-Imaging; Surrey, BC Canada). Images of strain growth and ascospore discharge assays were captured with a Nikon Coolpix 995 (Tokyo, Japan) except the images of growth on Bilay's + 1 mM BAPTA which were captured with by an Alpha Innotech FluorChem 8900 imaging system (San Leandro, CA).

Electrophysiology experiments

Cultures were prepared by inoculating agar blocks of mycelium of the *G. zeae* strains

onto strips (2.5 X 6 cm) of dialysis tubing that overlay Czapek medium (with 1.5% w/v agar) in Petri dishes, then incubating at 25°C for 3–4 days. The dialysis tubing was cut with a razor blade to a size of about 1 X 3 cm, which included the growing edge of the colony, placed inside the cover of a 30 mm Petri dish, and immobilized on the bottom with narrow strips of masking tape. The culture was flooded with 3 ml of buffer solution (BS) (in mM): KCl (10), $CaCl_2$ (1), $MgCl_2$ (1), sucrose (133), and MES (10), pH adjusted to 5.8 with KOH. Growth of hyphae at the colony edge resumed after flooding with BS (growth was monitored by taking thermal video prints of hyphae at the colony edge immediately after transfer to the microscope stage, and about 10 min later with a X10 objective). Electrical measurements were alternated between the three strains.

Trunk hyphae (3–10 μm diameter) about 0.5 cm behind the colony edge were selected (with a X40 water immersion objective) for potential and current voltage measurements using double barrel micropipettes. Micropipette fabrication was described in detail by Lew (2006). Voltage clamp methods have been described elsewhere for measurements performed in *Neurospora crassa* (Lew, 2006; 2007). Current was injected through one barrel and voltage monitored through the other barrel. The voltage clamp protocol was a bipolar staircase of resting potential and alternating positive and negative voltage clamps, each with a duration of 100 ms; voltage (to check voltage clamping fidelity) and clamping current were measured during the last 5 ms of the clamp. There was no indication of any difference in time dependent currents amongst the three strains: the clamping current had reached steady state by 100 ms (data not shown). Measurements of current density in hyphae are complicated by the cable properties of the hypha; but the length constant (a measure of current along the hypha) for *G. zeae* hyphae is not known, so that current densities (A m^{-2}) could not be calculated (*cf* Lew, 2007). The hyphal diameters of

the two mutant strains (*cch1* and *mid1*) were smaller than the PH1 wild-type. Since hyphal diameters will affect the input conductance measured from the slopes of the current-voltage relations, to compare the current-voltage relations of the three strains, the currents (and current-voltage slopes) were normalized to (hyphal diameter)^2.

The potential is comprised of contributions from the Goldman-Hodgkin-Katz potential for permeant ions and the activity of the plasma membrane electrogenic H^+-ATPase. To assess as directly as possible the contribution of the H^+-ATPase to electrogenicity at the plasma membrane, hyphae were treated with the respiratory inhibitor cyanide (0.5 ml from a 50 mM NaCN stock in BS, final concentration 7.1 mM) to deplete cellular ATP and inhibit the H^+-ATPase (Slayman et al., 1973; Lew and Kapishon, 2009).

Results

Function of Mid1 and Cch1 in *Gibberella zeae*.

Mid1 function was examined by replacing the entire *MID1* coding sequence with the dominant selectable marker *hph*, encoding hygromycin phosphotransferase, conferring hygromycin resistance. From a single transformation experiment using split marker constructs targeted to the *MID1* locus, 24 hygromycin resistant colonies were obtained. Two of three colonies examined displayed slowed vegetative growth and were designated Δ2 and Δ12. PCR analysis of the two mutants revealed amplicons consistent with replacement of *MID1* by *hph*. The remaining strain, designated E1, displayed wild-type growth and PCR analysis was consistent with ectopic insertion of the disruption construct. To generate a strain for Mid1 complementation, Δ2 was first crossed to *nit3* mutant PH-1 55 and progeny were screened for

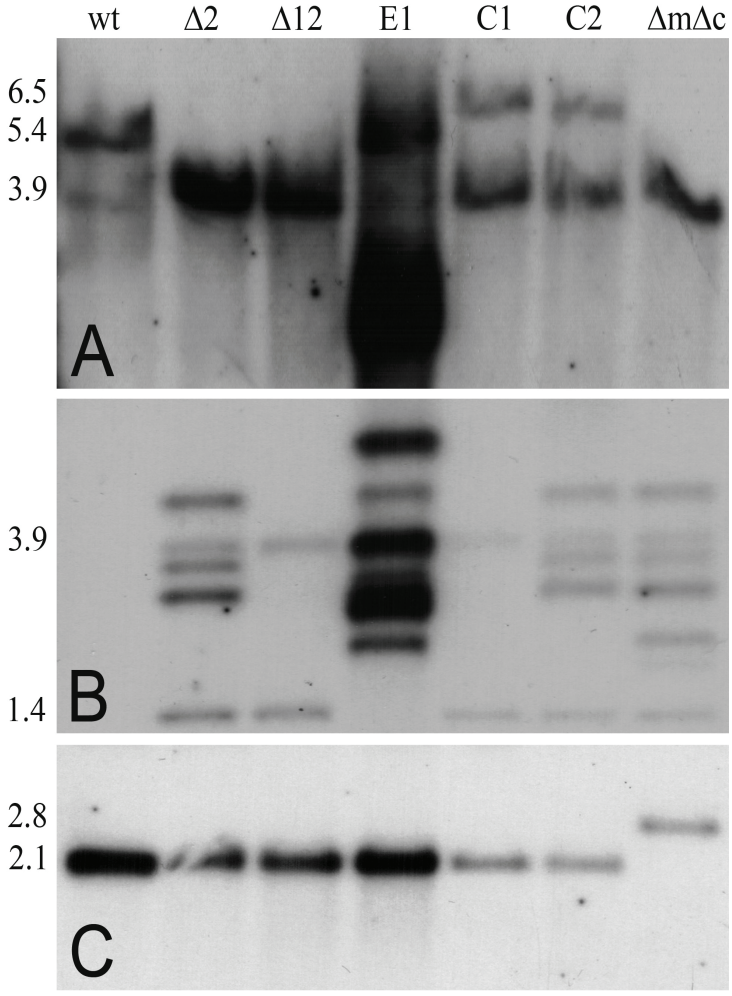

Figure 1. Southern analysis of *G. zeae* Mid1 deletion and complementation strains (A) Hybridization of the *MID1* probe. (B) Hybridization of the *hph* probe. (C) Hybridization of the *CCH1* probe. The numbers to the left indicate the approximate size of bands in kb. For all figures, strain genotypes are as follows: wt (*MID1 CCH1*), Δ2 and Δ12 (Δ*mid1 CCH1*), E1 (*MID1 CCH1*), C1 and C2 (Δ*mid1 CCH1* ::*MID1*), and ΔmΔc (Δ*mid1* Δ*cch1*).

the Δ*mid1 nit3* phenotype. From three recombinant cirrhi analyzed from the cross, 16 nit- colonies were isolated. PCR analysis indicated four progeny were Δ*mid1 nit3* double mutants. The Δ*mid1 nit3* double mutant, designated mn-11, was used for complementation. Cotransformation of mn-11 protoplasts with the MID1 complementation amplicon and split *NIT3* constructs was performed, resulting in selection of 25 nitrate-utilizing colonies. PCR analysis revealed that two transformants, designated C1 and C2, contained both *hph* and *MID1* sequences. Both complements exhibited wild-type vegetative growth and colony morphology. To generate Δ*mid1* Δ*cch1* double mutants, Δ*mid1 nit3* double mutant mn-11 was crossed with Δcch1-T14 (T14; Hallen and Trail, 2008). We isolated 24 colonies displaying slow but dense colony growth

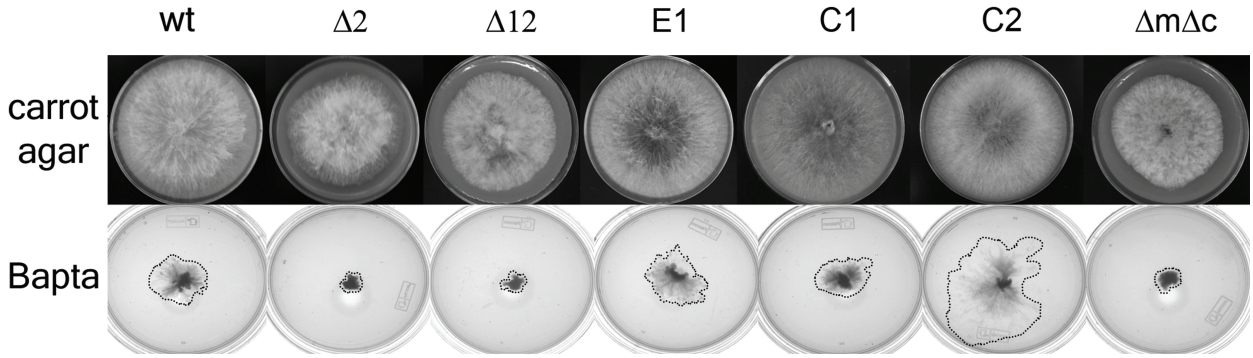

Figure 2. Growth of *G. zeae* strains on carrot agar and calcium-limited medium. **Top panel**: Growth (4 d) on CA. wt, E1, C1, and C2 fully colonized the medium; the remaining strains (Δ2, Δ12, ΔmΔc) did not. **Bottom panel:** Growth (14 d) on medium supplemented to 1 mM BAPTA; the extent of growth is outlined by black dotted lines.

on MMTS, indicating nit+ and calcium uptake deficiency phenotypes. PCR analysis of 12 isolates indicated that one strain lacked both *MID1* and *CCH1* coding sequences and was designated ΔmΔc The status of all strains was confirmed by Southern analysis (Fig. 1). The L (Left flank, see Methods) fragment of *Mid1* was expected to hybridize to a 5.4 kb band in PH-1 and a 3.9 kb fragment in the mutants. The probe hybridized to multiple unidentified fragments in E1 indicating that multiple ectopic insertions of the L5 containing replacement construct occurred (Fig1A). Complements C1 and C2 also displayed probe hybridization to the ~3.9 KB fragment and to a larger ~6.5 KB fragment, showing that *MID1* was deleted and complemented by an ectopic insertion of the wild-type *MID1* sequence. Unexpectedly, wild-type parent strain PH-1 and E1 showed hybridization to the ~3.9 KB fragment. To ensure that the unexpected hybridization was nonspecific rather than from contamination with a Δ*mid1* strain, an internal *hph* probe was used to hybridize to an identically prepared membrane (Fig. 1B). Hybridization to the expected ~3.9 KB and ~1.4 KB fragments if *MID1* was replaced occurred in all strains except PH-1 and E1. No hybridization of the *hph* probe occurred in PH-1, indicating that the unexpected hybridization of the L5 fragment was nonspecific. In strain E1, the *hph* probe hybridized to the ~3.9 KB and numerous other fragments of various sizes but not the ~1.4 KB

fragment also supporting the L5 probe results. Strains Δ2 and C2 also have multiple probe hybridizations to other fragments. The double mutant ΔmΔc has multiple other hybridized fragments because *CCH1* was also replaced using an *hph* construct.

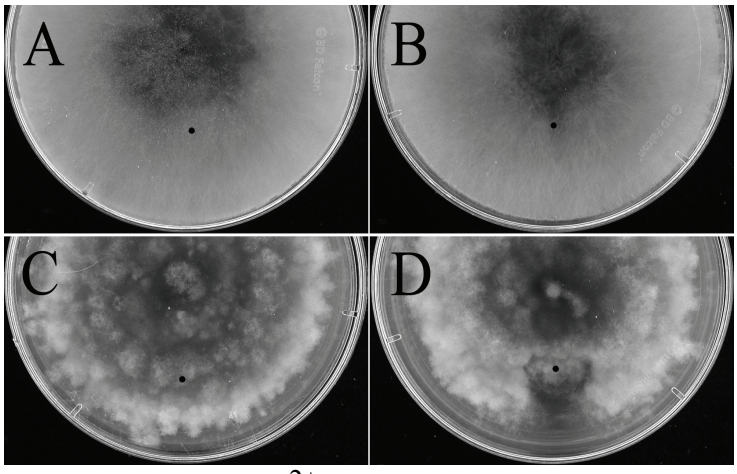

Figure 3. Effect of Ca^{2+} ionophore on *G. zeae* mycelial growth. (A) and (C) PH-1 and Δ2 controls, respectively. (B) and (D) PH-1 and Δ2 treated with A23187. The point of treatment is indicated by black dots and was made after 48 h initial growth. Images were taken 72 h after treatment.

Mutants lacking functional Mid1 grew at a slower rate than PH-1 (Fig. 2). No distinctive pattern of branching could be discerned that correlated with the fluffy phenotype. PH-1, E1, C1, and C2 grew in the presence of 1 mM chelating agent BAPTA for 4 days before growth was arrested, while mutants Δ2, Δ12, and ΔmΔc were unable to colonize (Fig. 2). Growth of PH-1 and Δ2 on V8 medium, spot amended with calcium ionophore A23187, or with ETOH (control) was examined. Both strains were unaffected on the control medium (Fig. 3A & C). PH-1 fully colonized the ionophore-amended medium and showed only a slight reduction of aerial hyphae at the point of ionophore application (Fig. 3B). Mutant Δ2 slowly colonized the ionophore amended medium and produce much less aerial hyphae than in the control (Fig. 3D). Addition of up to 1.2 M NaCl to Czapek-Dox agar showed similar growth reduction in both mutants and PH-1 (data not shown).

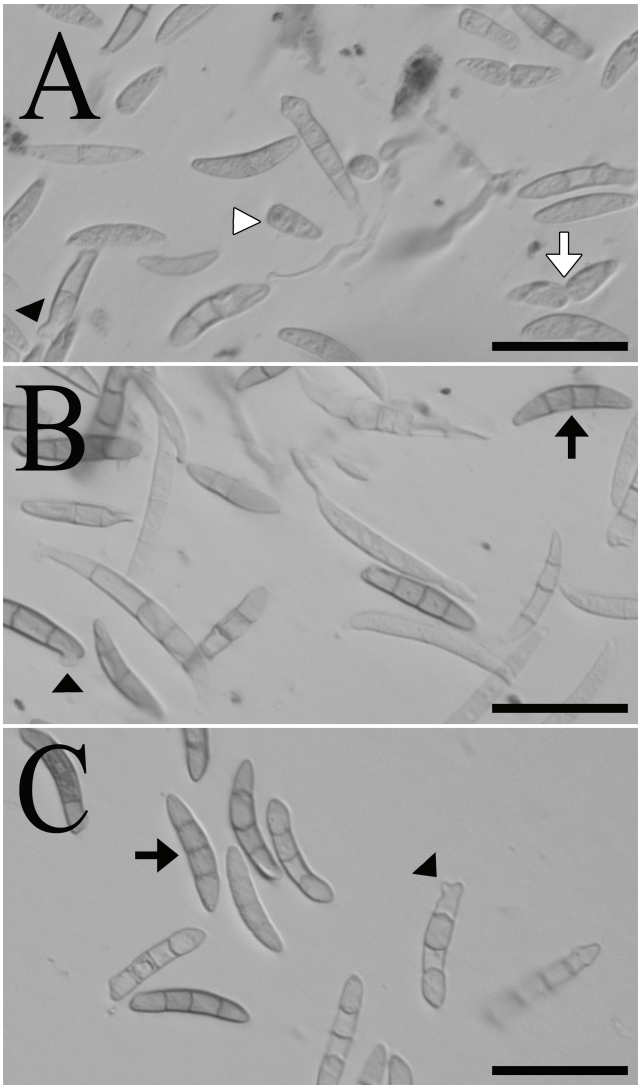

Figure 4. *G. zeae* ascospore morphology of mutant Δ2 (A), complemented strain C1 (B), and PH-1(C). White arrowhead indicate single cell fragments arising from two-celled abnormal ascospores. White arrow indicate two-celled abnormal ascospores with restricted septae that may fragment. Black arrowheads point to emerging germination tubes. Black arrows indicate wild-type four-celled ascospores. Bars = 20µm.

All strains produced morphologically normal mature perithecia. Examination of perithecial squash mounts by light microscopy at 24 h intervals from 4 to 6 d post induction showed that asci and spores of all strains appeared normal; however, perithecia reached maturity ~24 h later in the Δ*mid1* and Δ*mid1* Δ*cch1* mutants. The mutants also displayed abnormal ascospore development, producing predominately two-celled spores (Fig. 4A). Some mutant spores developed constrictions at the central septum and occasionally split in half after release from the ascus. PH-1, E1, C1, and C2 strains produced predominately normal four-celled ascospores (Fig. 4C & D). A qualitative examination of ascospore viability showed that spores from all strains germinated, but the hyphal density of the mutants was lower after two days of growth by germinating ascospores. Ascospore discharge was reduced in the mutants and partially restored by exogenous calcium added upon induction of the sexual stage (Fig. 5). Strains E1, C1,

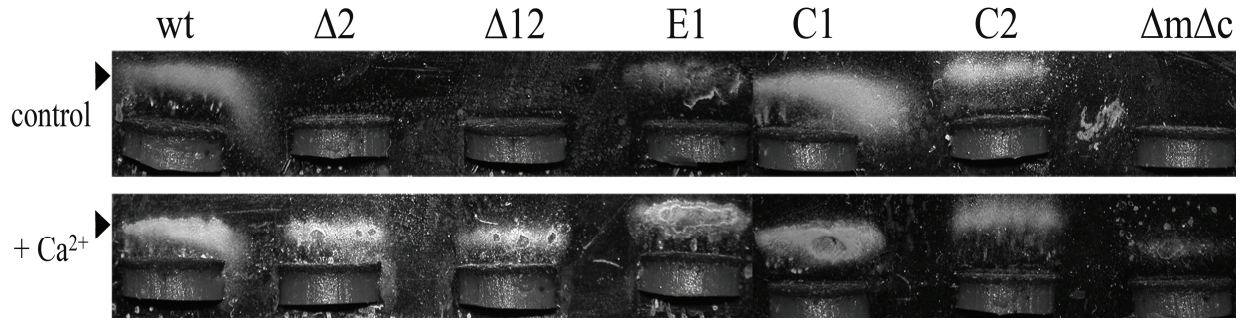

Figure 5. Effect of mutation and Ca^{2+} supplementation on *G. zeae* ascospore discharge. Agar plugs supporting mature perithecia (across the bottom of each panel) from each strain were oriented perpendicular to the glass slides so spores accumulated on slides (black arrowhead for each panel). Unamended medium (top) and medium amended with Ca^{2+} (bottom).

and C2 forcibly discharged ascospores as in PH-1. The Δ*mid1* and Δ*mid1* Δ*cch1* mutants failed to produce cirrhi and additional calcium did not provide a notable increase in cirrhus formation.

To better determine the effects of *MID1* deletion on growth and development, quantification of vegetative growth, ascospore discharge, and macroconidia production was performed on each strain (Fig. 6). On carrot agar, the Δ*mid1* mutants and the Δ*mid1* Δ*cch1* mutant showed large and significant reductions in vegetative growth rate when compared to PH-1 ($P < 0.001$) (Fig. 6A). The complement C1 also showed a smaller but significant reduction ($P < 0.05$). The growth rates of E1 and C2 strains did not differ significantly from PH-1. When grown on carrot agar + 80 mM Ca^{2+}, the growth rates of all mutants increased significantly from their growth rate on unamended carrot agar ($P < 0.05$) but were still significantly different at approximately 67% or less of PH-1 rates on unamended carrot agar ($P < 0.001$). The growth of PH-1, E1, C1, and C2 were not significantly different on carrot agar with or without calcium supplementation. The growth rates of all strains on carrot agar amended with 80 mM Mg^{2+} was not significantly different from growth rates on unamended carrot agar.On unmodified carrot agar, the mutants Δ2, Δ12, T14, and ΔmΔc showed significant reductions (12-, 14-, 10- and 19-

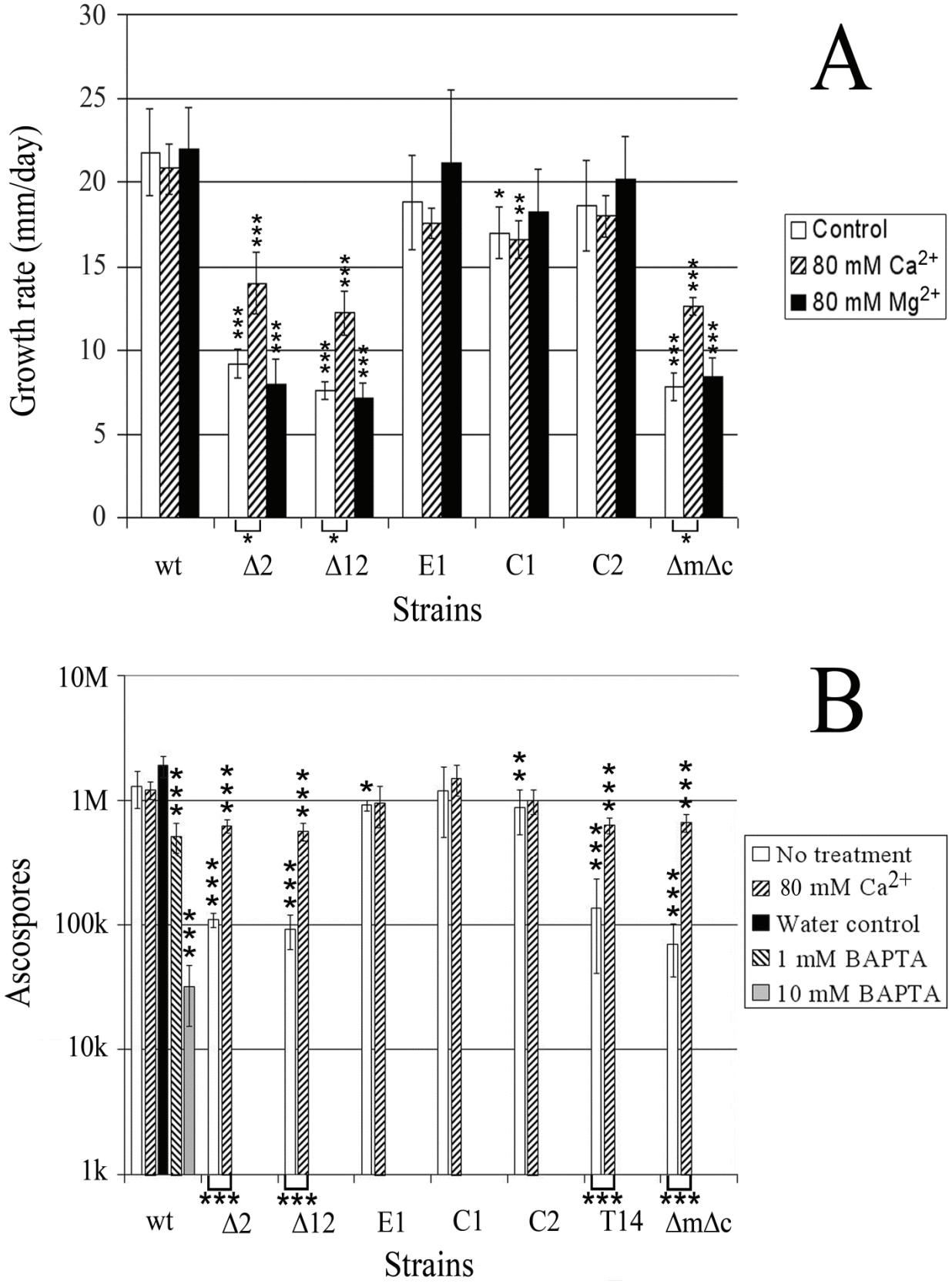
A
Growth rate (mm/day)
30
25
20
15
10
5
0
wt
Δ2
Δ12
E1
C1
C2
ΔmΔc
Strains
Control
80 mM Ca2+
80 mM Mg2+
B
Ascospores
10M
1M
100k
10k
1k
wt
Δ2
Δ12
E1
C1
C2
T14
ΔmΔc
Strains
No treatment
80 mM Ca2+
Water control
1 mM BAPTA
10 mM BAPTA

Figure 6

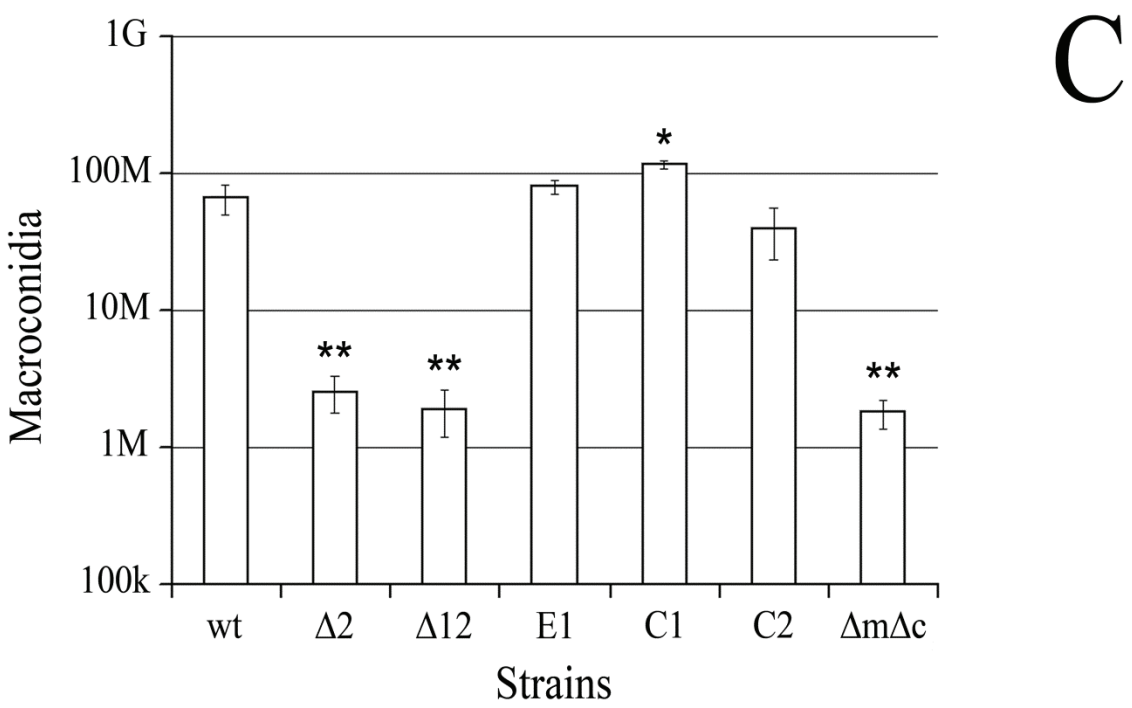

Figure 6 (cont'd)

Figure 6. Characterization of *G. zeae* growth and development. (A) Growth rates on carrot agar with and without Ca^{2+} or Mg^{2+} supplementation (change of diameter in mm/day). (B) Ascospore discharge. (C) Macroconidia production. Error bars represent the SD of the means of 5 (A), 10 (B), or 3 (C) biological replicates. Asterisks above open bars denote significant differences in the measurements of the indicated strains compared to PH-1 (wt). Asterisks below the bars denote significant differences in the measurements of the indicated strains between untreated and calcium supplemented treatments for that strain. * = $p < 0.05$ ** = $p < 0.01$ *** = $p < 0.001$. Strain genotypes are as listed in Fig. 1 except T14 (*MID1* Δ*cch1*).

fold, respectively) in ascospores discharged ($P < 0.001$; Fig. 6B). Complement C2 and ectopic E1 displayed smaller but significant reduction (~2-fold) in ascospore discharge ($P < 0.01$ and $P < 0.05$, respectively). E1 and C1 did not vary significantly from PH-1 levels. When supplemented with 80 mM $CaCl_2$, all mutants showed significant increases in ascospore discharge ($P < 0.001$). Additionally, wild-type on carrot agar treated with 1 mM or 10 mM BAPTA at the initiation of the discharge assay showed significant dose dependent reduction in ascospore release ($P < 0.001$) compared to wild-type on unmodified carrot agar, while the water control was not significantly different than untreated wild-type.

All mutants produced significantly fewer macroconidia compared to PH-1 ($P < 0.01$; Fig. 6C). Complement C1 produced significantly more macroconidia than wild-type ($P < 0.05$). Quantification of macroconidia production of the strains grown in CMC amended with 80 mM Ca^{2+} was unsuccessful. For all strains, the calcium supplemented culture stimulated secretion of a gelatinous substance that pelleted with the conidia, preventing an accurate tally.

To assess the impact of the loss of Mid1 on *G. zeae* pathogenicity, seven wheat plants were inoculated with macroconidia from each strain, and all were successfully infected. While infection by the mutants seemed slightly less vigorous than the other strains, no significant difference in the number of symptomatic kernels was found (data not shown).

Function of Mid1 in *Neurospora crassa*

The reciprocal crosses of *N. crassa* Δ*mid1* mutants produced normal perithecia and discharged ascospores. The discharged ascospores were compared to those from wild-type crosses and were found to be morphologically normal. Examination of perithecia squash mounts also revealed morphologically normal asci and ascospores arising from the Δ*mid1* crosses (data not shown).

***Gibberella* electrophysiology.**

PH-1, Δ2, and T14 strains were impaled successfully with double barrel micropipettes. A summary of electrical properties is shown in Figure 6 (examples of electrical traces in Fig. 6A, summary of potentials before and after cyanide treatment in fig. 6B, and current-voltage relations in Fig. 6C). When the micropipette was pressed against the cell, a small negative potential of –5 to –20 mV, presumably a Donnan potential for the wall, was occasionally observed. Upon

impalement into the cell, a stable negative-inside potential was obtained within about 1 min (Fig. 6A). The potentials of the three strains were similar: the wild-type was –149 ± 21 (n=14), the *mid1* mutant was –146 ± 19 mV (n=13) and the *cch1* mutant was –145 ± 18 mV (n=13). Electrophysiology experiments on asci were not possible due to size limitations.

To compare as directly as possible *in vivo* activity of the electrogenic H^+-ATPase in the three strains, ATP was depleted by treatment with the respiratory inhibitor cyanide, per experimental results in *N. crassa* (Slaymen et al., 1973) (Fig. 6B). The depolarized potentials — due to the Goldman-Hodgkin-Katz potential for permeant ions— were very similar: the wild-type was –47 ± 11 (n=14), the *mid1* mutant was –51 ± 12 mV (n=13) (P=0.402) and the *cch1* mutant was –56 ± 15 mV (n=13) (P=0.092). The ATP-dependent contribution to the potentials (potential after cyanide treatment *minus* the potential before cyanide treatment) was also very similar: the wild-type was 102 ± 19 (n=14), the *mid1* mutant was 95 ± 17 mV (n=13) (P=0.374) and the *cch1* mutant was 89 ± 14 mV (n=13) (P=0.057). Thus, both 'passive' (Nernstian) and active (H^+-ATPase) contributions are the same for the three strains.

After the potential achieved steady state, three current-voltage measurements were performed before and after cyanide treatment. Conductances were calculated from the slopes of the current *versus* voltage relations (which were linear, Fig. 7C). The conductance of the wild-type was significantly higher than that of either mutant: 32.3 ± 11.3 nS (n=14) compared to 17.8 ± 7.1 nS (n=13) for the *mid1* mutant (P=0.001), and 21.1 ± 10.0 nS (n=13) for the *cch1* mutant (P=0.008), but these differences can be attributed to the hyphal diameters of the measured cells. The wild-type had larger hyphae then either mutant: diameters of 8.0 ± 1.2 μm (n=14) compared to 5.4 ± 0.7 μm for the *mid1* mutant ($P<10^{-6}$) and 5.8 ± 0.8 μm for the *cch1* mutant ($P<10^{-4}$).

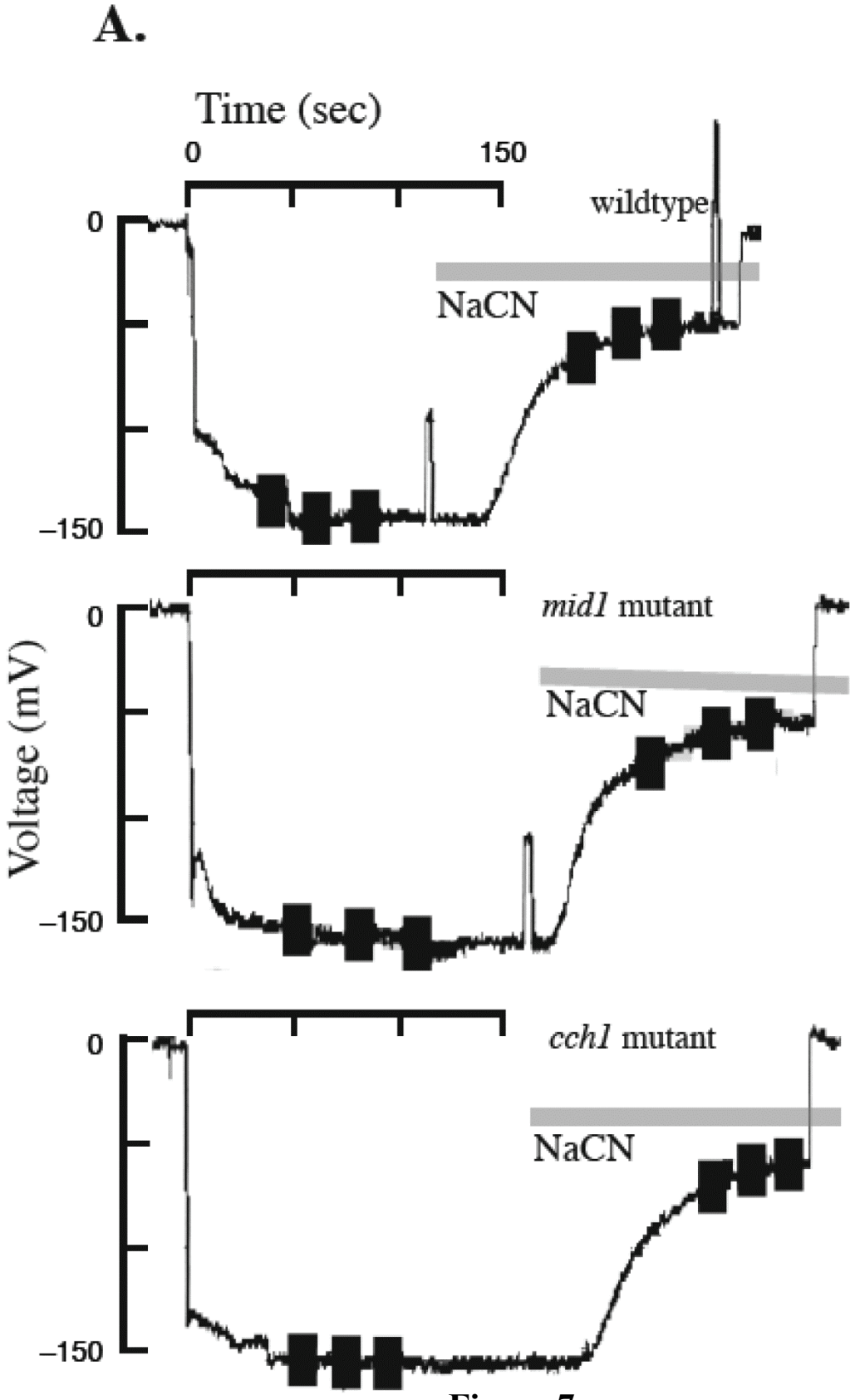
A.
Time (sec)
0
150
wildtype
0
NaCN
–150
mid1 mutant
0
NaCN
Voltage (mV)
–150
cch1 mutant
0
NaCN
–150

Figure 7

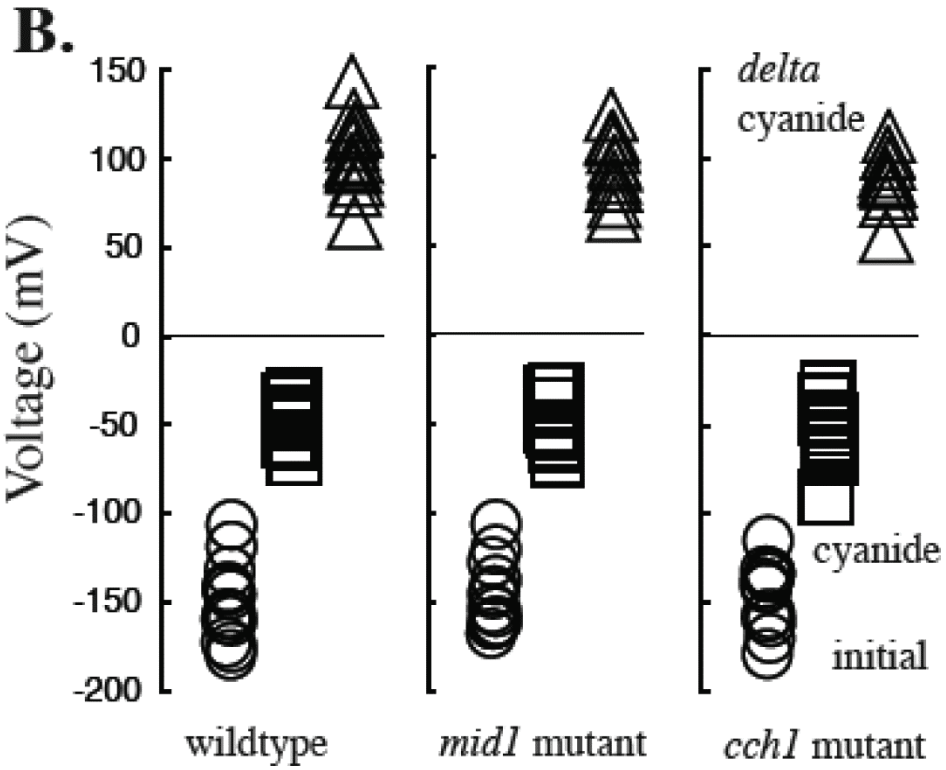

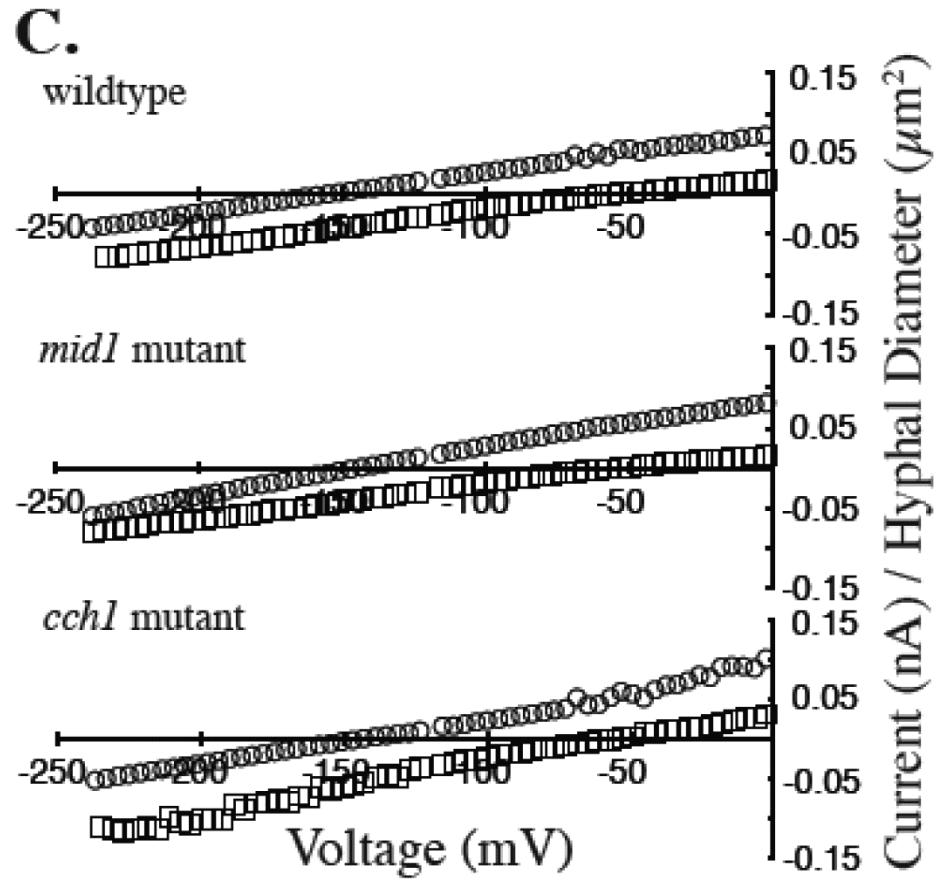

Figure 7 (cont'd)

Figure 7 (cont'd)

Figure 7. Electrical properties of the plasma membrane of hyphae from *G. zeae* strains PH-1, Δ2 (*mid1*), T14 (*cch1*). (A) Examples of electrical measurements for the three strains. After impalement, the potential stabilized within about 1 min. Then three current-voltage measurements were performed (vertical bars), followed by the addition of cyanide to deplete cellular ATP and inhibit the H^+-ATPase (horizontal bars, as marked). After the depolarized potential neared steady state, three more current voltage measurements were commenced, followed by removal of the micropipette from the cell. (B) Compiled measurements of initial E_m (circles), cyanide-induced depolarization (squares), and the difference (E_m after cyanide treatment *minus* E_m before cyanide treatment) (a measure of H^+-ATPase activity) (triangles). None of these measures are significantly different amongst the three strains. (C) Current-voltage relations for the three strains. These are the means (n=12) of the average current-voltage measurements (n=3) before (circles) and after (squares) cyanide treatment. These data have been normalized to the significantly different hyphal diameters of the three strains by dividing by the hyphal diameter (squared). The units (nA μm^{-2}) should not be interpreted as current density, which would require experimental measurements of the length constant of the hyphae (*cf* Lew, 2007).

Because input conductance (S) will be higher for larger hyphae if the specific conductance (S m^{-2}) is the same, the conductance were normalized to hyphal diameter by dividing by (hyphal diameter)^2 (the current-voltage relations in Fig. 7C have been so normalized).

After normalization, the wild-type conductance was 0.521 ± 0.225 nS μm^{-2} (n=13), the *mid1* mutant conductance was 0.609 ± 0.184 nS μm^{-2} (n=13) (P=0.294), and the *cch1* mutant conductance was 0.609 ± 0.316 nS μm^{-2} (n=12) (P=0.995). Thus, both potential and conductance were the same in wild-type and the two mutant strains. Changes in the conductance after cyanide treatment were small and not statistically different: wild-type, –0.051 ± 0.211 nS μm^{-2} (n=12); mid1, –0.179 ± 0.180 nS μm^{-2} (n=12) (P=0.125); *cch1*, 0.033 ± 0.481 nS μm^{-2} (n=12) (P=0.585).

Discussion

An obvious application for the stretch-activated channel Mid1 is membrane stretch during ascospore discharge, which stimulated our exploration of the Cch1/Mid1 complex in *G. zeae*. Here, we showed that Δ*mid1* mutants and the Δ*mid1* Δ*cch1* double mutant of *G. zeae* exhibited significantly reduced forcible ascospore discharge, slowed vegetative growth, reduced conidiation, and a high frequency of abnormal ascospores. These characteristics are similar to those of the Δ*cch1* mutant (Hallen and Trail 2008), but loss of Mid1 function resulted in more severe phenotypes than loss of Cch1 in *G. zeae.* Here we also show that neither the potential E_m nor the conductance g_m are affected in the Δ*mid1* and Δ*cch1*mutants indicating that, as transporters, the *mid1* and *cch1* gene products do not contribute measurably to the plasma membrane potential, nor are the downstream phenotypic effects (exemplified by poor growth) reflected by changes in plasma membrane ion transport. Furthermore, osmotic sensitivity experiments did not indicate any defect in osmotic response among the mutants. Supplementation of cultures of the Δ*mid1* and the Δ*mid1* Δ*cch1* mutants with exogenous Ca^{2+} partially rescued forcible discharge and vegetative growth, but did not rescue the abnormal development of ascospores. These results indicate that the defect in the *mid1* and *cch1* mutants is one of calcium signaling, supported by the ability to rescue the mutants with supplementary calcium. The sensitivity of the mutants to the ionophore A23187, which artificially elevates cytoplasmic calcium, suggests that there is also a lesion in calcium homeostasis. Assuming that the electrical properties are similar in asci and hyphae, we can conclude that the Cch1/Mid1 complex has a signaling role in ascospore discharge.

Should the *G. zeae MID1* and *CCH1* gene products contribute significantly to the overall electrical properties of the hyphal plasma membrane, either the potential or conductance would be affected in the mutants, which was not the case. The electrical potential reflects the contributions of permeant ions and active transport; this is commonly summarized by the equation $E_m = I_{pump}/g_m + E_G$, which states that the membrane potential is the sum of pump current divided by conductance (I_{pump}/g_m) and the Goldman-Hodgkin-Katz potential for permeant ions (E_G) (Spanswick, 2006). Conductance reflects the total voltage dependent ion transport across the plasma membrane. This is different from the situation in the *N. crassa*, for which the *mid1* mutant exhibits significantly lower H^+-ATPase activity as measured by cyanide-induced depolarization of the membrane. BLAST search reveals a very close match between the *N. crassa* plasma membrane H^+-ATPase (*pma-1*, NCU01680) and *G. zeae* (FGSG_01425) (identities 86% over 923 amino acids). Thus, despite the presence of *MID1*, *CCH1*, and *PMA1* in both organisms, the roles of Mid1 and Cch1 with respect to Pma1 are distinct in the hyphae.

As a respiratory inhibitor, the use of cyanide in *N. crassa* to deplete ATP is well-established (Slayman et al., 1973). Longer term (about 30 minutes), *N. crassa* becomes resistant to cyanide due to expression of an alternate oxidase (Lew and Levina, 2007); alternate oxidases are also found in *Fusarium* spp. (Alberghina and Benni, 1980). And, both fungi have cyanide-degrading enzymes (Basile et al., 2008). However, the cyanide-induced depolarizations in *G. zeae* and *N. crassa* are the same, so it is very likely that the rapid effect of cyanide-induced ATP-depletion leading to inhibition of the electrogenic H^+-ATPase occurs in *G. zeae*, similarly to *N. crassa*.

Previous studies have shown a role in higher fungi for stretch activated ion channels in thigmotropic responses to ridges on plant surfaces in the bean rust *Uromyces appendiculatus* (Zhou et al., 1992), responses to surface ridges and fungicide sensitivity in the human pathogen *Candida albicans* (Brand et al., 2009; Watts et al., 1998), pheromone responses in *S. cerevisiae* (Kanzaki et al., 1999), infection of plant tissues in *C. purpurea* (Bormann and Tudzenski, 2009) and vigorous mycelial growth of *N. crassa* (Lew et al., 2008). In *S. cerevisiae*, Cch1 and Mid1 were found to coimmunoprecipitate, yet respond to some stimuli differently, suggesting both cooperative and individual function (Locke et al., 2000; Courchesne and Ozturk, 2003; Tokes-Fuzesi et al., 2002). In *G. zeae,* the Δ*mid1* Δ*cch1* double mutant exhibited slightly more severe phenotypes than the Δ*mid1* mutant from which it was generated, supporting both dependent and independent roles for Mid1 and Cch1 in calcium entry. However, even in the absence of both calcium channels, the double mutant showed a partial rescue of the mutant phenotypes with calcium supplementation, suggesting the presence of one or more alternate calcium uptake routes.

The results from the quantification of vegetative growth, ascospore discharge, and macroconidia production demonstrate that complementation of Δ*mid1* mutants does not perfectly recapitulate the wild-type phenotypes, as complement strain C1 showed a significant reduction in growth rate and a significant increase in macroconidia production, and complement C2 showed a significant decrease in ascospore discharge. Since both complements show hybridization to a fragment of expected size for the replacement construct at the *MID1* locus and a second fragment larger than the fragment expected of the wild-type *MID1* locus (Fig. 1A), *MID1* is most likely being provided *in trans* and differences in distal *cis* regulatory elements at the integration site and the native *MID1* locus may explain the observed results. It is also possible that during the

integration event not all of the proximal *MID1* promoter integrated. Further investigation into the nature of these differences was not pursued.

In *Claviceps purpurea*, Δ*mid1* mutants were apathogenic (Bormann and Tudzynski, 2009) while pathogenicity of *Magneporthe grisea* Δ*mid1* and Δ*cch1* mutants were only slightly reduced (Nguyen et al., 2008). In *G. zeae* Δ*cch1* mutants (Hallen and Trail, 2008) and Δ*cch1* and Δ*cch1*Δ*mid1* mutants examined here showed a slightly slower progression of disease. However, reduction in conidium production and greatly reduced ascospore discharge characteristic of these mutants would likely result in reduced disease spread in these mutants in the field.

Despite the divergence of phenotypes among Δ*mid1* mutants of the fungi studied, the ability to complement using exogenous calcium appears to distinguish two phenotypes. Growth defects in *N. crassa* and *C. purpurea,* and the thigmotropism and sinusoid growth in *C. albicans* are unable to be chemically complemented. In contrast, *G. zeae* (except for ascospore shape), yeast and galvanotropism of *C. albicans* can be at least partially complemented. One possible explanation is a critical role for Mid1 in calcium transport in the former set, but not the latter. Interestingly, both *G. zeae* and *C. albicans* have phenotypes in both groups. In the case of ascospore shape in *G. zeae*, Mid1 may play a crucial role in transport during spore formation. Interestingly, Mid1 plays an important role in niche adaptation of *G. zeae* (ascospore discharge), *C. albicans* (sinusoidal growth for penetration of host tissues; Brand et al., 2009), *Cl. purpurea* (infection of hosts; Tudzynski, 2009), and yeast (mating; Iida et al., 1994). The diversity of roles this protein plays among fungi indicates its evolutionary malleability to support niche-specific activities.

Ascus function is unique in several respects: it is a one-way, single occurrence, destructive process, without a requirement to regenerate a functional ascus; it occurs after all of the nuclei are packaged within walled spores; and, it occurs rapidly (in *G. zeae,* one ascus fires every 45 sec under optimal conditions; Trail, unpublished observation). The ascus naturally stretches lengthwise when external pressure is applied. It seems likely that the natural conditions of humidity and wetness that trigger ascospore discharge would cause mature asci to swell, activating Mid1 and sending a signal for rapid firing of spores. The downstream targets of that signal are currently not known, and experiments designed to identify them are in progress. Localized vesicle fusion is thought to explain the calcium-regulated tip-reorientation of *C. albicans* (Gow, 2007). Vesicles are not prominent in the mature asci of *G. zeae* (unpublished observations) and the process appears to be more rapid than fusion would permit, so another mechanism must contribute to the rapid stretch of the asci leading to spore ejection.

Acknowledgments

The authors thank the Fungal Genetics Stock Center, which provided the Neurospora strains used in this study.

This work was supported by a grant from the National Science Foundation (0923794 to FT) and the Michigan Agricultural Experiment Station and was also funded in part by a Discovery Grant from the Natural Sciences and Engineering Research Council of Canada (RRL). In addition, the authors would like to acknowledge continued support by the USDA Wheat and Barley Scab Initiative.

CHAPTER 3

FIG1, A COMPONENT OF THE LOW AFFINITY CALCIUM UPTAKE SYSTEM, IS ESSENTIAL FOR PERITHECIUM DEVELOPMENT AND AFFECTS FILAMENTOUS GROWTH AND ASEXUAL DEVELOPMENT IN *FUSARIUM GRAMINEARUM*

Brad Cavinder and Frances Trail

I performed the work of this chapter in the Trail lab except for the following experiments. The Illumina genomic sequencing library for the insertional mutant was performed by Dr. Kristina Smith in Dr. Michael Freitag's lab at Oregon State University. For the wild-type *Fusarium graminearum* Illumina RNAseq, RNA extraction, sequencing library preparation, and the quality score filtering and trimming of the resultant reads were performed by Usha Sikhakolli in the Trail Lab.

ABSTRACT

The function of Fig1, a transmembrane protein of the low affinity calcium uptake system (LACS) in fungi, in the growth and development of the plant pathogen *Fusarium graminearum* was examined. The Δ*fig1* mutants failed to produce mature perithecia and sexual development was halted early in the formation of perithecium initials. Loss of Fig1 function also resulted in a reduced vegetative growth rate. Macroconidia production was reduced 70-fold in the Δ*fig1* mutants when compared to wild-type. Function of the high affinity calcium uptake system (HACS), comprised of Ca^{2+} channels Mid1 and Cch1, has also been explored in *F. graminearum.* To better understand the roles of LACS and HACS, Δ*fig1* Δ*mid1*, Δ*fig1* Δ*cch1*, and Δ*fig1* Δ*mid1* Δ*cch1* double and triple mutants were generated, and the phenotypes of these mutants were more severe than the Δ*fig1* mutants. Pathogenicity on wheat was unaffected for the Δ*fig1* mutants, but the Δ*fig1* Δ*mid1*, Δ*fig1* Δ*cch1*, and Δ*fig1* Δ*mid1* mutants, lacking both LACS and HACS function, were apathogenic. Supplementation with exogenous calcium did not rescue any of the mutant phenotypes. Additionally, Δ*fig1* mutants of *Neurospora crassa* were examined and did not affect the filamentous growth or female fertility in a Δ*fig1 mat A* strain, but the Δ*fig1 mat a* strain failed to produce fertile fruiting bodies. These results are the first report on Fig1 function in filamentous ascomycetes and expand its role to include complex fruiting body and ascus development.

Introduction

Calcium is a ubiquitous messenger in eukaryotic cells, acting both directly and indirectly to modulate protein activity, gene transcription, energy metabolism, endo- and exocytosis, and many other cellular processes (Berridge et al., 2003; Carafoli, 2005; Michalak et al., 2002). In fungi, two major calcium uptake pathways have been identified and characterized: the high affinity calcium uptake system (HACS), active during low calcium availability; and the low affinity calcium uptake system (LACS), active when calcium availability is high; (Erdman et al., 1998; Fischer et al., 1997; Iida et al., 1994; Martin et al., 2007; Paidhungat and Garrett, 1997). A third calcium uptake pathway was recently described in *S. cerevisiae,* but has yet to have its genetic components identified (Groppi et al., 2011). In the filamentous fungus, *Fusarium graminearum* (sexual stage *Gibberella zeae*), causal agent of head blight of wheat and barley, calcium signaling has been shown to have a role in hyphal growth, sporulation, and fruiting body function, and regulation of components of the HACS system have been shown to be involved in these processes (Cavinder et al., 2011; Hallen and Trail, 2008; Trail et al., 2002; Trail et al., 2005).

HACS is minimally composed of the voltage-gated Ca^{2+} channel (VGCC) Cch1 (Fischer et al., 1997; Paidhungat and Garrett, 1997), the stretch activated calcium channel/regulatory protein Mid1 (Iida et al., 1994), and the PMP22_Claudin superfamily member regulatory protein Ecm7 (Martin et al., 2007). In yeasts, HACS responds to environmental and endoplasmic reticulum stress and to exposure to mating pheromone (Courchesne et al. 2010; Brand et al., 2007; Brand et al., 2009; Hong et al. 2010; Iida et al., 1994; Locke et al., 2000; Peiter et al., 2005; Viladevall et al., 2004). In filamentous fungi, HACS mutants show both shared and variable phenotypes across species, including reduced vegetative growth and calcium

homeostasis lesions on the one hand, and effects on pathogenicity and sexual development, respectively (Bormann and Tudzynski, 2009; Cavinder et al., 2011; Hallen and Trail, 2008; Lew et al., 2008).

LACS is minimally composed of the Fig1 membrane protein, a PMP22_Claudin superfamily member like Ecm7, and is involved in calcium influx and membrane fusion during mating of *S. cerevisiae* and *Candida albicans* (Muller et al. 2003; Yang et al., 2011), mating projection development and cell wall degradation at the fusion site of appressed shmoos in *S. cerevisiae* (Erdman et al., 1998), and thigmotropism and repression of hyphal growth in *C. albicans* (Brand et al., 2007). Mammalian PMP22_Claudin superfamily members are involved in membrane-membrane interactions such as epithelial tight junction formation and signal transduction such as ion flux (Matter and Balda, 2003; Tsukita et al., 1999). The fungal members show little overall sequence identity with the mammalian orthologs, but most have similar secondary structure and topology including cytoplasmic N- and C- termini, four transmembrane domains, two extracellular and one intracellular loops, and a conserved GΦΦGXC(n)C motif (Φ = F, L, M, or Y hydrophobic residues, n = 8 > n > 20 amino acids) in the first extracellular loop (Brand et al., 2007; Erdman et al., 1998; Zhang et al., 2006).

In *F. graminearum*, deletion of *CCH1*, *MID1*, or both resulted in almost identical phenotypes, including reduced vegetative growth rate, conidiation, ascospore development and forcible ascospore discharge from asci. Chemical complementation with exogenous calcium rescued all phenotypes, at least partially, except the abnormal ascospore development seen in strains lacking Mid1, including the Δ*cch1* Δ*mid1* double mutant (Cavinder et al., 2011; Hallen and Trail, 2008). Because addition of calcium rescued the phenotypes even in the Δ*cch1* Δ*mid1* double mutant, and because LACS is involved in calcium importation, is active in environments

of high calcium availability, and is involved in sexual development of yeasts, we investigated the role of Fig1 in the growth and development of *F. graminearum.* We asked whether Fig1 is involved in the uptake of calcium essential for chemical complementation of the HACS mutant phenotype. We identified the putative *F. graminearum FIG1* ortholog, and generated Δ*fig1*, Δ*cch1* Δ*fig1*, Δ*fig1* Δ*mid1*, and Δ*cch1* Δ*fig1* Δ*mid1* strains to characterize *FIG1* function and interaction with HACS components. Additionally, we investigated the effect of Fig1 loss on growth, calcium homeostasis, and sexual development in *Neurospora crassa,* which has been shown to have different roles for HACS components than *F. graminearum* (Cavinder et al., 2011; Lew et al., 2008).

Materials and Methods

Strains, culture conditions

Strains used in this study are described in Table 1. Strains of *F. graminearum* were maintained on sterile soil at -20°C, as macroconidia (10^6-10^8 conidia/ml), and as colonized pieces of V8 agar in sterile 35% glycerol at -80°C. Macroconidia were produced in carboxymethylcellulose (CMC) liquid medium as previously described (Cappellini and Peterson, 1965) or on Bilay's agar medium (Booth, 1971). Sexual development was induced in culture on carrot agar by gentle removal of surface mycelia followed by treatment with 1 ml of 2.5% (w/v) Tween 60 solution as previously detailed (Bowden and Leslie, 1999; Trail and Common, 2000). Although *F. graminearum* is homothallic, it can outcross, a process accomplished by inoculating carrot agar with two different strains side by side. Recombinant perithecia are found along the centerline where the colonies meet.

N. crassa is heterothallic, with two mating type idiomorphs, a and A (Glass et al. 1988; Metzenberg and Glass, 1990). *N. crassa* wild-type and Δ*fig1 mat a* (Colot et al., 2006) strains were obtained from the Fungal Genetics Stock Center (FGSC) and were maintained on synthetic crossing medium (SC; Davis and de Serres, 1970) slants at -20°C. Sexual crosses were performed as previously described except cultures on SC were incubated for 7 d in ambient light instead of continuous fluorescent lighting (Cavinder et al. 2011).

Analysis of sexual crosses

All *F. graminearum* crosses were performed between *NIT3* nitrate-utilizing (nit^+) and *nit3* non-nitrate-utilizing mutant (nit^-) strains. Cirrhi (spores oozing from perithecia) from single perithecia were collected individually, the spores were suspended in water and distributed across the surface of MMTS medium as previously described (Bowden and Leslie, 1999; Cavinder et al., 2011). Recombinant perithecia can be easily identified by the presence of approximately equal numbers of nit^+ and nit^- progeny, which have different growth phenotypes on this medium. For strains that did not form cirrhi (*cch1* and *mid1* mutants), 10 perithecia at the interface between strains were collected, crushed in bulk on a glass slide in sterile diH2O to release ascospores, rinsed off the glass slides, and a portion of the suspension was spread onto the surface of MMTS agar. After 5-7 days of growth at RT, nit^+ and nit^- colonies from recombinant perithecia or bulk mixtures were individually collected. To confirm the nit phenotype, cultures were subsequently transferred to Czapek-Dox agar (Thom and Church, 1926) and Czapek-Dox agar supplemented to 470 mM potassium chlorate and 0.17% L-arginine (Wu and Linz, 1993). PCR was used to confirm the presence or absence of *CCH1, FIG1,* and *MID1*.

TABLE 3. Strains used in this study

Strain	Genotype	Abbreviation	Source
Fusarium graminearum			
PH-1(FGSC 9075)	wild-type (NRRL 31084)	wt	Trail and Common, 2000
PH-1 55	*nit3*	–	Cavinder et al., 2011
Δfig1-1	Δ*fig1*	Δf1	This Study
Δfig1-2	Δ*fig1*	Δf2	This Study
Δ*cch 1*–T11	Δ*cch 1*	–	Hallen and Trail, 2008
mn-11	Δ*mid1 nit3*	–	Cavinder et al., 2011
cn-5	Δ*cch1 nit3*	–	This Study
cn-7	Δ*cch1 nit3*	–	This Study
cmn-1	Δ*cch1* Δ*mid1 nit3*	–	This Study
cmn-9	Δ*cch1* Δ*mid1 nit3*	–	This Study
fm-1	Δ*fig1* Δ*mid1*	–	This Study
fm-5	Δ*fig1* Δ*mid1*	ΔfΔm	This Study
fc-1	Δ*fig1* Δ*cch1*	–	This Study
fc-6	Δ*fig1* Δ*cch1*	ΔfΔc	This Study
fcm-2	Δ*mid1* Δ*cch1* Δ*fig1*	ΔfΔcΔm	This Study
f12-C1	Δ*fig1* ::*FIG1*	Δf12-C1	This Study
f12-C2	Δ*fig1* ::*FIG1*	Δf12-C2	This Study
Neurospora crassa			
FGSC 2489	wild-type, *mat A*		Colot et al., 2006[a]
FGSC 4200	wild-type, *mat a*		Colot et al., 2006[a]
FGSC 17273	Δ*fig1 mat a*		Colot et al., 2006[a]
fig1A-18	Δ*fig1 mat A*		This Study
fig1A-20	Δ*fig1 mat A*		This Study
fig1A-21	Δ*fig1 mat A*		This Study

[a] Directly received from the Fungal Genetics Stock Center

To generate *N. crassa* Δ*fig1 mat A* mutants, a Δ*fig1 mat a* mutant strain (FGSG 17273) was crossed with wild-type *mat A* (FGSG 4200). To recover progeny, ascospores were then washed off the lids, subjected to heat shock to promote germination, and placed on SC amended to 1% sorbose and 0.05% glucose and fructose with sucrose omitted for germination as previously described (Shear and Dodge, 1927; Strickland and Perkins, 1973; Perkins, 2006).

Single spore isolates were transferred to SC, and PCR was used to confirm the presence or absence of *fig1* and *mat A-2* (present in *mat A* and absent in *mat a*).

Nucleic acids manipulation and genetic transformation

DNA was extracted from *F. graminearum* and *N. crassa* mycelium using a hexadecyltrimethylammonium bromide (CTAB) method as previously described (Cavinder et al., 2011). *F. graminearum* and *N. crassa* nucleotide data were obtained from the MIPS Fusarium graminearum Genome Database (http://mips.helmholtz-muenchen.de/genre/proj/FGDB/; version 3.2) and the MIPS Neurospora crassa Genome Database (http://mips.helmholtz-muenchen.de/genre/proj/ncrassa/; accessed: June, 2011), respectively. Primers used in this study are listed in Table 2. Phusion High-Fidelity DNA Polymerase (New England Biolabs, Ipswich, MA) was used for PCR unless otherwise noted. For targeted gene replacement constructs, a split marker protocol (Catlett et al., 2003; Fairhead et al., 1996; Fairhead et al., 1998) was performed as previously described (Cavinder et al., 2011) with modifications to target *FIG1* with the hygromycin resistance (*hph*) marker from pCB1004 (Carroll et al., 1994), as described below.

The split marker technique involves amplification of 500-750 bp fragments immediately upstream (L) and downstream (R) of the coding sequence of the target gene with 3' and 5' tails complementary to the 5' and 3' ends of the *hph* marker, respectively, allowing the fusion of the L and R flanks to overlapping partial *hph* amplicons by PCR. A successful gene replacement will result from a crossover between the *hph* fragments of the two merged products, and the replacement of the *FIG1* gene with the crossover fragment. In the case of *FIG1*, the annotated stop codon is 36 bp upstream from a contig gap, so we used 473 bp of coding sequence upstream

TABLE 4. Primers used in this study	
Name	Sequence (5'-3')
For replacement of the *F . graminearum FIG1* locus	
Fig1-L5	CGACCTGACTTGACTGACTGACTG
Fig1-L3-Hyg	GTAGCAACCAGGCGTGGTAGATGTGGTCGACTTTGTTCTCC
Fig1-R5-Hyg	CTTTTACTTTCACCAGCGTTGGCTAACCAGATCTCTCAGGTTTTGTACC
Fig1-R3	ACATGAGATAGGGGAACACAATCATGTCC
Fig1-HygF	GACCACATCTACCACGCCTGGTTGCTACGCCTGAATAAGTG
Fig1-HygR	GAGATCTGGTTAGCCAACGCTGGTGAAAGTAAAAGATGCTGAAGATC
3’ 1/2 HygF	AGTACTTCTACACAGCCATCGGTCCAGACG
5’ 1/2 HygR	CTGCTGCTTGGTGCACGATAACTTGGTGC
For complementation of *F. graminearum* Δ*fig1* mutants	
Fig1-compF	TAGAAGAGCGCTACGTAAGATCGTAGATC
Fig1-compR	CGTTATTCATGAACCAGTACACGGAGATG
For probe generation	
Cch1 probeF	CTCAATCTCCTGCGAAGTGGAATGAG
Cch1 probeR	GCAGACAAGGGACTAATAATCGCCAAC
Mid1 probeF	ACATCGCCTCACTTTGTGATCTACAGTG
Mid1 probeR	GCTTAGTACGGCTTCGATCTAGCG
For confirmation of *N. crassa fig1* and *mat A* locus presence or absence	
Nc Fig1-F	GTTGGTTTCTTCGGCATCTGCGTTAATC
Nc Fig1-R	CGATGATCAACAGCGTGAAGCTGAAC
Nc MAT-A2 F	TGCTATGCTCAACGAGAACGAAGTATCG
Nc MAT-A2 R	ACTTCTGAGGACCGACTCGGTAACTG

of the contig gap to generate the R fragment. Therefore, the final construct results in a partial gene replacement rather than full gene replacement with 475 nucleotides of reference gene sequence remaining in the genome of the replacement strains. For generation of the Δ*fig1* single mutants, the L-*hph* fragment (593 bp, supercontig_3.3: 4947747-4947176) was amplified by primers Fig1-L5 & Fig1-L3-Hyg while primers Fig1-R5-Hyg and Fig1-R3 generated a 474 bp R-*hph* fragment (supercontig_3.3: 4947302-4947775). Primers Fig1-L3-Hyg and Fig1-R5-Hyg have 5' tails of 15 and 20 bases complementary to the 5' and 3' ends of the *hph* marker from pCB1004 (Carroll et al., 1994), respectively, allowing for selection of transformants with hygromycin B (HygB). For split *hph*, Fig1-HygF and Fig1-HygR contain 5' tails of 13 and 15 bases complementary to the 3' and 5' ends of the FIG1 L- and R-*hph* fragments' *FIG1* sequences and were paired with primers 5' 1/2 HygR and 3' 1/2 HygF to generate the 5'- and 3' *hph* fragments, respectively. Using PCR, the 5' *hph* and L-*hph,* and the 3' *hph* and R-*hph* fragments were merged together. Both merged products were transformed into wild-type *F. graminearum* protoplasts.

For complementation of the Δ*fig1* mutants, a 1599 bp fragment of the *FIG1* locus (FGSG_06302; supercontig_3.3: 4946177-4947775), spanning 1,000 bp upstream of the first (supercontig_3.3: 4947177) and to 2 bp upstream of the last (supercontig_3.3: 4947777) *FIG1* coding nucleotides, was generated by PCR using primers Fig-compF and Fig1-compR. The amplicon was used to transform Δ*fig1* protoplasts.

Polyethylene glycol mediated transformation of protoplasts of *F. graminearum* was performed and Hyg+ strains were selected as previously described (Gaffoor et al., 2005). For complementation of Δ*fig1* mutants, protoplasts were regenerated on regeneration medium and then divided into three groups and overlaid regeneration medium containing 0.57 mM, 1.4 mM,

or 3.1 mM of calcium ionophore A23187. Colonies growing to the surface of the overlays were transferred to V8 agar containing 450 µg/ml HygB or unammended V8 agar as appropriate. Transformants thriving on selective medium were then transferred to V8 agar for maintenance, storage, and subsequent phenotype analysis.

RNA was extracted from lyophilized *F. graminearum* mycelia using the TRIzol reagent (Life Technologies, Carlsbad, California) as per the manufacturer's protocol with two phenol (pH 6.6):chloroform:isoamyl alcohol (25:24:1) followed by two chloroform extraction steps after the initial TRIzol:chloroform phase separation. Sample aliquots of 120 µg were purified using the RNeasy Mini Kit (Qiagen, Germantown, MD), following the manufacturer's RNA cleanup instructions and eluting with nuclease free H_2O (Promega). All RNA was stored at -80°C.

One µg RNA was used as template for cDNA synthesis reactions. The SMARTer RACE cDNA Amplification Kit (Clontech, Mountain View, CA) was used for cDNA synthesis for subsequent 5'- and 3'-rapid amplification of cDNA ends (RACE) reactions per the manufacturers' instructions. Along with the kit included universal primer, primers Fig1 RACE R1 and Fig1 RACE F1 for the 5'- and 3' RACE reactions, respectively, and Phusion High-Fidelity DNA polymerase (New England Biolabs) were used in the RACE reactions. Amplified fragments were then cloned into pCR2.1-TOPO using the TOPO TA Cloning kit (Life Technologies) and sequenced at Michigan State University's Research Technology Support Facility using an ABI PRISM 3730 Genetic Analyzer (Life Technologies).

Characterization of Δ*fig1* phenotypes

To characterize vegetative growth and sexual development of Δ*fig1* in *F. graminearum*, individual strains were grown on carrot agar amended with 80 mM $CaCl_2$, 80 mM $MgCl_2$ or

unamended, and incubated at RT under continuous light. Radial growth was measured at 24 h intervals for 3 d with four biological replicates for each strain. The first day's growth was discounted. The growth rate was calculated by subtracting colony diameter at 24 h from the diameter at 48 h and was averaged between the replicates. Significance between the growth of Δ*fig1* strains compared to PH-1 and among the treatments was assessed. Bilay's medium (Booth, 1971) was supplemented to 1 mM with the extracellular calcium chelator 1,2-bis(2-aminophenoxy)ethane-*N,N,N,N,*-tetraacetic acid tetrapotassium salt (BAPTA) to determine the ability of Δ*fig1* mutants to grow in limited calcium conditions, as previously described for Δ*cch1* mutants (Cavinder et al., 2008). To determine the effect of increased intracellular calcium levels, strains were center inoculated on V8 agar, and after 48 h growth, a point treatment of 10 µl of either a 9.5 mM solution of calcium ionophore A23187 (in ETOH) or 100% ETOH (control) was applied to a point slightly ahead of the leading edge of mycelial growth.

To quantify conidiation in *F. graminearum* mutants, strains were grown shaking in 100 ml CMC for 4 d at room temperature (RT). Macroconidia were harvested by filtration through sterilized Miracloth (Calbiochem). The macroconidia were pelleted by centrifugation, resuspended in 1 ml of sterile diH_2O, and quantified.

PCR identified Δ*fig1 mat A* progeny of *N. crassa* were reciprocally crossed to wt *mat a*, wt *mat A,* and Δ*fig1 mat A* strains both to test the mating type determination and to assess the effect of the loss of *fig1* on sexual development. Squash mounts of perithecia from the crosses were examined microscopically to observe ascus and ascospore development. Culture dish lids of the crosses were monitored for discharged ascospores.

Statistical Analysis

To assess the significance of intragroup variation and intergroup interaction and to return associated p-values for all pairwise comparisons, analysis of variance (ANOVA) and Tukey's HSD were performed using the R language and environment for Windows (R Development Core Team, 2010).

Illumina sequencing and bioinformatics

Genomic DNA from an insertional mutant generated from wild-type strain PH-1 was sequenced using Illumina GAII (San Diego, CA) with 76 bp paired-end reads and a 400 bp average library insert size. The 3'-ends of the reads were trimmed with a Biopython script (Cock et al., 2009) script and a Phred scale quality cutoff score of 28. The reads were assembled using the Velvet assembler, using k-mer values of 37-49 nucleotides (version 1.1.03; Zerbino and Birney, 2008; Zerbino et al., 2009). No reads were manually discarded because of length, but reads shorter than the k-mer size used in an assembly are automatically ignored by Velvet. The *FIG1* locus was located in the assembly using standalone BLAST+ (Camacho et al., 2009). Using wild-type RNA collected from perithecia at 96 hr after sexual development induction, a sequencing library was constructed and sequenced using Illumina GA II 36 bp single end reads and a 400 bp average cDNA library insert size (to be published separately)

Burrows-Wheeler Aligner (BWA, version 0.5.9; Li and Durbin, 2009) was used to align the RNAseq reads to either the genomic *FIG1* sequence from the Velvet assembly or to the same sequence with introns removed. The 5'- and 3'-RACE clone sequences were aligned manually. Multiple alignment of the putative full length *F. graminearum* Fig1 protein to Fig1 sequences from multiple fungi was performed with T-Coffee (Di Tommaso et al., 2011). The multiple

sequence alignment was viewed and edited in with Jalview (Waterhouse et al., 2009) and Seaview (Gouy et al., 2010). The putative full length *F. graminearum* Fig1 protein sequence was used search the Conserved Domains Database (Marchler-Bauer et al., 2011).

Microscopy and Imaging

For microscopic examination, samples were fixed in 2X phosphate-buffered saline (PBS) containing 4% (w/v) paraformaldehyde for 20 min on ice, washed twice with 2X PBS, and stained with 0.06% (w/v) toluidine blue in sterile H_2O overnight. Stained samples were washed twice each in 50%, 75%, and 100% ethanol in sterile water before being stored in sterile H_2O.

A Zeiss Standard microscope was used to observe samples and images were captured with a Zeiss AxioCam MRc color camera using AxioVision 4.8.2 (Göttingen, Germany). Non-microscopic images were captured with a Nikon Coolpix 995 (Tokyo, Japan). Image processing, manipulation, and annotation were performed with ImageJ (Abramoff et al., 2004) or Adobe Photoshop CS2 (San Jose, CA).

Results

Identification of *Fig1* through RACE and Illumina sequencing

The reference sequence of *F. graminearum* contains a contig gap in the region of *FIG1* (*Fusarium* Comparative Sequencing Project, Broad Institute of Harvard and MIT; http://www.broadinstitute.org/annotation/genome/fusarium_graminearum/MultiHome.html; assembly 3; contigs 204-205). Due to the gap, the FIG1 annotation (at both the MIPS Fusarium graminearum Genome Database and the Broad Institute Fusarium Comparative Database) contains two introns and three exons (Fig. 1A) ending 36 bp upstream of the contig gap and

predicting a protein of 156 amino acids that is more than 100 aa shorter than most filamentous ascomycete homologs. To recover the missing sequence, 5'- and 3'-RACE were performed, and two clones from each preparation were sequenced, revealing the presence of a third intron and fourth exon (Fig. 1B). Subsequently, we performed Illumina sequencing on genomic DNA from a strain derived from wild-type (to be published separately). In addition, Illumina RNAseq was performed on developmental stages of wild-type (to be published separately). *FIG1 g*enomic sequence was identified from the Velvet assembly of the genomic DNA by BLAST. Sequence spanning the annotated end of the previous gene upstream to the start of the next gene downstream of *FIG1* was used for alignment. The RACE sequences and RNAseq reads were aligned to the Velvet *FIG1* sequence and both sets of data aligned well to the exons, but not the introns (Fig. 1B). The introns were removed from the Velvet *FIG1* genomic sequence and the RNAseq reads were aligned to the putative spliced transcript, resulting in read coverage across the splice junctions instead of the loss of coverage seen with introns included (Fig. 1C).

To assess whether the new longer *F. graminearum FIG1* sequence from the Velvet assembly represents the full length of the gene, the translated protein sequence was aligned to 20 Fig1 homologs from ascomycetes. The Claudin motif found in all Fig1 homologs was present in the new longer sequence, the longer protein aligned well across the full length of the protein especially to other filamentous species (data not shown), a search of the Conserved Domains Database (Marchler-Bauer et al., 2011) found a full length Fig1 domain (data not shown), indicating that longer sequence includes the complete *F. graminearum FIG1* ortholog.

Generation and characterization of *FIG1* mutants in *F. graminearum*.

Mutants of *FIG1* in *F. graminearum* were generated by replacing the first 125 bp of the

coding sequence with *hph* as described in the Methods. From a single transformation experiment, 10 transformants resistant to hygromycin were obtained. PCR amplicons of three transformants were consistent with replacement of the targeted *FIG1* sequence with *hph* and the remaining 7 transformants were not tested (not shown). Two of these three transformants, designated Δfig1-1 and Δfig1-2, were used in subsequent experiments. To generate Δ*cch1 nit3* and Δ*cch1* Δ*mid1 nit3* strains, crosses were initiated between Δ*cch1*-T11 (Δ*cch1*) and mn-11 (Δ*mid1 nit3*). PCR screening of 12 progeny growing slowly and sparsely on MMTS (indicative of nit-) revealed two strains, cn-5 and cn-7, that produced amplicons expected from a Δ*cch1* genotype and two strains, cmn-1 and cmn-9, that produced amplicons expected from a Δ*cch1* Δ*mid1* genotype. Crosses between Δ*fig1* 1 x mn-11, Δ*fig1* 1 x cn-7 (Δ*cch1 nit3*) and Δ*fig1* 1 x cmn-1 (Δ*cch1* Δ*mid1 nit3*) were performed to isolate Δ*fig1* Δ*mid1*, Δ*cch1* Δ*fig1*, and Δ*cch1* Δ*fig1* Δ*mid1* strains, respectively. Six progeny displaying slow and dense growth on MMTS (indicative of nit+) were recovered from each of the three crosses. Screening by PCR confirmed the presence of the appropriate amplicons for two Δ*fig1* Δ*mid1* strains (fm-1 and fm-5), two Δ*cch1* Δ*fig1* strains (fc-1 and fc-6), and one Δ*cch1* Δ*fig1* Δ*mid1* strain.

To examine the effects of *FIG1* deletion on vegetative growth, calcium uptake, and calcium homeostasis, all strains were grown on media with or without the addition of calcium, magnesium, calcium chelator BAPTA, and calcium ionophore A23187 (which raises the cytosolic concentration of calcium). Differences in mycelial growth were tested under several conditions. Growth on unamended carrot agar revealed that all LACS and HACS mutants grew at a slower rate than wild-type (Fig. 2A). Growth on Bilay's medium containing 1 mM BAPTA, was used to test growth in calcium restrictive medium. Strains lacking Mid1 or Cch1 grew slightly for one day and failed to colonize further, but Δ*fig1* mutants fully colonized the medium

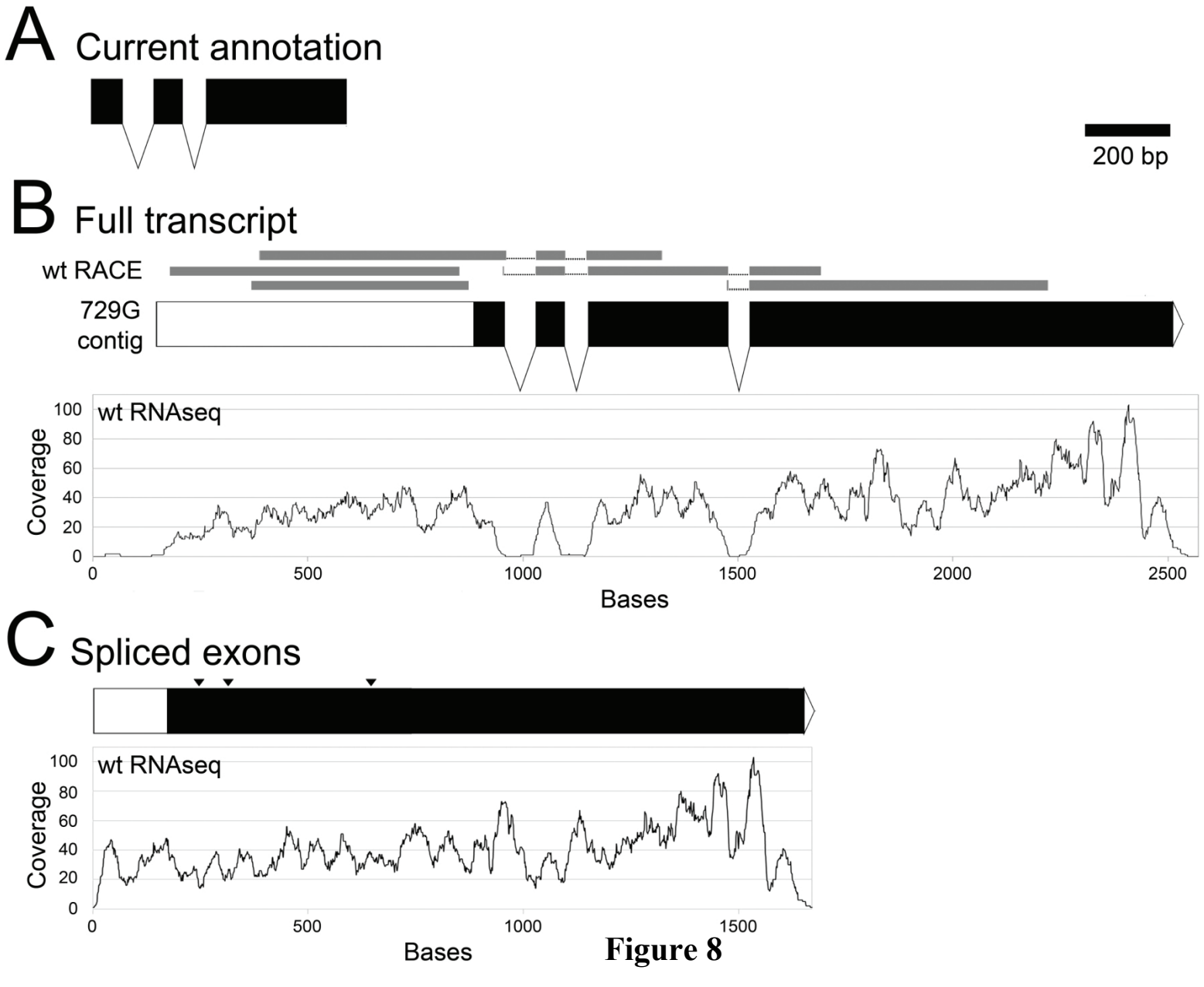
A Current annotation
200 bp
B Full transcript
wt RACE
729G
contig
wt RNAseq
Coverage
100
80
60
40
20
0
0
500
1000
1500
2000
2500
Bases
C Spliced exons
wt RNAseq
Coverage
100
80
60
40
20
0
0
500
1000
1500
Bases

Figure 8

Figure 8 (cont'd)

Figure 8. *F. graminearum FIG1* gene models. (A) Current gene model from MIPS. (B) Predicted gene model from a Velvet assembly of insertion mutant 729g-112 . Gray bars above the model are aligned 5'- and 3'-RACE clone sequences. The graph below the model shows the coverage of aligned wt RNAseq reads. (C) Predicted spliced transcript from wt RACE and RNAseq alignments in B. The black arrowheads above the model are the locations of the intron splice sites. Alignment of the wt RNAseq reads to the model is graphed below the model. Scale bar = 200 bp.

as did wild-type. Growth on V8 agar spot amended with either calcium ionophore A23187 or ETOH (control) showed that wild-type fully colonized the A23187 treated medium while the remaining strains were unable colonize the treated spot (Fig. 2B). All strains colonized the ETOH control medium.

Quantification of growth rates and macroconidia production was performed to better understand the effect of Fig1 loss on vegetative growth and asexual reproduction. When grown on unamended carrot agar, LACS mutants without functional Fig1 grew at a significantly slower rate than wild-type while mutants having both LACS and HACS defects grew at a significantly slower rate than Δf1 (Fig. 3A). Growth of all strains on carrot agar amended with 80 mM calcium or 80 mM magnesium was not significantly different than growth of the same strain on unamended carrot agar. In contrast, the Δ*cch1* Δ*fig1* Δ*mid1* triple mutant grew significantly slower on carrot agar amended with magnesium than on both carrot agar and carrot agar amended with calcium. All mutants produced significantly fewer macroconidia in CMC than wild-type, but were not significantly different from each other (Fig. 3B).

To observe the effect of the loss of Fig1 on sexual development, strains were inoculated onto carrot agar and after fully colonizing the medium were induced to undergo sexual development. Strains lacking a functional Fig1 failed to develop perithecia, although they produced the characteristic black pigment seen in the top 2-4 mm of the medium after induction

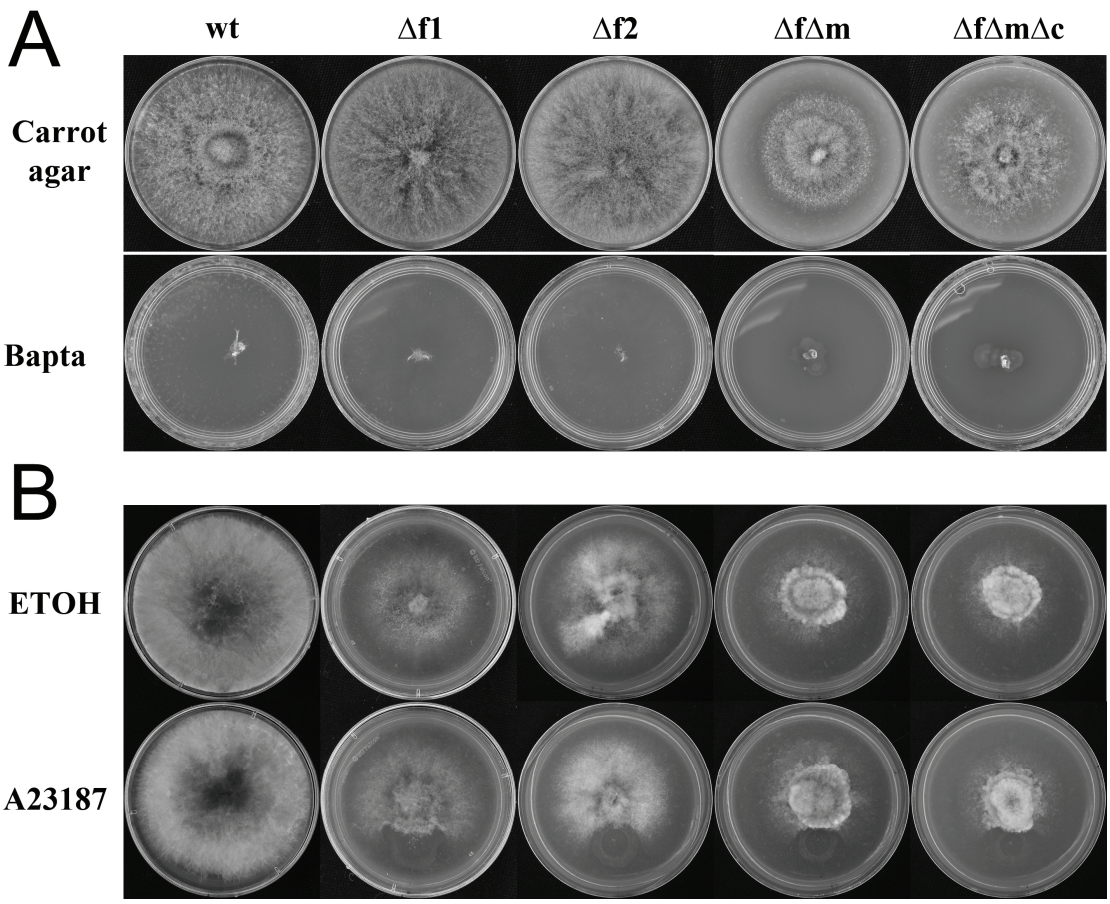

Figure 9. Growth of Δf1, Δf2, ΔfΔm and ΔfΔmΔc strains on carrot agar, carrot agar with BAPTA to limit available calcium, and on V8 agar and V8 agar with Ca^{2+} ionophore A23187. (A) **Top panel**: Growth (4 d) on CA. wt, Δf1, and Δf2 fully colonized the medium. Strains ΔfΔm and ΔfΔmΔc did not. **Bottom panel:** Growth (14 d) on medium supplemented to 1 mM BAPTA. wt, Δf1, and Δf2 fully colonized the medium, but ΔfΔm and ΔfΔmΔc ceased growing after some initial colonization. (B) **Top panel**: Growth on V8 agar treated with EtOH control. wt fully colonized the medium. Strains Δf1 and Δf2 colonized the medium but with less aerial hyphae than wt. Strains ΔfΔm and ΔfΔmΔc were similar but more severe and did not fully colonize the medium. **Bottom panel:** wt fully colonized the ionophore treated medium but the remaining strains failed to do so.

(Fig. 3A). To determine whether sexual development initiates at all or if it halts at a specific stage of development, wild-type and the Δ*fig1* single mutants were inoculated onto carrot agar with several pieces of cellulose membrane placed onto the surface of the medium. After full colonization, sexual development was induced. At 24 hr and 48 hr post induction, the

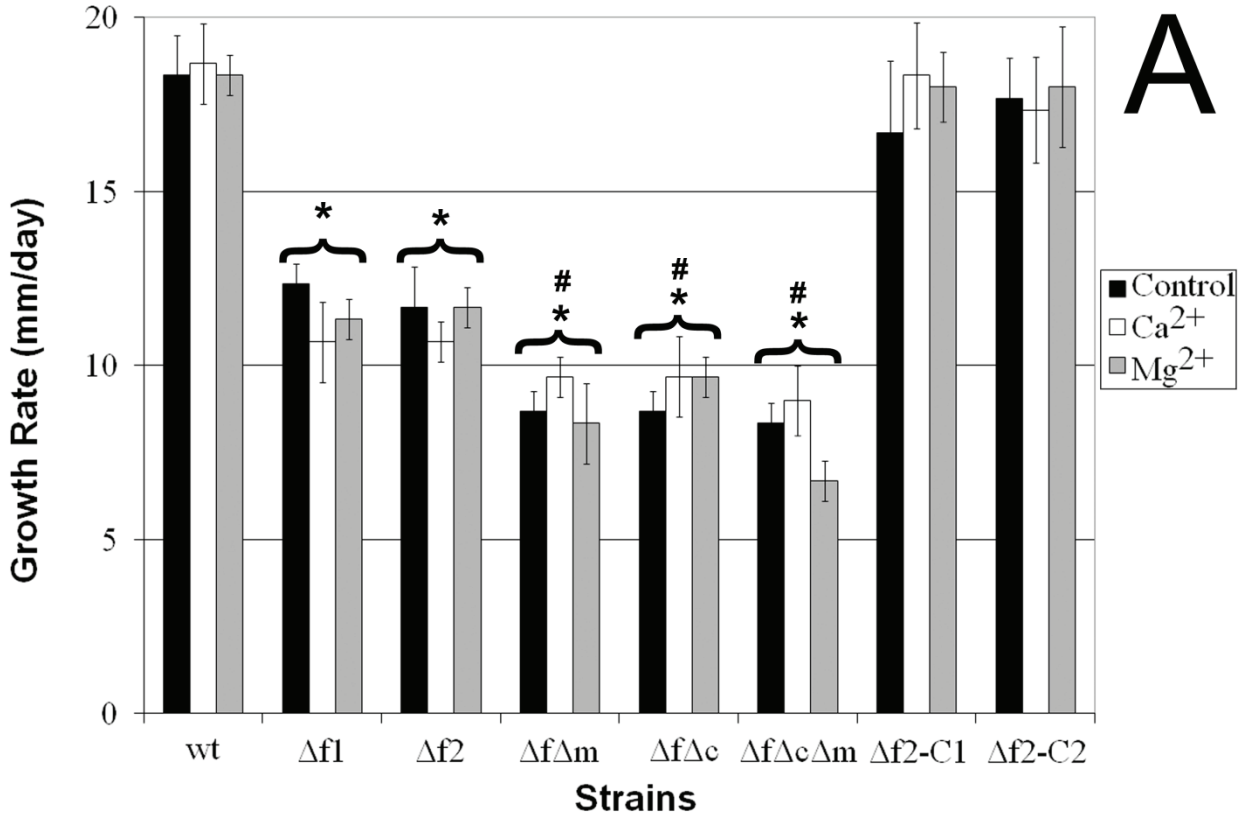
A
Growth Rate (mm/day)
20
15
10
5
0
Control
Ca2+
Mg2+
wt
Δf1
Δf2
ΔfΔm
ΔfΔc
ΔfΔcΔm
Δf2-C1
Δf2-C2
Strains

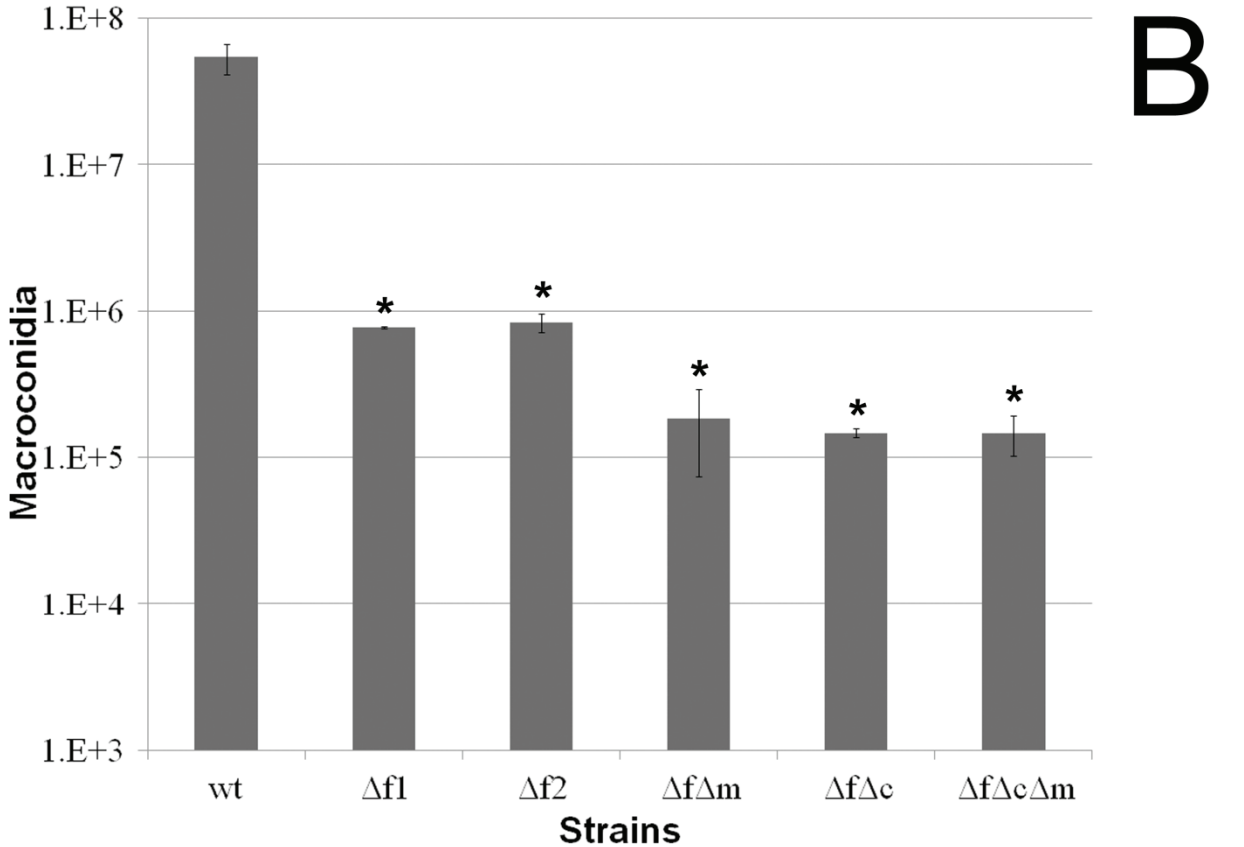
B
Macroconidia
1.E+8
1.E+7
1.E+6
1.E+5
1.E+4
1.E+3
wt
Δf1
Δf2
ΔfΔm
ΔfΔc
ΔfΔcΔm
Strains

Figure 10

Figure 10 (cont'd)

Figure 10. Characterization of *F. graminearum* growth and asexual development. (A) Growth rates on carrot agar with and without Ca^{2+} or Mg^{2+} supplementation (change of diameter in mm/day). Asterisks above brackets indicate a significant difference between all growth conditions of the bracketed strain and wild-type on carrot agar. Number signs above brackets indicate a significant difference between the bracketed strain on carrot agar and Δf1, but not Δf2, on carrot agar. (B) Macroconidia production. Error bars represent the SD of the means of 3 biological replicates. * = $p < 0.005$; # = $p < 0.05$.

cellulose membranes were removed from the carrot agar. The tissue on the membranes were fixed, stained with toluidine blue, destained, and viewed by light microscopy (Fig. 3B). At 24 hr, wild-type developed perithecium initials, but the Δ*fig1* mutants only had hyphae curving back onto themselves. By 48 hr, the membranes with wild-type contained larger immature perithecia with developing walls, and the Δ*fig1* mutants developed perithecium initials that failed to develop any further.

Characterization of *FIG1* mutants in *N. crassa*

The *N. crassa fig1* ortholog (NCU02219) was identified by BLAST using the *S. cerevisiae* Fig1 protein sequence. A Δ*fig1 mat a,* but not a Δ*fig1 mat A* strain, was generated by Colot et al. (2006), so the Δ*fig1 mat a* strain was crossed to wt *mat A* to generate Δ*fig1 mat A* progeny. Twenty-four progeny were screened by PCR for the absence of *fig1* and the presence of *mat A-2*. PCR analysis revealed that three progeny, *fig1A-18, fig1 A-20,* and *fig1 A-21*, lacked *fig1*, but harbored *mat A*-2. Strain *fig1 A-21* was used for subsequent experiments.

To examine the effect of Fig1 loss on calcium homeostasis, YEPD agar was inoculated wt *mat a*, wt *mat A*, Δ*fig1 mat a*, and Δ*fig1* mat *A*, and spot treated with calcium ionophore A23187 or ETOH as a control. The cultures were examined 38 hr post inoculation and all strains colonized the treated medium without any noticeable difference (data not shown). Crosses were

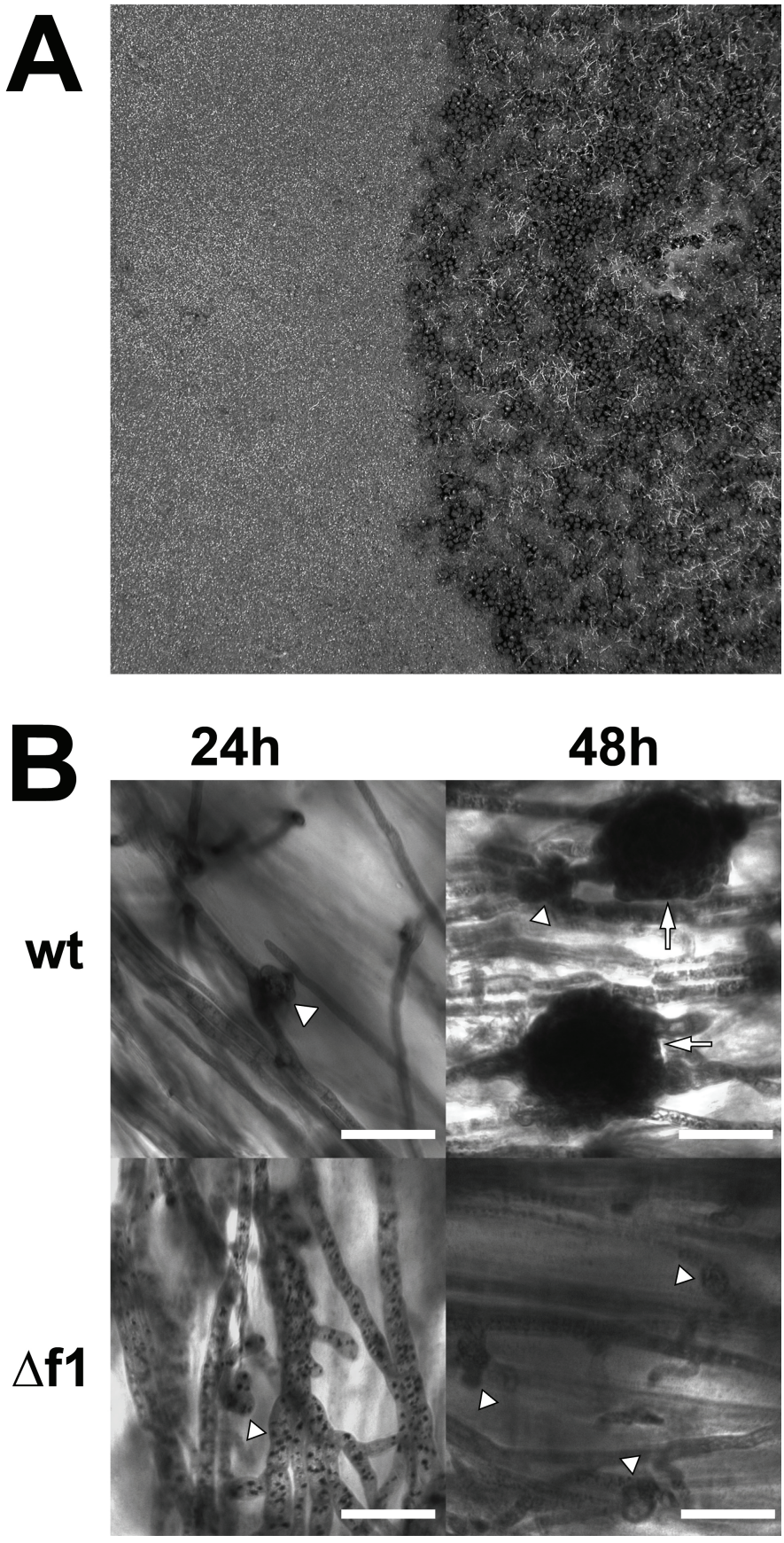

Figure 11

Figure 11 (cont'd)

Figure 11. Sexual development in wt and Δf1. (A) Mature wt culture has normal sexual development (right side) and Δf1 exhibits an absence of perithecia development. (B). Sexually induced cultures at 24 and 48 hr stained with toluidine blue. Perithecium initials (white arrowheads) develop at 24 hr in wt. Initials in Δf1 developed more slowly. By 48 hr, immature walled perithecia (white arrow) are found in wt but in Δf1 perithecium initials are noticeable, but do not develop further. Scale bars = 20 μM.

initiated between the Δ*fig1* strains of both mating types to each other and to the reciprocal mat wild-type strains to observe the effects of Fig1 loss on sexual development. Microscopic examination of squashed perithecia found that the fruiting bodies of the Δ*fig1 mat a* strain were not fertile as they were devoid of asci but the Δ*fig1 mat A* strain developed normally (Data not shown).

Discussion

The results presented here demonstrate divergent roles for Fig1 in *F. graminearum* and *N. crassa*. In *F. graminearum*, Fig1 function affects all stages of the life cycle examined and is essential for sexual development. In *N. crassa*, loss of Fig1 resulted in little to no effect on vegetative growth, but reduced the female fertility and halted perithecium development in a *mat a* background. Fig1 is required for both Ca^{2+} influx dependent and independent responses to exposure to mating pheromone in yeasts (Erdman et al., 1998; Lockhart et al., 2003; Yang et al., 2011; Zhang et al., 2006), however, to date there have been no reported functional studies of Fig1 in filamentous species. The apparent divergence of LACS function between *N, crassa* and *F. graminearum* is reminiscent of that previously reported for HACS function between *F. graminearum* and *N. crassa* in which both similar (slowed vegetative growth, calcium homeostasis lesion) and divergent phenotypes (reduced ascospore discharge and abnormal ascospore morphology in *F. graminearum* and altered hyphal electrophysiology in *N. crassa*)

were observed (Cavinder et al, 2011; Lew et al. 2008). That the roles of HACS and LACS both show divergence points to the evolutionary malleability of calcium signaling.

Recent studies, including the analysis of genomes in the Origins of Multicellularity Database (http://www.broadinstitute.org/annotation/genome/multicellularity_project/MultiHome.html; accessed: July. 2011) have shown that some components of calcium signaling once thought to be unique to either fungi or metazoans appeared before the divergence of these lineages approximately a billion years ago (Cai and Chlapman, 2011; Rokas 2008; Ruiz-Trillo et al. 2007). This sequence database contains basal members of the Unikonts, organisms with cell bearing only one flagellum type that includes metazoans, fungi, and amoebae. Metazoans and fungi are further subdivided into the Opisthokonts, cells bearing a single posterior flagellum. Comparative analyses of the genome in the database are being utilized to understand the origins, commonalities, and differences of multicellularity between animals and fungi. The genome of *Thecamonas trahens*, a member of the phylum Apusozoa, contains the only known ortholog of Mid1 outside of the true fungi. In addition, *T. trahens* contains several homologs of mammalian VGCC, rather than a fungal Cch1 ortholog. The Apusozoa are a possible sister group to the Opisthokonts, having diverged before the fungal-metazoan split (Cavalier-Smith, 2009; Glücksman et al., 2010), so Mid1 was present before Apusozoa and Opisthokonts diverged. In addition, *Allomyces macrogynus*, a Blastocladiomycete (James et al., 2006), possesses six Cch1 homologs (Cai and Chlapman, 2011). Although the presence of Fig1 and other PMP22_Claudin superfamily members was not examined by Cai and Chlapman (2011), multiple members are already known to exist in both metazoans and fungi, suggesting that at least one member was present in the common ancestor. Lineage specific adaptation resulting in the loss, gain, or

expansion of calcium signaling components in combination with the changes to the specific roles may account for the differences seen in the extant species of Unikont organisms.

Members of the PMP22_Claudin superfamily, of which Fig1 is a member, are involved in membrane-to-membrane interactions and also commonly form diffusion barriers that selectively allow ions, water, and other solutes to pass between cells (Furuse, 2010; Grey et al., 2003; Rosenthal et al., 2010; Wu et al., 2004). The known functions of Fig1 in fungi fit well with those known for non-fungal proteins in the PMP22_Claudin superfamily, involving cell to cell interactions and ion flux. Fig1 is involved in the sexual development of *C. albicans* and *S. cereviseae*, and the results here show that it is also involved in the sexual development of *F. graminearum* and *N. crassa*. Fig1 expression and calcium uptake increases in response to mating pheromone and Fig1 localizes to the mating projections and membranes destined for fusion during mating in both *S. cerevisiae* and *C. ablicans*. Deletion of *Fig1* resulted in lowered pheromone-induced calcium accumulation and decreased cell fusion during mating of both yeasts. In *S. cerevisiae*, undigested cell wall remaining between the appressed shmoos was observed, which was rescued by addition of exogenous calcium, and this phenotype was not seen in *C. albicans* (Alby et al., 2010; Erdman et al., 1998). Cell to cell interactions and membrane dynamics appear to be central to the function of Fig1 in yeast mating and point to a possible similar role in filamentous fungi that may explain the blocking of sexual development in *F. graminearum* and the reduced female fertility *N. crassa* seen in Δ*fig1* mutants. Cellular fusion is critical to the formation of the coiled perithecium initials and the formation of parenchymatous tissue from hyphae during fruiting (Trail and Common 2000). Although the blocking of *F. graminearum* sexual development at the perithecium initials stage did not allow investigation of the role of Fig1 in later stages of development in the present study, it seems likely that Fig1

would also be involved at later stages of *F. graminearum* sexual development. Membrane dynamics and trafficking are essential for asci development (Beckett and Crawford, 1973; Hung, 1977; Read and Beckett, 1996) and for the delimitation of ascospores by the formation of double membranes around the progeny nuclei (Czymmek and Klomparens, 1992; Wu and Kimbrough, 2001). As Fig1 is involved in membrane fusion, a role for Fig1 in ascus development and ascospore delimitation is possible.

The role of Fig1 during vegetative and hyphal grow is also variable among the fungi. Loss of Fig1 did not affect the growth rate or calcium accumulation of *S. cerevisiae* or *C. albicans* vegetative yeast cells (Brand et al., 2007; Muller et al., 2003). During hyphal growth of *C. albicans*, Fig1 expression is low and fluorescence from Fig1-GFP fusion proteins was undetectable but was readily detected after increased expression upon exposure to mating pheromone (Yang et al., 2011). Deletion of *FIG1* resulted in increased conversion to hyphal growth of yeast grown on agar, indicating Fig1 plays a role in hyphal suppression in some environments (Brand et al., 2007). Additionally, loss of Fig1 did not decrease calcium uptake in *C. albicans* hyphae, but did affect the thigmotropic response of hyphae to physical ridges, resulting in the reduced frequency of hyphal tip growth reorientation upon contact with a ridge compared to wild-type (Brand et al., 2007). Our results show that Fig1 has no detectable effect on *N. crassa* vegetative growth. However in *F. graminearum*, *FIG1* deletion results in similar phenotypes to HACS mutants: reduced vegetative growth, reduced macroconidiation, and defective calcium homeostasis (Cavinder et al. 2011; Hallen and Trail, 2008). However, the mycelium of HACS mutants is fluffy compared to wild-type, while Δ*fig1* strains have mycelia that are appressed to the substrate surface with little aerial hyphae. The nutrient availability seems to affect this phenotype some as less aerial hyphae is produced on V8 agar than on the

more nutrient rich carrot agar. Another difference is that the Δ*fig1* mutants grow on calcium limited medium, supplemented with BAPTA, as well as wild-type, but Δ*mid1* and Δ*cch1* strains fail to colonize the BAPTA containing medium, supporting the need for HACS, but not LACS, to support calcium influx in calcium limited environments. It would be interesting to see if LACS has a function in the hyphal electrophysiology of *F. graminearum* and *N. crassa*. HACS disruption in *N crassa* resulted in altered electrical properties as measured by voltage clamp (Lew et al., 2008). In contrast, HACS disruption in *F. graminearum* did not alter hyphal electrochemical properties (Cavinder et al., 2011).

The results presented here, taken together with the previous HACS and LACS results in other fungi and the analysis of calcium signaling components in the origins of multicellularity database, show the evolutionary flexibility of calcium signaling in the different lineages of extant eukaryotes. Even within the Sordariomycetes, the roles of HACS and LACS has diverged as seen by the results with Cch1, Mid1, and Fig1 in *F. graminearum* and *N. crassa*. Although not examined here because of the block in sexual development, we think it is likely that Fig1 plays a role in sexual development after the transition from perithecium initials to immature perithecium, and application of sexual development stage specific or inducible RNAi would allow the investigation of any such role. Additionally, the importance of calcium importation genes in sexual development suggest that the roles of other calcium signaling components will also be involved. Finally, the end targets of calcium signaling during sexual development are not known and investigations to identify them are being pursued.

CHAPTER 4

DEVELOPMENT OF INDUCED RNA INTERFERENCE VECTORS FOR USE IN *FUSARIUM GRAMINEARUM* AND RELATED FILAMENTOUS FUNGI

Brad Cavinder and Frances Trail

ABSTRACT

Since its discovery, RNA interference (RNAi) has become an important tool for biologists, allowing the investigation of genes whose loss is lethal. Here a doxyxyline inducible expression system was adapted for use in *Fusarium graminearum* and was utilized to drive expression of an inverted repeat transgene targeting *MYO2*, a type V myosin. Induction of RNAi during sexual development resulted in severely slowed ascus growth, and altered vesicle trafficking and ascospore delimitation. Removal of the inducing agent resulted in the recovery of normal sexual development. Induction of RNAi of *MYO2* during vegetative growth did not affect the growth rate. In addition, RNAi of *PKS3*, a gene involved in synthesis of the black perithecial pigment was explored. A transformant containing the *PKS3* RNAi construct was found to lack perithecium pigment without doxycycline induction. This result may be from transcriptional read-through from upstream sequences or from the influence of an enhancer drove expression of the RNAi construct. If an enhancer is involved, then RNAi constructs can be used for developmentally specific enhancer trapping provided that a suitable target for RNAi with a useful phenotype is known. These results show that the doxycycline induced expression system is effective in *F. graminearum*, and coupled to RNAi constructs, the system can be used effectively to examine the role of genes at desired time points.

Introduction

Fusarium graminearum is a cosmopolitan filamentous ascomycete fungus and a plant pathogen capable of infecting numerous hosts. In North America, *F. graminearum* is the primary cause of Fusarium Head Blight (FHB) of wheat and barley and has caused significant financial losses in the past two decades (Nganje et al., 2001; Trail, 2009). Both ascospores and macroconidia are inoculum for FHB, but ascospores are thought to be the primary inoculum in the field. Ascospores were found to adhere to wheat spikes more robustly than macroconidia (Markell and Francl, 2003), and air sampling studies consistently find more airborne ascospores than macroconidia, although macroconidia are occasionally found in equal or greater numbers (Fernando et al., 2000; Inch et al., 2005; Markell and Francl, 2003). Desjardins et al (2006) found that ascospore non-producing strains of *F. graminearum* were significantly less able to cause FHB epidemics than wild-type ascospore producing strains. Finally, phylogenetic studies from around the world characterizing field isolates showed high genetic diversity among the isolates, little to no linkage disequilibrium between genetic markers, and almost as many haplotypes as isolates, suggesting a high rate of recombination and thus sexual reproduction in the field (Karugia et al., 2009; Tóth et al., 2005; Walker et al., 2001; Ward et al., 2008, Zeller et al., 2003).

Ascus development is a dynamic process that results in the destruction of asci upon the forcible discharge of ascospores, meaning that the process is one way and asci do not need to recover from the changes they undergo during development. Membrane dynamics is an important part of ascus development as karyogamy, meiosis, and a round of mitosis all occur in the ascus to generate eight progeny nuclei and a double layer of membranes is used to delimit progeny ascospores (Czymmek and Klomparens, 1992; Read and Beckett, 1996). In *Sordaria*

macrospora, actin and myosin were shown to be required for the transition from crozier to ascus. These two proteins also played a role in ascospore delimitation, as pharmacological inhibition of either actin polymerization or actin-myosin interaction function disrupted these processes (Thompson-Coffe and Zickler, 1993). This function is likely carried out by class V myosins, which are involved in vesicle transport in *S. cerevisiae* (Pruyne et al., 2004). The class V myosin ortholog in *F. graminearum* is *MYO2* (FGSG_07469).

RNA interference (RNAi) is the process by which mRNAs are posttranscriptionally downregulated by short 21-25 nucleotide double-stranded RNA (dsRNA) fragments. The process starts when Dicer, an RNAse III enzyme, digests dsDNA into short interfering RNA (siRNA) that are incorporated into the RNA induced silencing complex (Bernstein et al. 2001; Pham et al., 2004; Tomari et al., 2004).The RNA induced silencing complex utilizes the siRNA to target complementary sequences in mRNA for digestion. Since its discovery, RNAi has become a widely used tool to study gene function. RNAi techniques have used constitutive, induced, and tissue and developmental stage specific expression systems for transcription of the RNAi construct (Lee and Kumar, 2009; Rao et al., 2006). A doxycycline induced expression system employing an engineered tet-ON system derived from the *Escherichia coli* tetracycline-resistance operon was adopted for use in the filamentous ascomycete *Aspergillus nidulans* (Vogt et al., 2005). This system consists of two parts. The first part is a reverse transactivator (rtTA2S-M2) fusion protein between the DNA binding domain of TetR, a transcriptional repressor protein that binds to tetracycline operator sequences (*tetO*), and a multimerized minimal VP16 transcriptional activator domain. The fusion protein contains additional mutations to increase binding affinity to doxycycline. The second part is an expression construct with seven copies of *tetO* (*tetO*$_7$) followed by an *A. nidulans* minimal *gpdA* promoter (Pmin). In the presence of

doxycycline, rtTA2S-M2 will bind to *tetO7* and drive expression from Pmin. RNAi was effectively applied in *F. graminearum* to knockdown the expression of the *TRI6* gene, a transcription factor needed for trichothecene mycotoxin production, using a constitutively expressed inverted repeat transgene (IRT) construct with ~600 bp *TRI6* repeats to generate a hairpin RNA with a long dsRNA region (McDonald et al., 2005).

Our goal in this study was to develop inducible RNAi for studies of genes important in perithecium development and function. Many of these genes cause loss of sexual development in knockout strains (Kim et al., 2007; Oide et al., 2007; Turgeon et al., 2008; Urban et al., 2003). Here we combined the doxycycline induced expression system of Vogt et al. (2005) with the IRT RNAi expression construct of McDonald et al (2005) for use in *F. graminearum*. To this end, targeted IRT RNAi expression vectors for *PKS3* (FGSG_17168), a polyketide synthase needed to produce the dark perithecium pigment of *F. graminearum*, and *MYO2* were constructed and introduced into *F. graminearum* using the doxycycline inducible system. The results illustrate the ability to down regulate gene expression at specific time points to affect development and understand gene function. Taken with the previous results of driving reporter gene expression, the doxycycline inducible expression system can be used for both positive and negative regulation of gene expression.

Material and Methods

Strains, culture conditions

Strains of *F. graminearum* used in this study are listed in Table 1. Strains were maintained as macroconidia and colonized V8 agar pieces in 35% sterile glycerol at -80°C. Macroconidia were produced in carboxymethylcellulose (CMC) broth as previously described

TABLE 5. Strains used in this study		
Strain	Genotype	Source
Fusarium graminearum		
PH-1(FGSC 9075)	wild-type (NRRL 31084)	Trail and Common, 2000
PH-1 55	*nit3*	Cavinder et al., 2011
502-4	*nit3* rtTA2s-M2	This Study
M2-II	*MYO2* RNAi	This Study
M2-2	*MYO2* RNAi rtTA2s-M2	This Study
M2-5	*MYO2* RNAi rtTA2s-M2	This Study
M2-7	*MYO2* RNAi rtTA2s-M2	This Study
P3-1	*PKS3* RNAi	This Study

(Cappellini and Peterson, 1965). Sexual development was induced by removing the surface hyphae from fully colonized carrot agar and adding 1 ml of a sterile 2.5% (w/v) Tween 60 solution (Bowden and Leslie, 1999; Trail and Common, 2000). Outcrosses were performed by inoculating carrot agar plates with two strains and inducing sexual development after full colonization of the medium. Recombinant perithecia form at the interface of the two strains.

Saccharomyces cerevisiae strain FY834 (Winston et al., 1995) was used for yeast transformations and was received from Dr. Angus Dawe (New Mexico State University, Las Cruces, NM). *S. cerevisiae* strains were stored at -80°C in an appropriate liquid growth medium amended to 35% glycerol. One Shot TOP10 Chemically Competent *Escherichia coli* cells (Life Technologies, Carlsbad, CA) were used for bacterial transformations.

Nucleic acids manipulation

DNA was extracted from *F. graminearum* mycelium grown in liquid yeast extract-sucrose medium using a hexadecyltrimethylammonium bromide (CTAB) method as previously described (Cavinder et al., 2011; Hallen and Trail, 2008). *F. graminearum* nucleotide data were obtained from the MIPS Fusarium graminearum Genome Database (http://mips.helmholtz-

muenchen.de/genre/proj/FGDB/). A standard alkaline lysis protocol was followed to extract plasmid DNA from *E. coli* (Sambrook and Russell, 2001). Plasmid DNA was extracted from *S. cerevisiae* cells using the Zymoprep Yeast Plasmid Miniprep II kit (Zymo Research) or by incubating cells in 400 µl of 50 mM potassium phosphate, pH 7.5 with 5 µl (25 U) of Zymolyase (Zymo Research) for 45 min at 37°C followed by the standard *E. coli* alkaline lysis protocol. Extracted plasmids were screened by PCR to identify clones with the desired constructs.

The Primers used in this study are listed in Table 2. Phusion High-Fidelity DNA Polymerase (New England Biolabs) was used for PCR. All PCR products were size fractionated by agarose gel electrophoresis. The appropriately sized band for a given reaction was cut out of the gel and purified using the Wizard SV Gel and PCR Clean-Up System (Promega, Madison, WI) following the manufacturer's protocol. Single and double restriction enzyme digests were performed using the manufacturer's suggested reaction conditions and digested DNA fragments were purified using the DNA Clean & Concentrator-5 kit (Zymo Research, Irvine, CA). DNA ligations were performed using T4 DNA ligase (New England Biolabs, Ipswich, MA) following the manufacturer's protocol. Plasmids p500 and p502 (Vogt et al., 2005) were obtained from the Fungal Genetics Stock Center, and pTMH44.2 (McDonald et al., 2005) and pRS426 (Christianson et al., 1992) were gifts from Dr. Nancy Keller (University of Wisconsin, Madison, WI) and Dr. Angus Dawe (New Mexico State University, Las Cruces, NM), respectively.

Vector construction

Vectors were generated by a combination of merging PCR amplified DNA fragments with short overlaps to each other by PCR and by homologous recombination in *Saccharomyces*

TABLE 6. Primers used in this study	
Name	Sequence (5'-3')
For genertion of pYUCH	
2μm-F	GATCTTTTCTACGCACCTGAACGAAGCATCTGTGCTTCA
2μm-R	CTGTGGTATGGTGCGAAGTTCCTATTCTCTAGAAAGTA
Ura3-F	GAATAGGAACTTCGCACCATACCACAGCTTTTCAATTCAATTCATC
Ura3-R	GACCCCGTAGAAACAGTTTTTTAGTTTTGCTGGCCGCATCTTC
Ori-F	GAAGCATAAAGTGTAAAGCGCGTTGCTGGCGTTTTTCCATAG
Ori-R	GTTCAGGTGCGTAGAAAAGATCAAAGGATCTTCTTGAGATCC
MCS-F	CTTTCACCAGCGTTCCATTCAGGCTGCGCAACTGTTG
MCS-R	CAGCAACGCGCTTTACACTTTATGCTTCCGGCTCGTATG
CAT/*hph* -F	CAAAACTAAAAAACTGATGGAGAAAAAAATCACTGGATATACCACCGTTG
CAT/*hph* -R	CAGCCTGAATGGAACGCTGGTGAAAGTAAAAGATGCTGAAGATC
For generation of pYUCH-RNA	
TcgrA-F	TTTCCCAGTCACGACGACAGCAGAAGAATCTCTCTCCGCTGT
TcgrA-R	GTAAACTCGATCGAGGGATTCATGACGTATATTCACCGAGATAGTC
tetO7-F	GCAAAACTAAAAAACTGTTTCTACGGGGTCTGACGCTCAGTG
tetO7-R	ACTGAAGATGGGCACATGCATGCCATAGGGTACCGA
Pmin-F	ATGGCATGCATGTGCCCATCTTCAGTATATTCATCTTCCCATC
Term-R	CGTAGCAACCAGGCGTCCAAGCTCTAGAAAGAAGGATTACCTCTA
pYUCH-F	
pYUCH-R	

TABLE 6 (cont'd)	
Name	Sequence (5'-3')
For generation of pYUCH-RNA-MYO2 and pYUCH-RNA-PKS3	
pCode-F	CATGGGGCGGAATTCGGGCTATGTGCAGGAGAGAACCATCT
pCode-R	CGCCGCGCCACTAGTTGATGTCTGCTCAAGCGGGGTAGC
pTemp-F	CGTGAATCGCGGCCGCGCTTGAGATCCACTTAACGTTACTGAAATCATC
pTemp-R	AAGCTTGGACAATTGCTCAATGTTGTGTCTGATCTTGAAGTTGACC
Myo2 Code-F	TGTCGCAAGGAATTCGTCTTCGCTCTTCGGTGGATGAGATC
Myo2 Code-R	TGTCTTCAGACTAGTCTCGACCTTGTCGCGCATCCTTG
Myo2 Temp-F	ATTGTCTTCGCGGCCGCCTCGACCTTGTCGCGCATCCTTG
Myo2 Temp-R	TGTCGCAAGCAATTGGTCTTCGCTCTTCGGTGGATGAGATC
PKS3 Code-F	CCCTTACCCGAATTCGCGGTTTCGCCATGAATTGTAATGACC
PKS3 Code-R	ACCACTGACACTAGTTTCTGGACCTTGAAGGAAGTTGCGAAG
PKS3 Temp-F	GTCAGTGGTGCGGCCGCTTCTGGACCTTGAAGGAAGTTGCGAAG
PKS3 Temp-R	CCCTTACCCCAATTGGCGGTTTCGCCATGAATTGTAATGACC
For TAIL-PCR	
AD2	NGTCGASWGANAWGAA
AD3	WGTGNAGWANCANAGA
AD5	NTCGASTWTSGWGTT
AD7	TGWGNAGWANCASAGA
AD8	AGWGNAGWANCAWAGG

cerevisiae along with traditional cloning in *E. coli*. Plasmids amplified by PCR for cloning cotransformations in *S. cerevisiae* were cut with DpnI (New England Biolabs) directly in the PCR reactions to digest methylated DNA from the starting plasmid template. Plasmid p502 contains a reverse tetracycline transactivator (rtTA2s-M2) expression construct and a hygromycin phosphotransferase *(hph*) marker and was transformed as is into *F. graminearum* strain PH-1 55 protoplasts without modification. Plasmid maps were generated using PlasMapper (Xiaoli et al., 2004), and are shown in Fig. 1.

Construction of pYUCH. A 1,049 bp fragment containing the *URA3* marker and a 1,003 bp fragment containing the 2 micron origin of replication (2 μM) for selection and episomal maintenance in *S. cerevisiae* were amplified from pRS426 using primers Ura3-F and Ura3-R and 2μm-F and 2μm-R, respectively. Three fragments of 430, 638, and 2,499 bp containing the pBR322 origin of replication (Ori), the pBC SK+ multiple cloning site (MCS), and the chloramphenicol acetyltransferase (CAT) and *hph* markers (CAT-*hph*) for episomal maintenance, traditional cloning, and selection in *E. coli* and *F. graminearum* were amplified by PCR from pCB1004 (Carroll et al., 1994), using primers Ori-F and Ori-R, MCS-F and MCS-R, and CAT/*hph*-F and Cat/*hph*-R, respectively. Primers Ura3-R and CAT/*hph*-F contain 5' tails of 23 and 24 bp complementary to the 5' sequence of the CAT/*hph* and URA3 fragment, respectively, and the fragments were merged by PCR, generating a 3,570 bp *URA3*-CAT/*hph* fragment. Primers MCS-R and Ori-F contain 11 and 18 bp 5'overlaps to the 5' end of Ori and 3' end of MCS, respectively, and the fragments were merged by PCR, generating the bp MCS-Ori fragment. Primers MCS-R and 2μm-F contain 5' tail of 25 and 23 bp complementary to the 5' end of the 2 μm fragment and the 3' end of the MCS fragment, respectively, and PCR was used to merge the fragments into the bp MCS-Ori-2μm fragment. Primers Ura3-F and CAT/*hph*-R

contain 5' overlaps of 13 and 12 bp to the 3' and 5' ends of the MCS-Ori-2µm fragment, and primers MCS-F and 2µm-R contain 14 bp 5' tails complementary to the 3' and 5' end of the *URA3*-CAT/*hph* fragment, respectively. The URA3-CAT/*hph* and MCS-Ori-2µm fragments were cotransformed into *S. cerevisiae* to generate pYUCH by homologous recombination.

Construction of pYUCH-RNA. A 276 bp fragment containing the *A. nidulans cgrA* terminator (T*cgrA*) and a 330 bp fragment containing seven repeats of the tetracycline operator (*tetO*$_7$) were amplified from p502 using primers TcgrA-F and TcgrA-R and tetO7-F and tetO7-R, respectively. Primers TcgrA-R and tetO7-F contain a 5' tails of 16 and 18 bp complementary to the 5' end of the *tetO*$_7$ and the 3' end of the T*cgrA* fragments, respectively, and the fragments were merged by PCR to generate a 635 bp TcgrA-*tetO*$_7$ fragment. A 1,194 bp fragment (eRNAi) containing a minimal *A. midulans gpdA* promoter, the empty IRT RNAi sequence with two cloning sites separated by a partial *GFP* sequence spacer, and the *A. midulans trpC* terminator was amplified by PCR from pTMH44.2 using primers Pmin-F and Term-R. Primers tetO7-R and Pmin-F contain 5' overlaps of 16 and 14 bp to the 5' end of the eRNAi and the 3' end of *tetO*$_7$ fragments, respectively. The T*cgrA-tetO*$_7$ and eRNAi fragments were merged by PCR to generate the 1,830 bp T*cgrA-tetO*$_7$-eRNAi fragment. Primers TcgrA-F and Term-R respectively contain 13 and 17bp 5' overlaps complementary to internal MCS sequences. The entire pYUCH plasmid excluding 223 bp of internal MCS sequence (pYUCH-amp) was amplified by PCR using primers pYUCH-R and pYUCH-F that contain 5' tails of 17 and 12 bp complementary

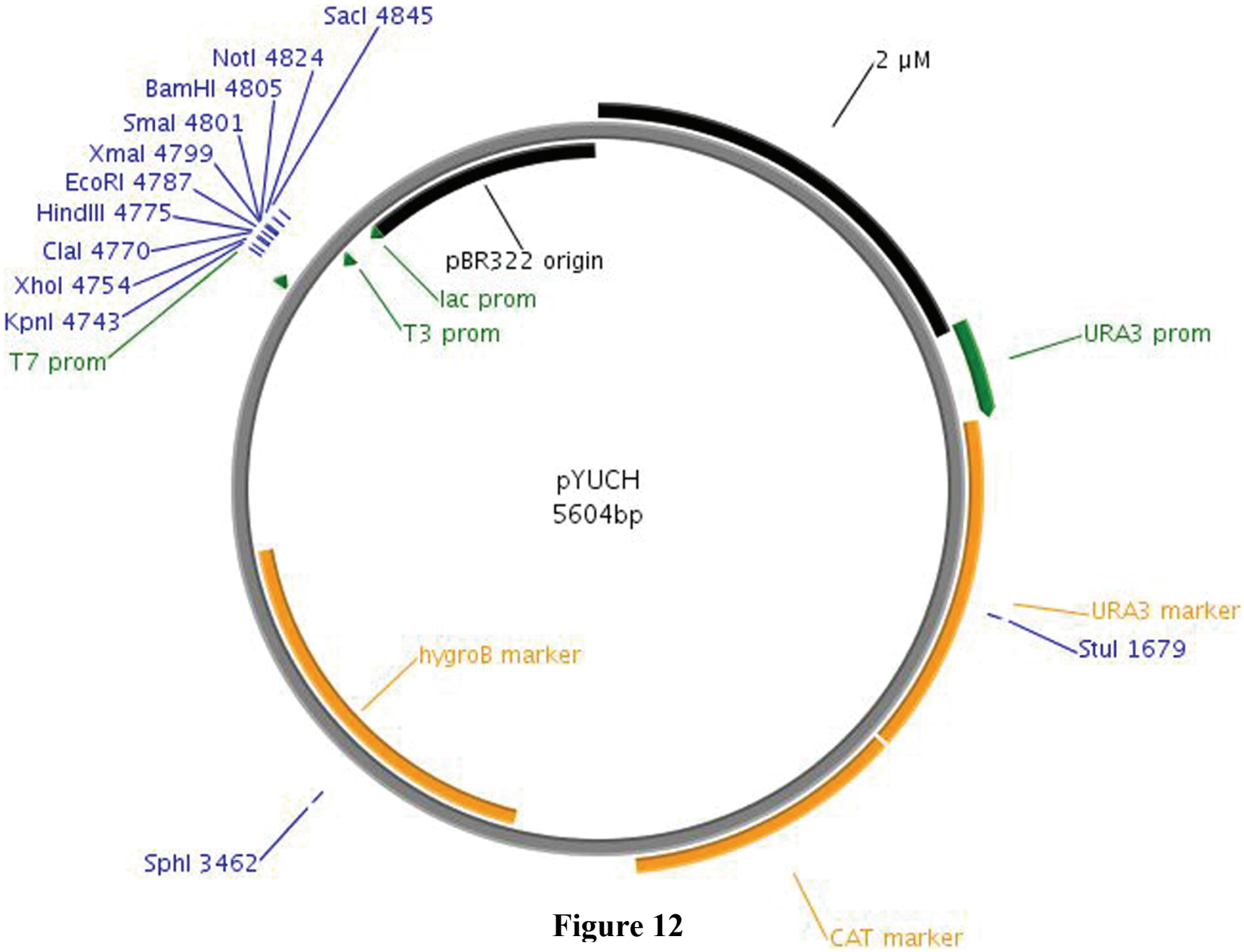
SacI 4845
NotI 4824
BamHI 4805
SmaI 4801
XmaI 4799
EcoRI 4787
HindIII 4775
ClaI 4770
XhoI 4754
KpnI 4743
T7 prom
2 µM
pBR322 origin
lac prom
T3 prom
URA3 prom
pYUCH
5604bp
URA3 marker
StuI 1679
hygroB marker
SphI 3462
CAT marker

Figure 12

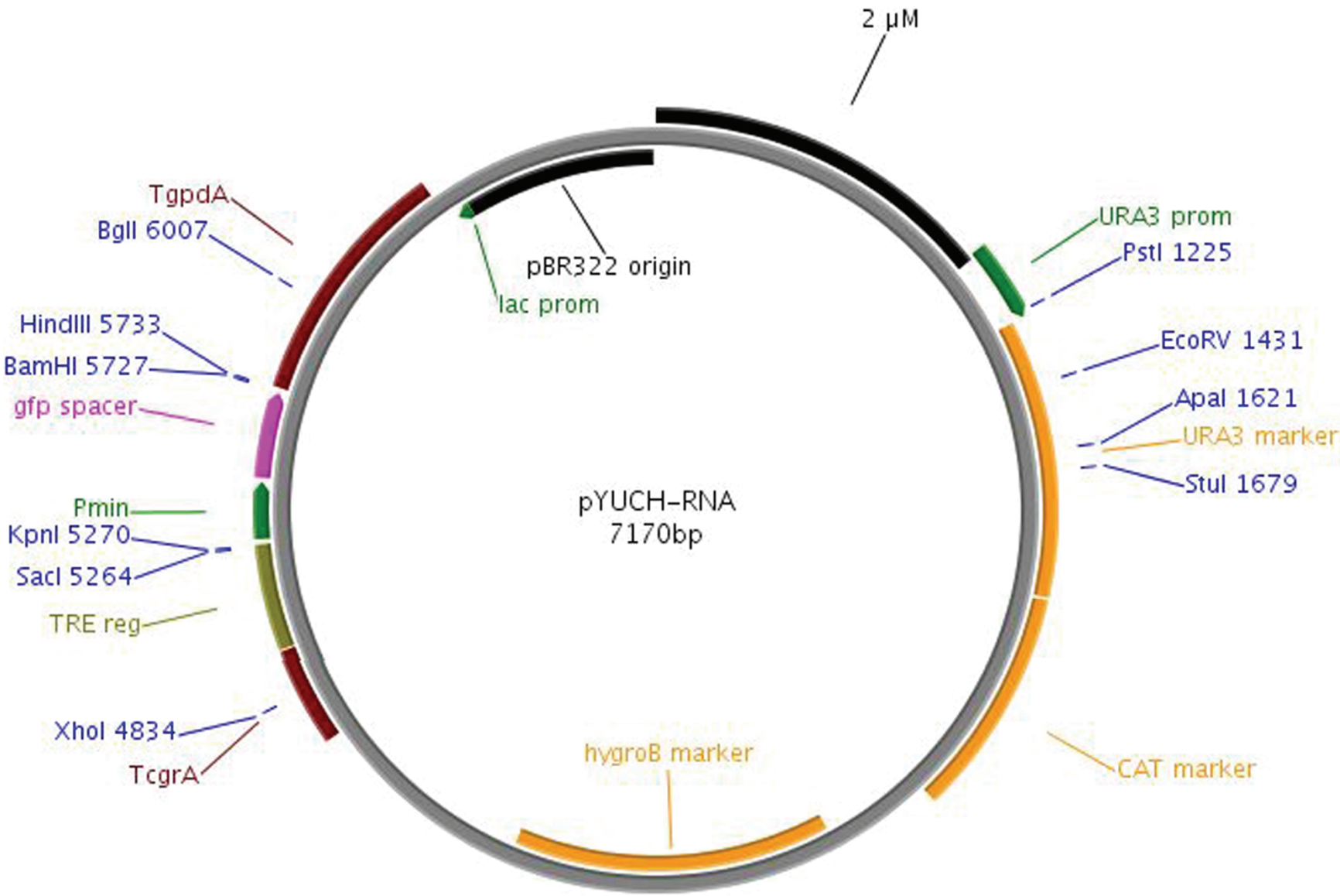

Figure 12 (cont'd)

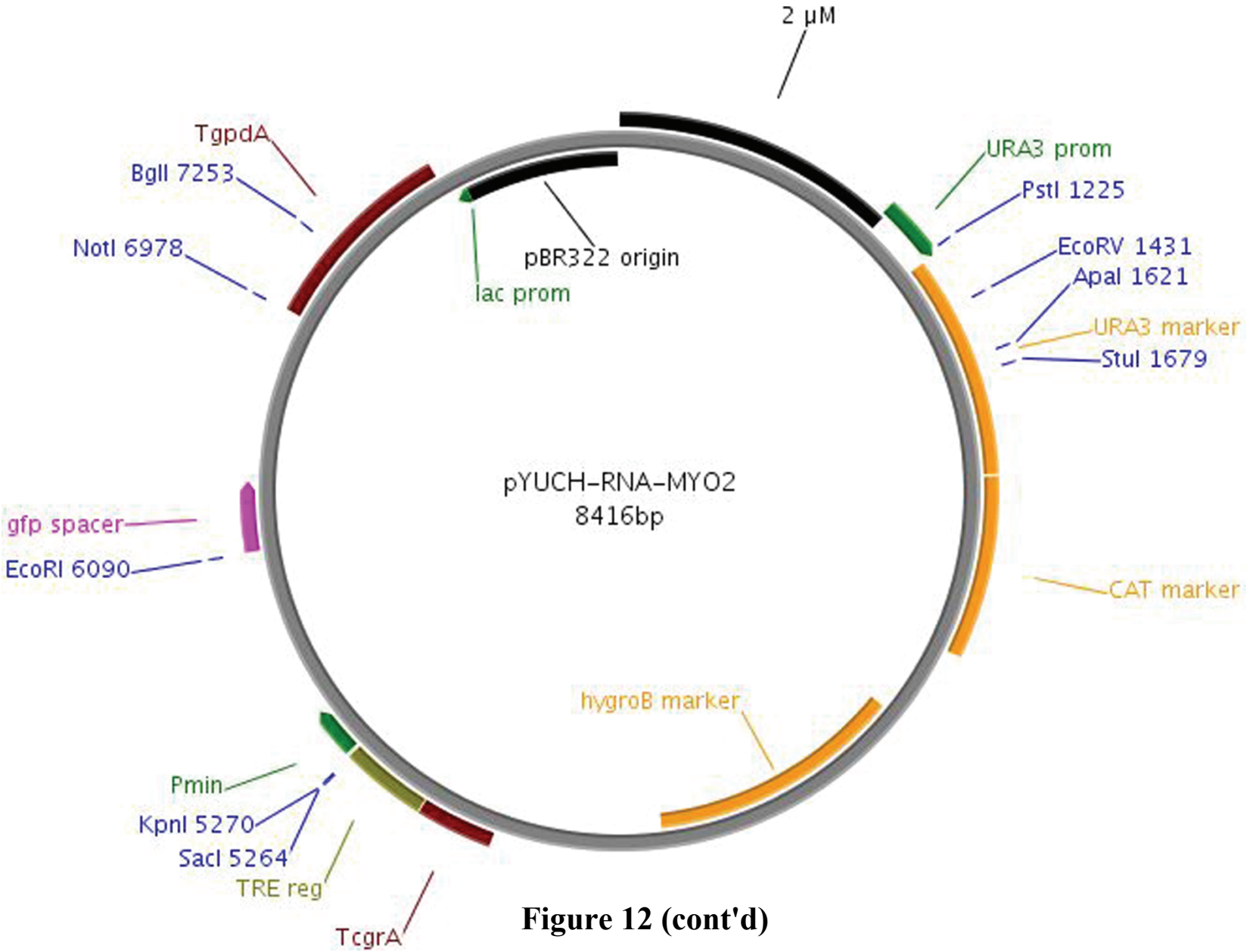

Figure 12 (cont'd)

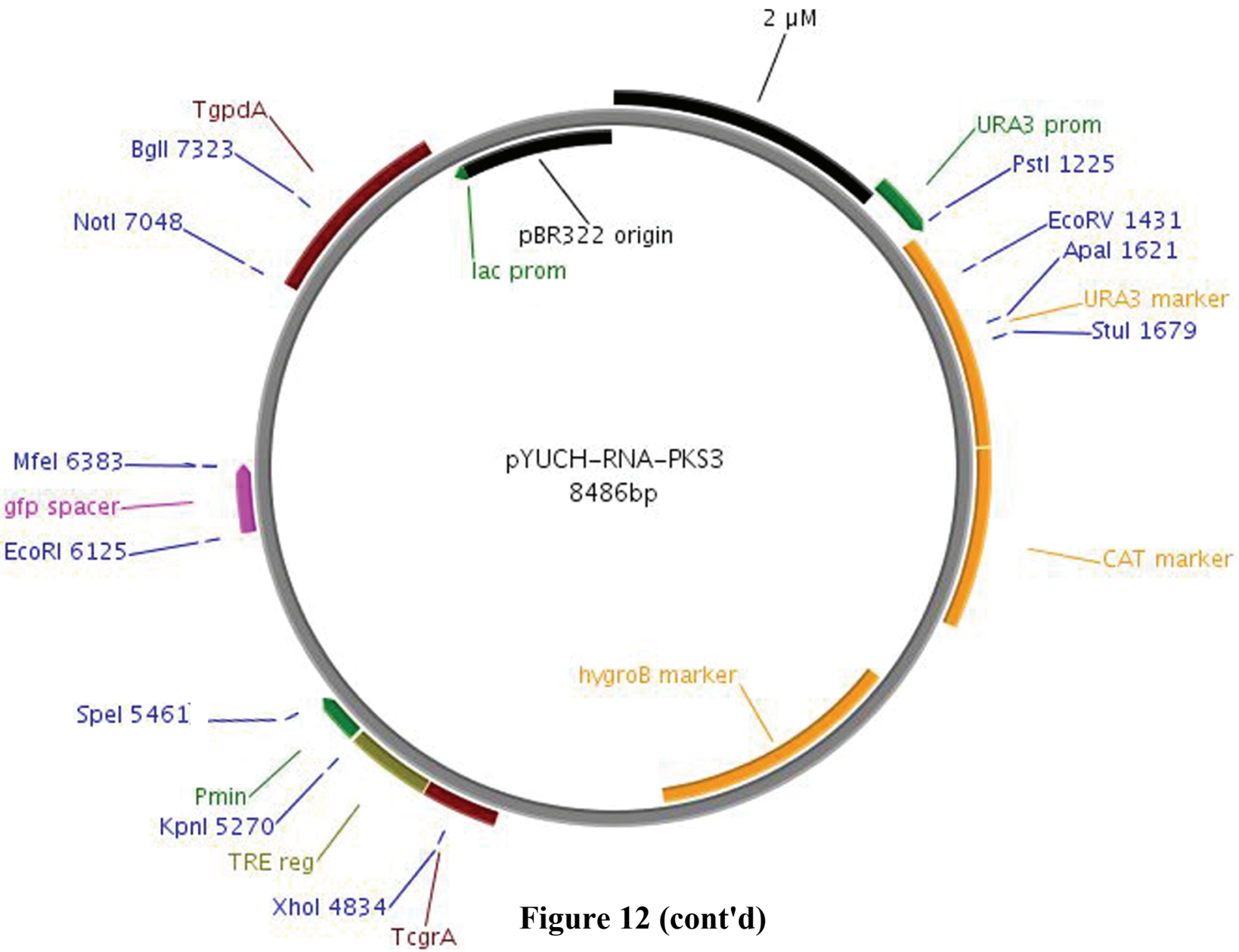

Figure 12 (cont'd)

Figure 12 (cont'd)

Figure 12. Plasmid maps of constructed vectors (pages 88-91). Unique sites of commonly used restriction enzymes are shown with their nucleotide position. For interpretation of the reference to color in this and all other figures, the reader is referred to the electronic version of this dissertation.

to the 5' and 3' ends of the T*cgrA-tetO7*-eRNAi fragment, respectively. The overlapping pYUCH-amp and T*cgrA-tetO7*-eRNAi fragments were cotransformed into *S. cerevisiae* to generate pYUCH-RNA by homologous recombination.

Construction of targeted RNAi vectors pYUCH-RNAi-Myo2 and pYUCH-RNAi-PKS3. A 644 bp fragment of *MYO2* (FGSG_07469) and a 658 bp fragment of *PKS3* (FGSG_17168) were amplified by PCR (Code fragments: fragments to be cloned in one orientation) using primers Myo2 Code-F and Myo2 Code-R and PKS3 Code-F and PKS3 Code-R, respectively. The same fragments were also amplified by primers MyoC Temp-F and Myo2 Temp-R and PKS3 Temp-F and PKS3 Temp-R (Temp fragments: fragments to be cloned in the reverse orientation of the Code fragments), but differ from the Code fragments in the restriction enzyme restriction sites contained in 5' tails of the primers. When the Code fragment is ligated into the first IRT cloning site and the Temp fragment is ligated into the second IRT cloning site, the Code and Temp gene fragments will be in the reverse orientation of each other, thus generating the hairpin loop. The Code-F and Code-R primers for both Myo2 and *PKS3* contain 5' tails with a EcoRI or SpeI recognition site and the next 9 bp of the genomic sequence, respectively. Similarly, the Temp-F and Temp-R primers contain 5' tails containing a NotI or MfeI recognition site and the next 9 bp of the genomic sequence. The entire pYUCH-RNA plasmid except some sequence between and including the NcoI and AscI restriction sites of the first IRT cloning site was amplified by PCR (pCode fragment) using primers pCode-F and pCode-R that are complementary to the 25 and 24

bp immediately downstream of the AscI site and upstream of the NcoI site followed by a EcoRI or SpeI recognition site and the next 9 bp of the pYUCH-eRNAi sequence, respectively. Double EcoRI-HF and SpeI (New England Biolabs) digests on the pCode, Myo2 Code, and PKS3 Code fragments were, individually, performed and purified as previously described. The digests were purified using the DNA Clean & Concentrator-5 kit (Zymo Research, Irvine, CA), and the digested pCode fragment was ligated to the digested Myo2 and PKS3 fragments separately and each ligation was transformed into *E. coli* to generate pYUCH-RNAi-Myo2c and pYUCH-RNAi-PKS3c. Primers pTemp-F and pTemp-R were used to amplify the entire from pYUCH-RNAi-Myo2c and from pYUCH-RNAi-PKS3c plasmids by PCR (pTemp fragments) except for sequence between the BamHI and HindIII recognition sites in second IRT cloning site. NotI-HF and MfeI-HF (New England Biolobs) double digestions of the Myo2 and *PKS3* pTemp and Temp fragments were performed and purified. The digested *MYO2* pTemp and Temp fragments and *PKS3* pTemp and Temp fragments were ligated and transformed into *E. coli* to isolate the final doxycycline inducible RNAi vectors pYUCH-RNAi-Myo2 and pYUCH-RNAi-PKS3 that were used to transform PH-1 protoplasts. Vectors were constructed as detailed with at least two clones of the desired construct obtained from each *E. coli* transformation.

Genetic transformations

Transformation of chemically competent One Shot TOP10 *E. coli* (Life Technologies) with a ligation reaction was performed per the manufacturer's protocol and transformed cells were spread on LB agar with an appropriate antibiotic for selection. Single transformed colonies were transferred to LB broth amended with the appropriate antibiotic for further screening. Competent cells of *S. cerevisiae* strain FY834 were prepared and transformed using the Frozen-

EZ Yeast Transformation II Kit (Zymo Research) per the manufacturer's protocol. Polyethylene glycol mediated transformation of *F. graminearum* protoplasts was performed and hygromycin B resistant (hyg^R) strains were selected as previously described (Gaffoor et al., 2005). All transformations were performed with undigested plasmid. To identify transformants containing complete constructs, DNA extracted from putative transformants was used as template for PCR with primers Pmin-F and TcgrA-R for the rtTA2s-M2 construct in p502 and TcgrA-F and GFP-R and GFP-F and Term-R for the doxycycline inducible IRT RNAi constructs in pYUCH-RNAi-Myo2 and pYUCH-RNAi-PKS3. Primers Pmin-F and PKS3 Code-R were also paired individually with GFP-R for PCR using pYUCH-RNAi-PKS3 transformant P3-1 DNA as template. Amplification from the GFP spacer sequence to the start or end of the construct was performed because PCR across both IRT sequences was unsuccessful using either plasmid or transformant DNA as the template likely because the IRT sequences anneal to each during thermocycling. To determine if the plasmid insertions affect sexual development, all hyg^r transformants were grown on carrot agar and sexual development was induced and monitored by visual examination of the cultures and microscopic examination of perithecium squash mounts during the course of development.

Analysis of sexual crosses

*F. graminearum c*rosses were performed individually between *NIT3* nitrate-utilizing (nit^+) strains, containing the doxycycline inducible RNAi expression construct from pYUCH-RNAi-Myo2 or from pYUCH-RNAi-PKS3, and a *nit3* non-nitrate-utilizing mutant (nit^-) strain, containing the rtTA2s-M2 expression construct, which have different growth phenotypes on

minimal medium supplemented with tergitol and L(-)sorbose (MMTS; Bowden and Leslie, 1999). Ascospores in cirrhi from individual perithecia were suspended in water and spread onto MMTS. Progeny from recombinant perithecia were identified as MMTS plates containing nearly equal numbers of progeny displaying the nit^+ and nit^- growth phenotypes. Nit^+ progeny were selected from these plates and individually transferred to Czapek-Dox agar (Thom and Church, 1926) amended to 450 µg/L hygromycin B, and strains displaying vigorous growth were then transferred to V8 agar for maintenance and subsequent phenotypic characterization, DNA extraction, and macroconidia production. PCR analysis of DNA extracted from the progeny was used to screen progeny for those that contained both the rtTA2s-M2 and the doxycycline inducible RNAi expression constructs, using the same primers for the constructs used to verify transformants above.

Characterization of the effects of doxycycline on PH-1 and inducible RNAi strains

To determine the effects of doxycycline on *F. graminearum* vegetative growth, PH-1, Myo2-2, Myo2-5, and Myo2-7 were grown on carrot agar and carrot agar amended to 200 µg/ml doxycycline, which is well above the minimum 15 µg/ml doxycycline found to effectively induce expression of an *hph* marker using the rtTA2s-M2 and *tetO*$_7$-Pmin system in *A. nidulans* (Vogt et al., 2005). Hyphae from the strains were center inoculated and the colony diameters were measures after 24 and 48 hr of growth. The first day's growth was subtracted from the second day's growth to give the growth rate. The effect of doxycycline on sexual development was also examined. Sexual development was induced on carrot agar normally for each strain, and at 48 hr post-induction, 12 mm diameter circles were removed from the cultures, trimmed to ~5 mm thickness, and transferred to carrot agar amended to 200 µg/ml doxycycline and to carrot

agar amended to 400 µg/ml doxycycline. Squash mounts of perithecia of all strains were made at 120, 144, and 168 hr post-induction and were examined by microscopy

TAIL-PCR

Three sets of TAIL-PCR reactions were performed on a transformant P3-1 using a standard protocol modified as follows: 98°C for 45 s initial melting step and 20 s for all other cycles in all reactions; and 60°C as the annealing temperature for the construct specific primers (Liu and Whittier, 1994; Nakayama et al., 2001). All three sets consisted of five reactions that individually used degenerate primers AD2, AD3, AD5, AD7, and AD8 (Nakayama et al., 2001) and nested primers specific for the *PKS3* doxycycline inducible RNAi construct. The first set used specific primers 3' GFP-R, GFP-R. and 5' GFP-R in the primary, secondary, and tertiary TAIL-PCR reactions, respectively. The second and third sets used the primers PKS3 TAIL1, PKS3 TAIL2, and Pmin TAIL3 and PKS3 TAIL2, Pmin TAIL3, and Pmin TAIL4 for the primary, secondary, and tertiary reactions, respectively. The secondary and tertiary reactions were size-fractionated by gel electrophoresis with the reactions for the same AD primer in adjacent lanes. Amplicons in the tertiary reactions that were of an appropriately smaller size than bands in the secondary reactions were gel purified and submitted for sequencing with the specific primer used in the tertiary reaction. Samples were sequenced by Michigan State University's Research Technology Support Facility using an ABI PRISM 3730 Genetic Analyzer (Applied Biosystems, Carlsbad, CA).

Statistical Analysis

To assess the significance of intragroup variation and intergroup interaction, analysis of variance

was performed using the R Language and Environment for Windows (R Development Core Team, 2010).

Microscopy and Imaging

A Leica DM LB microscope (Leica Microsystems GmbH, Wetzlar, Germany) with differential interference contrast (DIC) capabilities was used to observe samples and images were captured with a Zeiss AxioCam MRc color camera using AxioVision 4.8.2 (Göttingen, Germany). Non-microscopic images were captured with a Nikon Coolpix 995 (Tokyo, Japan). Image processing, manipulation, and annotation were performed with ImageJ (Abramoff et al., 2004) or Adobe Photoshop CS2 (San Jose, CA).

Results

Six hyg^r transformants were recovered from transformation of wild-type protoplasts with pYUCH-RNAi-Myo2, the *MYO2* targeting doxycycline inducible RNAi vector. PCR analysis identified one transformant, designated M2-II, which contained the full Myo2 RNAi construct, when induced on carrot agar. Sexual development of M2-II was normal. Six nit^- hyg^r transformants were isolated from transformation of PH-1 55 (nit^-) protoplasts with p502 containing the rtTA2s-M2 expression construct conferring transformants with constitutive expression of the doxycycline responsive transactivator and the selectable *hph* marker. PCR analysis of the PH-1 55 nit+ colonies revealed one transformant, designated 502-4, that

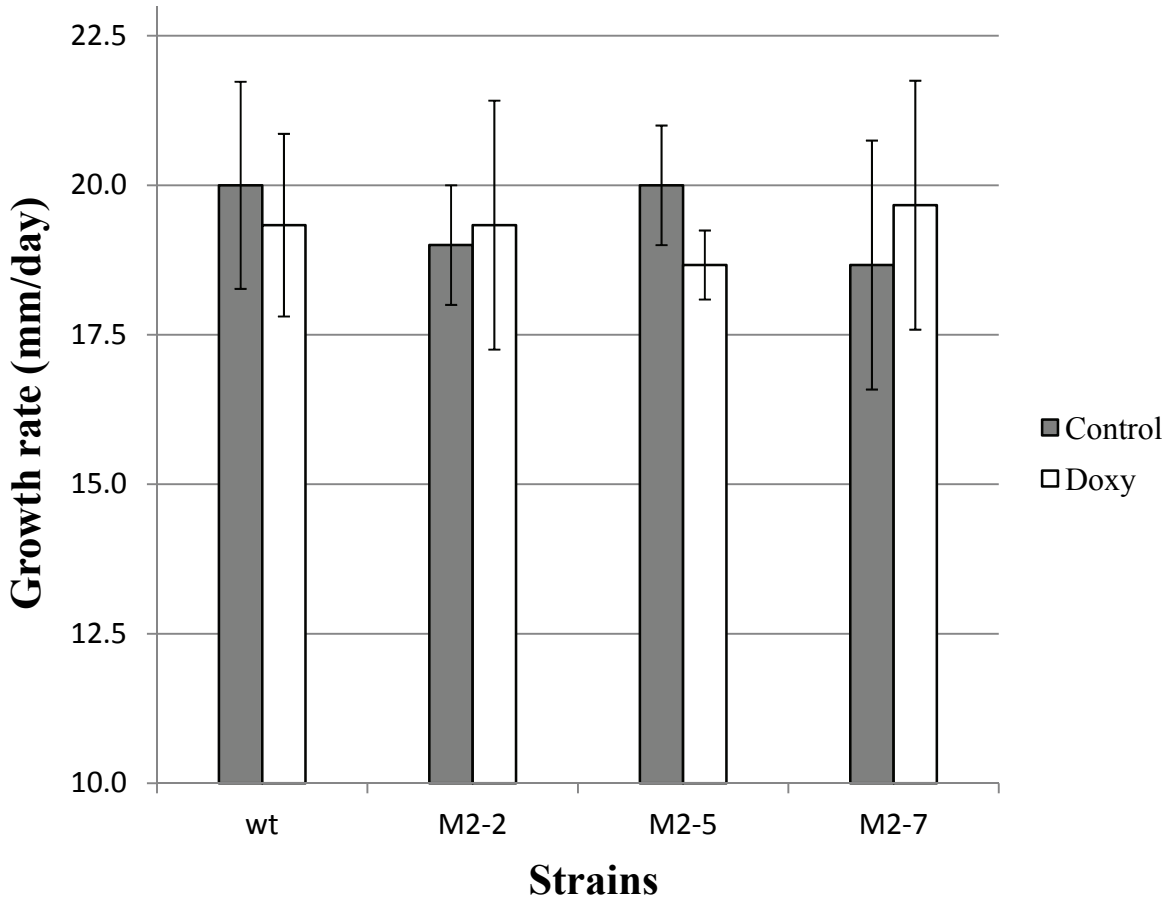

Figure 13. Growth rates of wild-type *MYO2* RNAi strains. Growth rates on carrot agar for all strains were not significantly different from each other with or without doxycycline treatment.

contained the full rtTA2s-M2 expression construct. Sexual development of 502-4 was similar to wild-type PH-1.

M2-II was crossed to 502-4, and 8 nit+ progeny were recovered with 5 progeny being hyg^r. PCR analysis indicated that 3 nit+ hyg^r progeny harbored both the p502 rtTA2s-M2 expression construct and the full pYUCH-RNAi-Myo2 doxycycline inducible RNAi expression construct and were designated M2-2, M2-7, and M2-5. The growth rates of PH-1, M2-2, M2-5, and M2-7 on carrot agar and carrot agar amended to 200µg/ml doxycycline were assessed (Fig. 2). No significant differences were found between the strains with or without doxycycline treatment.

Sexual development of the strains was induced on carrot agar, and at 72 hr post-induction, portions of the cultures were transferred to carrot agar with 200 µg/ml doxycycline. Development of both sets of cultures was monitored by microscopic examination of perithecia squash mounts (Figure 3). On carrot agar, all strains developed normal perithecia.

For the cultures transferred to carrot agar with 200 µg/ml doxycycline, sexual development was normal for wild-type, but was altered in M2-2, M2-5, and M2-7, which exhibited phenotypes of different severity (M2-7 > M2-2 >M2-5; Figure 3). Exposure to doxycycline slowed development in all three strains. Specifically, croziers (young, hook-shaped asci) remained for an extended time before developing further into asci and were still numerous at 168 hr post-induction, normally beyond the time when asci are fully mature in wild-type (Trail and Common, 2000; Hallen et al, 2009). Asci that were delayed in development were filled with vesicles even at 168 hr post-induction, the time-point at which normal maturation is complete. Delimitation and development of ascospores in these strains was also altered with a combination of reduced delimitation and abnormal morphology of ascospores. Asci of wild-type are normally filled with vesicles during early stages of development, but they become more sparse as development progresses until there are almost no vesicles in the ascus cytosol at ascus maturity (144 - 168 hr). In addition to those involved in ascospore delimitation, these vesicles merge with the outer ascus membrane and are the source of material for ascus elongation (Trail and Common, 2000). Development of all strains, including wild-type, transferred to carrot agar amended to 400 µg/ml doxycycline was slowed (data not shown), so these cultures were not used further. Transfer of M2-2, M2-5, and M2-7 cultures from carrot agar with 20 µg/ml doxycycline to unamended carrot agar at 168 hr post-induction resumed normal development (personal observation).

Five hyg^r transformants were recovered from a single transformation experiment of wild-type protoplasts with pYUCH-RNAi-PKS3, the doxycycline inducible RNAi vector targeting *PKS3*. Sexual development of the 5 transformants was normal. However, strain P3-1 lacked the dark perithecium pigment that requires *PKS3* function in order to be produced (Fig. 4). PCR analysis on extracted P3-1 DNA failed to produce an amplicon with primers TcgrA-F and GFP-R. Approximately sized amplicons, of 990 and 756 bp, were produced using primers Pmin-F and PKS3 Code-R, individually, with GFP-R, respectively. These results suggest that only some of the T*cgrA* sequence inserted with the rest of the construct during integration of pYUCH-RNAi-PKS3 into the *F. graminearum* genome. To determine the extent of the T*cgrA*-Pmin end of the *PKS3* construct that integrated and the adjacent genomic sequence, three sets of TAIL-PCR reactions were performed. The first set of reactions used nested primers that were all complementary to the *gfp* spacer of the RNAi construct. An amplicon in the AD8 tertiary reaction was purified and sequenced. The sequence contained *gfp* sequence, the EcoRI recognition site used for cloning, and then *PKS3* Code fragment (see methods) sequence but did not reach Pmin sequence.

Discussion

Doxycycline induced IRT expression targeting *MYO2* effectively reduced the rate of crozier to ascus transition, ascus maturation, and disrupted ascospore delimitation, demonstrating that Myo2 function is important for proper ascus and ascospore development, but not for filamentous growth. These results share similarities with previous results in *S. macrospora* using Cytochalasin D, an inhibitor of actin polymerization, and, separately, the actin-myosin interaction inhibitor 2,3-butanedione monoxime (BDM), which found that both actin and

myosins are required for crozier developmental progression and play a role in ascospore delimitation and development (Thompson-Coffe and Zickler, 1993). However, BDM has been found to inhibit ATPase acitvity of type II myosins, but not type I or type V. The specific targeting of *MYO2* and the ability to target the other *F. graminearum* myosins will allow the individual examination of their function in ascus development.

Uninduced expression of a *PKS3* targeting RNAi vector resulted in perithecia lacking pigment, a phenotype seen in *PKS3* knockouts (Gaffoor et al., 2005). Although the genetic location of the insertion is not yet known, it is likely that transcription read-through from a gene in the 5' direction from Pmin or transcriptional activation by an enhancer may be involved in the loss of *PKS3* function. These results suggest that the doxycycline inducible RNAi vectors can be used without the rtTA2s-M2 expression vector for developmentally specific enhancer trapping provided that a suitable target for RNAi with a useful phenotype is known.

The tet-ON inducible expression is known to display some leaky expression (Ostap, 2002), and Vogt et al. (2005) found that only 10-15% of strains with both rtTA2s-M2 and an inducible expression construct were inducible. However, the variation in the severity of the phenotypes between M2-2, M2-5, and M2-7 is somewhat different given that they are siblings from the same cross and progeny from the same insertion event. The leaky expression of the tet-On system refers to expression from Pmin without addition of doxycycline. Here that would result in RNAi against *MYO2*, but this effect was not seen in M2-2, M2-5, and M2-7, which developed similarly to wild-type when doxycycline was absent. The differences seen with these strains may result from differing amounts of the reverse transactivator rtTA2s-M2 being produced and, thus, differing capability of these strains to respond to doxycycline. Though PH-1 55 was generated from PH-1 and no noticeable phenotypic differences are seen between the

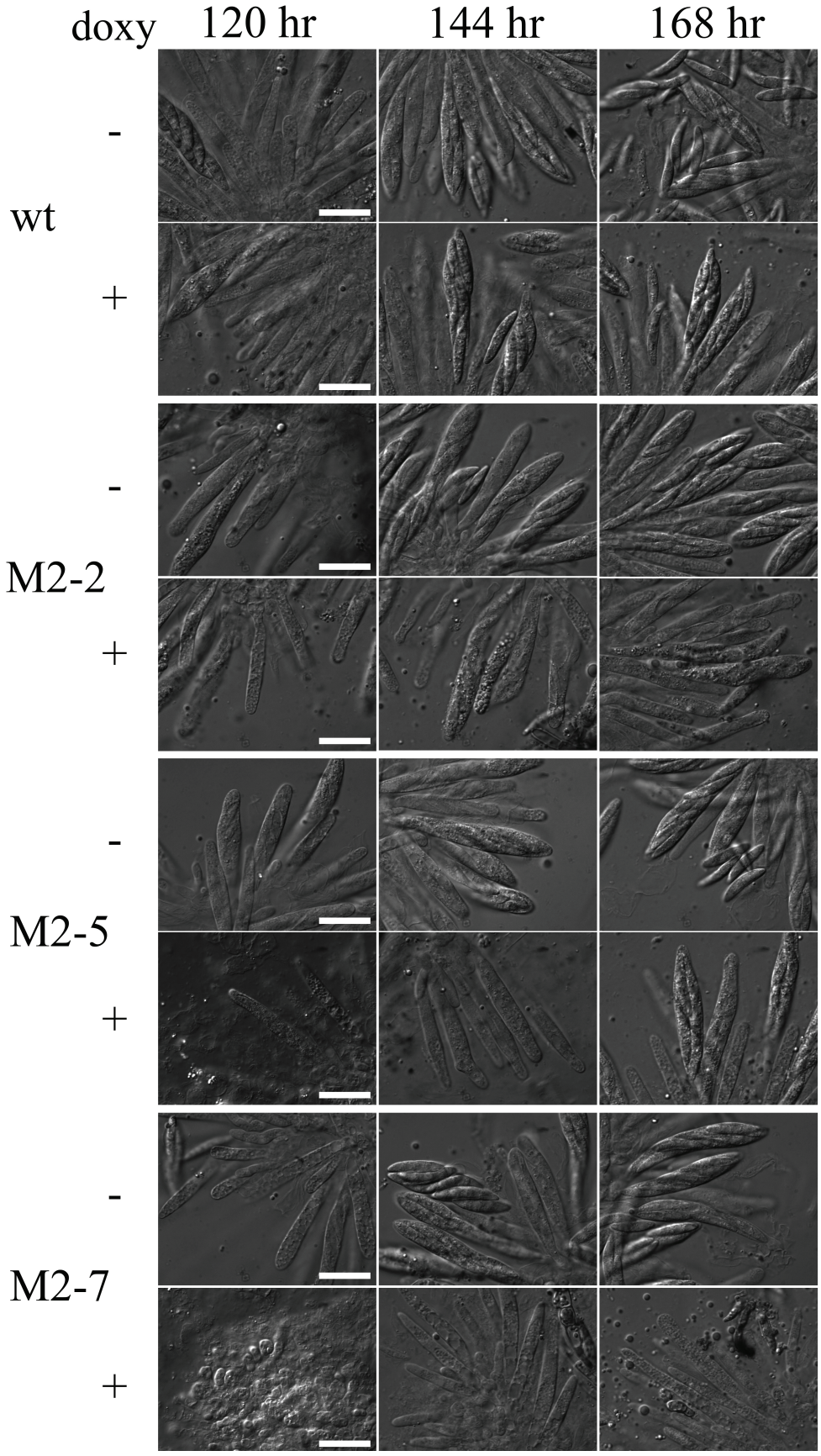

Figure 14

Figure 14 (cont'd)

Figure 14. Asci of wild-type and *MYO2* RNAi strains with or without doxycycline treatment. Wild-type is unaffected at all time points by doxycycline treatment. Strains M2-2, M2-5, and M2-7 develop normally on unamended carrot agar but development is slowed on carrot agar containing doxycycline. The effect is greatest in M2-7. Even at 168 post-sexual induction, there are many immature asci filled with vesicles and very few ascospores are developing. Scale is the same for all images, and scale bars = 20 µm.

strains other than nitrate utilization capability, there could be other genetic mutations present in PH-1 55 that segregated differently in three siblings. These results suggest other factors may be involved such as differences in genetic background or in epigenetic regulation from recombination during meiosis. While it would be interesting to know the cause of the differences seen here, they do not diminish the utility or versatility of doxycycline induced RNAi. The doxycycline induced expression system used here to can be used to influence gene expression both positively and negatively, expressing a desired gene or RNAi construct, respectively, and provides a powerful tool for investigations into essential or process essential genes in *F. graminearum* and other filamentous fungi.

Figure 15. Loss of perithecium pigment in P3-1. Sexual development was induced in co-culture of P3-1 and wild-type. The left side of the image is P3-1 with wild-type on the right. A P3-1 perithecium is indicated by the white arrowhead. The black arrow head points to a wild-type wt perithecium.

CONCLUSION

This work has provided insight into some of the pathways involved in *F. graminearum* growth and development and has generated tools for use in filamentous fungi. The results of the work presented here show that calcium signaling and myosin function play important roles in the sexual development of *F. graminearum*. Gene deletion strains of all three HACS and LACS components *MID1* and *CCH1* and *FIG1*, respectively, significantly reduce *F. graminearum* growth and development. There are likely more components to both of these calcium uptake systems. Fig1 is involved in importation of calcium, but it has no primary sequence or structural domains that suggest it functions as a calcium channel itself. Its role in membrane-membrane interaction seems a likely reason for the aborted perithecium development seen in the Δ*fig1* mutants. The mechanism and gene(s) directly involved in LACS calcium importation remain cryptic. *MID1* is also mostly thought to play a modulatory role in calcium uptake, but there are some results in studies of *S. cervisiae* that suggest it may form channels itself (Kanzaki et al., 1999; Locke et al., 2000; Tada et al., 2003). The role of *CCH1* is well established as a calcium channel orthologous to mammalian L-type voltage gated calcium channels, though the fungal members appear to have amino acid substitutions in the voltage sensing domains that may reduce voltage sensing (Liu and Gelli, 2008; Hong et al., 2010).

Future studies should be geared towards determining the other genes and proteins involved in the ascospore discharge mechanism. Is calcium regulation involved in their function as well? It is clear that *MYO2* is crucial for ascus development, but a direct role in discharge has not been examined yet. These results also show that a doxycycline inducible expression system can be utilized in this fungus to drive expression of a RNAi construct, and presumably, any other desired construct or gene whether an endogenous or transgenic sequence. Targeting the other two

F. graminearum myosins for RNAi during sexual development is partially completed and it will be interesting to see if they also are involved in sexual development. *FIG1* is also a prime target for gene expression knockdown by the doxycycline induced RNAi, because examination of its role in later stages of sexual development was not possible with deletion mutants. Other genes involved in membrane dynamics, cytoskeleton organization, and polarized growth are also candidate targets. Without the reverse transactivator, rtTA2s-M2, the T*cgrA tetO*$_7$-Pmin constructs could be used in enhancer trapping experiments, using either a reporter gene or an RNAi construct.

A working model of ascus development and ascospore discharge is presented in Fig. 1.

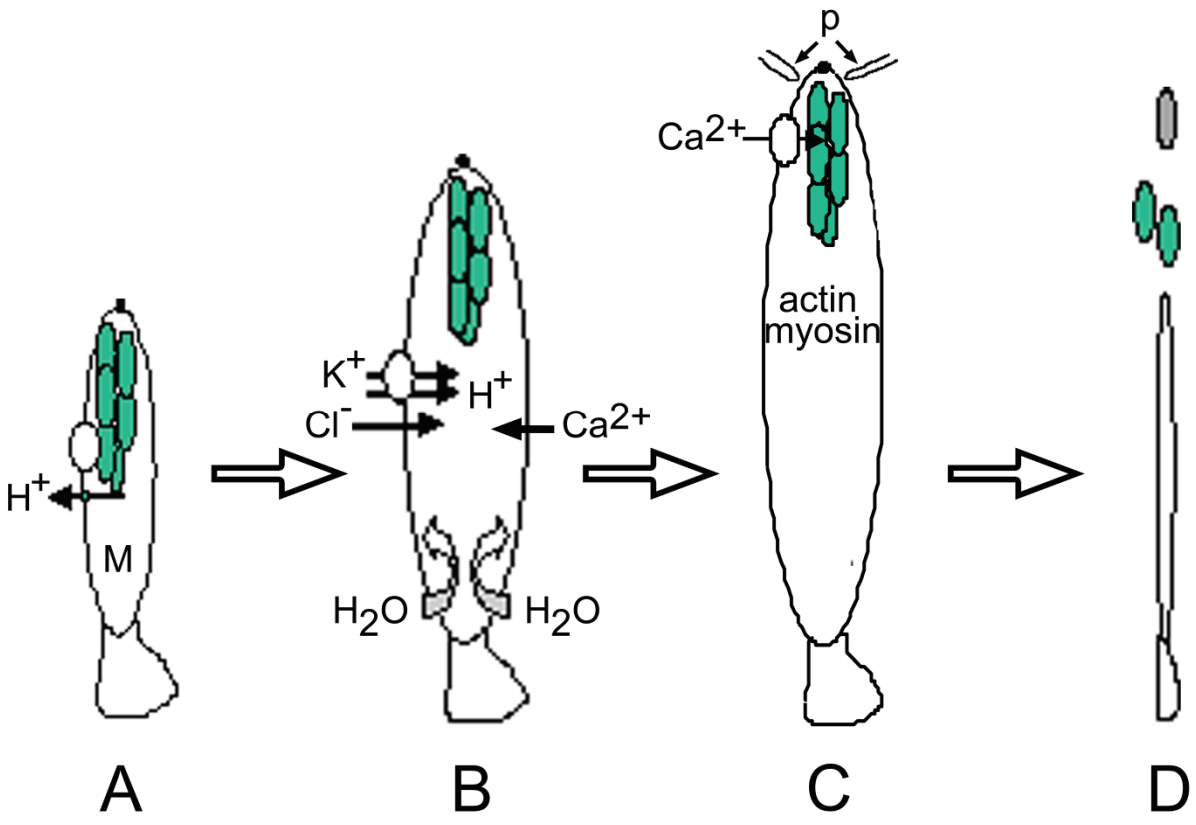

Figure 1. Working model of ascospore discharge. (A) Osmolyte primimg (B) Osmolyte accumulation and rapid ascus expansion. (C) Possible discharge trigger. (D) Forcible ejection of ascospores. Not to scale. M = mannitol, p = periphyses

Calcium or other signals activate a proton pumping ATPase. Mannitol buildup may be the result of the lipid catalysis that occurs during the middle to late stages of sexual development. Whether a calcium signal is involved is not known. The plasma membrane H^+-ATPase pumps H^+ ions out of the ascus. H^+ efflux drives the influx of K^+ and Cl^- ions into the ascus, and the increased concentration of mannitol drives the initial influx of water and ascus expansion. This expansion activates Mid1 and Cch1 in the ascus membrane, causing an influx if calcium. The Ca^{2+} influx activates calcineurin which interacts with Cch1 to decrease calcium influx, providing cytosolic calcium availability feedback. Actin reorganization during development may be influenced by calcium signals and allows the ascus to freely stretch. Increasing turgor pressure throughout the process may facilitate ascus expansion. As an expanding ascus reaches the ostiole, it comes into contact with the periphyses that line the inside of the ostiole. This contact may trigger mechanosensitive calcium influx through Mid1/Cch1. This calcium signal may induce further actin reorganization. Actin and myosins may be involved in ascospore discharge by the transportation of vesicles containing cell wall degrading enzymes to the ascus pore where they degrade the pore, by the generation or release of tension on actin filaments and myosins at the pore to either pull apart or allow the opening of the pore, respectively, or both mechanisms. It is also possible that enzymes secreted from the periphyses help degrade the ascus wall and pore from the outside. Regardless of the mechanism, the opening of the pore releases the ascospores. Further work remains to identify the genes involved in ascospore discharge and to clarify the proposed roles of the components of this working model of *F. graminearum* ascospore discharge.

REFERENCES

REFERENCES

Alberghina, A., and A. Benni. 1980. Different sensitivity to mitochondrial inhibitors of respiration in *Fusarium oxysporum* and *Fusarium solani*. Phytopathologische Zeitschrift. **99**:138-145.

Allbritton, N.L., T. Meyer, and L. Stryer. 1992. Range of messenger action of calcium ion and inositol 1,4,5-trisphosphate. Science **258**: 1812-1815.

Atanasoff, D. 1920. Fusarium-blight (scab) of wheat and other cereals. Journal of Agricultural Research **10**.

Armstrong. D.L. 1989. Calcium channel regulation by calcineurin, a Ca^{2+}-activated phosphatase in mammalian brain. Trends in Neurosciences **12**: 117-122.

Basile L. J., R. C. Willson, B. T. Sewell, and M. J. Benedik. 2008. Genome mining of cyanide-degrading nitrilases from filamentous fungi. Appl. Microbiol. Biotechnol. **80**: 427-435.

Bement, W.M., and M.S. Mooseker. 1995. TEDS Rule: A molecular rationale for differential regulation of myosins by phosphorylation of the heavy chain head. Cell Motility and the Cytoskeleton **31**: 87-92.

Bennett, J.W., and M. Klich. 2003. Mycotoxins. Clinical Microbiology Reviews **16**: 497-516.

Berridge, M.J., M.D. Bootman, and H.L. Roderick. 2003. Calcium Signalling: Dynamics, Homeostasis and Remodelling. Nat. Rev. Mol. Cell. Biol. **4**: 517-529.

Berridge, M.J. 2007. Calcium signalling, a spatiotemporal phenomenon. In: Calcium: a matter of life or death, Eds. J. Krebs and M. Michalak, Elsevier Science.

Beckett, A., and R.M. Crawford. 1973. The Development and Fine Structure of the Ascus Apex and its Role During Spore Discharge in *Xylaria longipes*. New Phytologist **72**: 357-369.

Biess, A., E. Korkotian, and D. Holcman. 2011. Barriers to Diffusion in Dendrites and Estimation of Calcium Spread Following Synaptic Inputs. PLoS Computational Biology **7**: e1002182. doi:10.1371/journal.pcbi.1002182

Bistis, G.N., 1981. Chemotropic Interactions between Trichogynes and Conidia of Opposite Mating-Type in Neurospora crassa. Mycologia. **73**: 959-975.

Bonila, M., K.K. Nastase, and K.W. Cunningham. 2002. Essential role of calcineurin in response to endoplasmic reticulum stress. The EMBO Journal **21**: 2343-2353.

Booth, C. 1971. The genus *Fusarium*. Commonwealth Mycological Institute, Kew, Surrey, England.

Bowden, R.L., and J. F. Leslie. 1999. Sexual recombination in *Gibberella zeae*. Phytopathology **89**: 182-188.

Brand, A., K. Lee, V. Veses, N. Gow. 2009. Calcium homeostasis is required for contact-dependent helical and sinusoidal tip growth in Candida albicans hyphae. Molecular Microbiology **71**: 1155-1164.

Brand, A., S. Shanks, V. Duncan, M. Yang, K. Mackenzie, and N. Gow. 2007. Hyphal orientation of *Candida albicans* is regulated by a calcium-dependent mechanism. Current Biology **17**: 347-352.

Brenner, J., N. Gomez-Ospina, and R. Dolmetsch. 2007. Temporal and spatial regulation of calcium-dependent transcription. In: Calcium: a matter of life or death, Eds. J. Krebs and M. Michalak, Elsevier Science.

Bucheli, T.D., F.E. Wettstein, N. Hartmann, M. Erbs, S. Vogelgsang, H-R. Forrer, and R.P. Schwarzenbach. 2008. *Fusarium* Mycotoxins: Overlooked Aquatic Micropollutants?. Journal of Agricultural and Food Chemistry **56**: 1029-1034.

Buller, A.H.R. 1909. Researches on Fungi. Longmans, Green and CO., London, England. 287 pp.

Burgess, L. w., Dodman, R. L, Pont, W. and Mayers, P. 1981. Fusarium diseases of wheat, maize and grain sorghum in Eastern Australia. In Fusarium: Diseases, Biology, and Taxonomy, P.E. Nelson, T.A. Toussoun and R.J. Cook eds., The Pennsylvania State University Press, University Park, PA.

Canero, E., J.C. Ribas, B. Garcia, A. Duran, and Y. Sanchez. 2000. *Schizosaccharomyces pombe* ehs1p is involved in maintaining cell wall integrity and in calcium uptake. Mol. Gen. Genet. **264**: 173-183.

Cappellini, R.A., and J.L. Peterson. 1965. Macroconidium formation in submerged cultures by a non-sporulating strain of *Gibberella zeae*. Mycologia **57**: 962-966.

Carafoli, E.L. 2005. Calcium - a universal carrier of biological signals. The FEBS Journal **272**: 1073-1089.

Carafoli, E. 2007. The unusual history and unique properties of the calcium signal. New Comprehensive Biochemistry **41**: 3-22.

Carafoli, E., L. Santella, D. Branca, and M. Brini. 2001. Generation, control, and processing of cellular calcium signals. Critical Crit Rev Biochem Mol Biol. **36**:107-260.

Carroll, A.M., J.A. Sweigard, and B. Valent. 1994. Improved Vectors for Selecting Resistance to Hygromycin. Fungal Genetics Newsletter **41**: 22.

Carroll, G.C. 1969. A study of the fine structure of ascosporogenesis in *Saccobolus kerverni*. Arch Mikrobiol **66**: 321-339.

Catlett, N.L., B. Lee, O.C. Yoder, and B.G. Turgeon. 2003. Split-marker recombination for efficient targeted deletion of fungal genes. Fungal Genetics Newsletter **50**: 9-11.

Chongo G., B.D. Gossen, H.R. Kutcher J. Gilbert, T.K. Turkington, M.R. Fernandez, and D. Mclaren. 2001. Reaction of seedling roots of 14 crop species to *Fusarium graminearum* from wheat heads. Canadian Journal of Plant Pathology **23**: 132-137.

Chrismas, M. 1980. Ascospore Discharge and Germination in *Xanthoria Parietina*. The Lichenologist **12**: 403-405.

Clapham, D.E. 2007. Calcium Signaling. Cell **131**: 1047-1058.

Clarkson, J., J. Staveley, K. Phelps, C. Young, and J. Whipps. 2003. Ascospore release and survival in *Sclerotinia sclerotiorum*. Mycological Research **107**: 213-222.

Connorton, J.M., K.D. Hirschi, and J.K. Pittman. 2011. Mechanism and Evolution of Calcium Transport Across the Plant Plasma Membrane. In: The Plant Plasma Membrane, Eds. A.S. Murphy, B. Schulz, and W. Peer, Springer.

Coons, G.H. 1918. Twentieth Annual Report of The Michigan Academy of Science. Fort Wayne Printing Company, Fort Wayne, IN.

Courchesne, W., and S. Ozturk. 2003. Amiodarone induces a caffeine-inhibited, MID1-depedent rise in free cytoplasmic calcium in *Saccharomyces cerevisiae*. Molecular Microbiolgy **47**: 223-234.

Courchesne, W.E., C. Vlasek, R. Klukovich, and S. Coffee. 2011. Ethanol induces calcium influx via the Cch1-Mid1 transporter in *Saccharomyces cerevisiae*. Arch Microbiol **193**: 323-334.

Craig, R., and J.L. Woodhead. 2006. Structure and function of myosin filaments. Current Opinion in Structural Biology **16**: 204-212.

Cyert, M.S. 2001. Genetic analysis of calmodulin and its targets in *Saccharomyces cerevisiae*. Annual Review of Genetics **35**: 647-672.

Czymmek, K.J., and K.L. Klomparens. 1992. The ultrastructure of ascosporogenesis in freeze-substituted *Thelebolus crustaceus:* enveloping membrane system and ascospore initial development. Canadian Journal of Botany **70**: 1669-1683.

Dänicke, S., K.-P. Brüssow, H. Valenta, K.-H. Ueberschär, U. Tiemann, and M. Schollenberger. On the effects of graded levels of *Fusarium* toxin contaminated wheat in diets for gilts on feed intake, growth performance and metabolism of deoxynivalenol and zearalenone. Molecular Nutrition and Food Research **49**: 932-943.

Davis, R.H. 2000. *Neurospora*. Contributions of a model organism. Oxford University Press, New York.

Davis, R.L., and D. de Serres. 1970. Genetic and microbial research techniques for *Neurospora crassa*. Methods Enzymology **27A**: 79-143.

DeBary, A. 1887. Comparative Morphology and Biology of the Fungi Mycetozoa and Bacteria. Clarendon Press, Oxford.

Demaurex, N., and C. Distelhorst. 2003. Apoptosis - the calcium connection. Science **300**: 65-67.

Desjardins, A.E., R.H. Proctor, G. Bai, S.P. McCormick, G. Shaner, G. Buechley, and T.M. Hohn. Reduced virulence of trichothecene-nonproducing mutants of *Gibberella zeae* in wheat field tests. Molecular Plant-Microbe Interactions **9**: 775-781.

Desnos, C., S. Huet, and F. Darchen. 2007. 'Should I stay or should I go?': myosin V function in organelle trafficking. Biology of the Cell **99**: 411-423.

Desrivières, S., F.T. Cooke, H. Morales-Johansson, P.J. Parker, and M.N. Hall. 2002. Calmodulin controls organization of the actin cytoskeleton via regulation of phosphatidylinositol (4,5)-bisphosphate synthesis in *Saccharomyces cerevisiae*. Biochemical Journal **366**: 945-951.

Di Tommaso, P., S. Moretti, I. Xenarios, M. Orobitg, A. Montanyola, J.M. Chang, J.F. Taly, and C. Notredame. 2011. T-Coffee: a web server for the multiple sequence alignment of protein and RNA sequences using structural information and homology extension. Nucleic Acids Research **39**: W13-W17.

Dill-Macky, R., and R.K Jones. 2000. The effect of previous crop residues and tillage on Fusarium head blight of wheat. Plant Disease **84**: 71-76.

Dill-Macky, R., and B. Salas. 2002. Effect of cereal residue burning on the incidence and stratified distribution of Fusarium graminearum and Cochliobolus sativus in wheat and barley plants. In: 2002 National Fusarium Head Blight Forum Proceedings. East Lansing, MI, USA: Michigan State University, 140.

Dodge, B.0. 1935. Mechanics of Sexual Reproduction in Neurospora. Mycologia. **27**: 418-438.

Dorn, G.W.II. 2009. Apoptotic and non-apoptotic programmed cardiomyocyte death in ventricular remodelling. Cardiovascular Research **81**: 465-473.

Erdman, S.E., L. Lin, M. Malczynski, and M. Snyder. 1998. Pheromone regulated genes required for yeast mating differentiation. J. Cell Biol. **140**:461-483.

Fairhead, C., A. Thierry, F. Denis, M. Eck, and B. Dujon. 1998. 'Mass-murder' of ORFs from three regions of chromosome XI from *Saccharomyces cerevisiae*. Gene **223**: 33-46.

Fairhead, C., B. Llorente, F. Denis, M. Soler, and B. Dujon. 1996. New vectors for combinatorial deletions in yeast chromosomes and for gap-repair cloning using 'split-marker' recombination. Yeast **12**: 1439-1457.

Fischer, M., J. Cox, D.J. Davis, A. Wagner, R. Taylor, A.J. Huerta, and N.P. Money. New information on the mechanism of forcible ascospore discharge from *Ascobolus immersus*. Fungal Genetics and Biology **41**: 698-707.

Fischer, M., N. Schnell, J. Chattaway, P. Davies, G. Dixon, and D. Sanders. 1997. The *Saccharomyces cerevisiae* CCH1 gene is involved in calcium influx and mating. Federation of European Biochemical Societies Letters **419**: 259-262.

Fernando, W.G.D., J.D. Miller, W.L. Seaman, K. Seifert, and T.C. Paulitz. 2000. Daily and seasonal dynamics of airborne spores of *Fusarium graminearum* and other *Fusarium* species sampled over wheat plots. Canadian Journal of Botany **78**: 497-505.

Franca-Koh, J., Y. Kamimura, and P. Devreotes. 2006. Navigating signaling networks: chemotaxis in *Dictyostelium discoideum*. Current Opinion in Genetics & Development **16**: 333-338.

Fujisaki, H., J.P. Albanesi, and E.D, Korn. 1985. Experimental Evidence for the Contractile Activitoife sA canthamoeba Myosins IA and IB. The Journal of Biological Chemistry **260**: 11183-11189.

Gaffoor, I., D.W. Brown, R. Plattner, R.H. Proctor, W. Qi, and F. Trail. 2005. Analysis of the polyketide synthase genes in the filamentous fungus *Gibberella zeae* (anamorph *Fusarium graminearum*). Eukaryotic Cell **4**: 1926-1933.

Glass, N.L., S.J. Vollmer, C. Staben, J. Grotelueschen, R..L Metzenberg and C. Yanofsky. 1988. DNAs of the two mating-type alleles of *Neurospora crassa* are highly dissimilar. Science **241**:570-573.

Gouy M., S. Guindon, and O.Gascuel. 2010. SeaView version 4: a multiplatform graphical user interface for sequence alignment and phylogenetic tree building. Molecular Biology and Evolution **27**: 221-224.

Gregory, P.H., and O.J. Stedman. Spore dispersal in *Ophiobolus graminis* and other fungi of cereal foot rots. Transactions of the British Mycological Society **41**: 449-456.

Groppi, S., F. Belotti, R.L. Brandão, E. Martegania, and R. Tisi. 2001. Glucose-induced calcium influx in budding yeast involves a novel calcium transport system and can activate calcineurin. Cell Calcium **49**:376-386.

Guenther, J., H.E. Hallen-Adams, H. Bücking, Y. Shachar-Hill, and F. Trail. 2009. Triacylglyceride metabolism by *Fusarium graminearum* during colonization and sexual development on wheat. Molecular Plant-Microbe Interactions **22**: 1492-1503.

Guenther, J. and F. Trail. 2005. The development and differentiation of G*ibberella zeae* (anamorph: *Fusarium graminearum*) during colonization of wheat. Mycologia **97**: 229-237.

Hackett, C.J., and K.C. Chen. 1976. Ultrastructure of developing ascospores in *Sordaria brevicollis*. Journal of Bacteriology **126**: 883-894.

Hallen H.E., M. Huebner, S.H. Shiu, U. Güldener, and F. Trail. 2007. Gene expression shifts during perithecium development in Gibberella zeae (anamorph Fusarium graminearum), with particular emphasis on ion transport proteins. Fungal Genet. Biol. **44**: 1146-56.

Hallen, H., and F. Trail. 2008. The L-Type calcium ion channel Cch1 affects ascospore discharge and mycelial growth in the filamentous fungus *Gibberella zeae* (anamorph *Fusarium graminearum*). Eukaryotic Cell. **7**:415-424.

Hartmann, N., M. Erbs, H.-R. Forrerm S. Vogelgsang, F.E. Wettstein, R.P. Scharzenbach, and T.D. Bucheli. 2008. Occurrence of Zearalenone on *Fusarium graminearum* Infected Wheat and Maize Fields in Crop Organs, Soil, and Drainage Water. Environmental Science and Technology **42**: 5455-5460.

Healy, R.A. 2003. *Mattirolomyces tiffanyae*, a new truffle from Iowa, with ultrastructural evidence for its classification in the Pezizaceae. Mycologia **95**: 765-772.

Hille, B. 1994. Modulation of ion-channel function by G-protein-coupled receptors. Trends in Neuroscience **17**: 531-536.

Hong, M.P., K. Vu, J. Bautos, and A. Gelli. 2010. Cch1 restores intracellular Ca^{2+} in fungal cells during ER stress. The Journal of Biological Chemistry **285**: 10951-10958.

Iida, H., H. Nakamura, T. Ono, M.Okumura, and Y. Anraku. 1994. MID1, a novel *Saccharomyces cerevisiae* gene encoding a plasma membrane protein, is required for Ca^{2+} influx and mating. Mollecular and Cellular Biology **14**: 8259-8271.

Inch, S., W.G.D. Fernando, and J. Gilbert. 2005. Seasonal and daily variation in the airborne concentration of *Gibberella zeae* (Schw.) Petch spores in Manitoba. Canadian Journal of Plant Pathology **27**: 357-363.

Ingold, C. T. 1939. Spore Discharge in Land Plants. Clarendon Press: Oxford.

Ingold, C.T., 1966. Aspects of spore liberation: violent discharge. In: Madelin, M.F. (Ed.), The Fungus Spore, Proceedings of the Eighteenth Symposium of the Colston Research Society, Bristol, England. Buttersworths, London, pp. 113–132.

Ingold, C.T., 1971. Fungal Spores: Their Liberation and Dispersal. Clarendon Press, Oxford.

James, T.Y., P.M. Letcher, J.E. Longcore, S.E. Mozler-Standridge, D. Porter, M.J. Powell, G.W., Griffith, and R. Vilgalys. 2006. A molecular phylogeny of the flagellated fungi (Chytridiomycota) and description of a new phylum (Blastocladiomycota). Mycologia **98**: 860-871.

Jones, S.G. 1926. The Development of the Perithecium of Ophiobolus graminis, Sacc. Annals of Botany **os-40**: 607-629.

Jung, G., and J.A. Hammer III. 1994. The actin binding site in the tail domain of *Dictyostelium* myosin 1C (myoC) resides within the glycine- and proline-rich sequence (tail homology region 2). FEBS Letters **342**: 197-202.

Karugia, G.W., H. Suga, L.R. Gale, T. Nakajima, K. Tomimura, and M. Hyakumachi. 2009. Population structure of the Fusarium graminearum species complex from a single Japanese wheat field sampled in two consecutive years. Plant Disease. **93**: 170-174.

Kanzaki, M., M. Nagasawa, I. Kojima, C. Sato, K. Naruse, M. Sokabe, and H. Iida. 1999. Molecular identification of a eukaryotic, stretch-activated nonselective cation channel. Science **285**: 882-886.

Khonga, E.B., and Sutton, J.C., 1988. Inoculum production and survival of *Gibberella zeae* in maize and wheat residues. Canadian Journal of Plant Pathology **10**: 232-240.

Krementsov, D.N., E.B. Krementsova, and K.M. Trybus. 2004. Myosin V regulation by calcium, calmodulin, and the tail domain. The Journal of Biological Chemistry **164**: 877-886.

Kretsinger, R.H., and C.E. Nockolds. 1973. Carp Muscle Calcium-binding Protein II. structure determination and general description. The Journal of Biological Chemistry **248**: 3313-3326.

Krichevsky, A., S.V. Kozlovsky, G.-W. Tian, M.-H. Chen, A. Zaltsman, and V. Citovsky. 2007. How pollen tubes grow. Developmental Biology **303**: 405-420.

Kurtz, S., A. Phillippy, A.L. Delcher, M. Smoot, M. Shumway, C. Antonescu, and S.L. Salzberg. 2004.Versatile and open software for comparing large genomes. Genome Biology **5**: R12.

Laude, A.J., and A.W.M. Simpson. Compartmentalized signalling: Ca^{2+} compartments, microdomains and the many facets of Ca^{2+} signalling. The FEBS Journal **276**: 1800-1816.

Lee, J., I.-Y. Chang, H. Kim, S.-H. Yun, J.F. Leslie, and Y.-W. Lee. 2009. Genetic Diversity and Fitness of Fusarium graminearum Populations from Rice in Korea. Appl. Environ. Microbiol. **75**: 3289-3295.

Leslie, J.F., and B.A. Summerell. 2006. The Fusarium Laboratory Manual. Blackwell Professional, Ames, Iowa.

Lew, R. R., Z. Abbas, M. Anderca, and S. Free. 2008. Phenotype of a mechanosensitive channel mutant, *mid-1*, in a filamentous fungus, *Neurospora crassa*. Eukaryotic Cell **7**: 647-655.

Lew, R.R. 2006. Use of double barrel micropipettes to voltage-clamp plant and fungal cells, p. 139-154. In A. G. Volkov (ed.), Plant electrophysiology - theory and methods. Springer, Berlin, Germany.

Lew, R.R. 2007. Ionic currents and ion fluxes in *Neurospora crassa*. J. Exp. Bot. **58**: 3475-3481. doi:10.1093/jxb/erm204.

Lew, R.R. and N.N. Levina. 2004. Oxygen flux magnitude and location along growing hyphae of *Neurospora crassa*. FEMS Microbiology Letters. **233**: 125-130.

Lew, R.R., and V. Kapishon. 2009. Ptk2 contributes to osmoadaptation in the filamentous fungus *Neurospora crassa*. Fungal Genetics and Biology. **46**: 949-955.

Link, H.F. 1809. Observationes in ordines plantarum naturales. Magazin der Gesellschaft Naturforschenden Freunde Berlin **3**: 3-42.

Liu, M., and A. Gelli. 2008. Elongation Factor 3, EF3, associates with the calcium channel Cch1 and targets Cch1 to the plasma membrane in *Cryptococcus neoformans*. Eukaryotic Cell **7**: 118-1126.

Locke, E, Bonilla, M., Liang, L., Takita, Y., Cunningham, K. 2000. A homolog of voltage-gated Ca^{2+} channels stimulated by depletion of secretory Ca^{2+} in yeast. Mol. Cell Biol. **20**: 6686-6694.

Lortie, M., and J.E. Kuntz. 1963. Ascospore discharge and conidium release by nectria galligena bres. under field and laboratory conditions. Canadian Journal of Botany **41**: 1203-1210.

Lowey, S., G.S. Waller, and K.M. Trybus. 1993. Skeletal muscle myosin light chains are essential for physiological speeds of shortening. Nature **365**: 454-456.

MacHardy, W. E. 1996. Apple Scab: Biology, Epidemiology, and Management. The American Phytopathological Society, St. Paul, MN.

Marchler-Bauer, A. et al. 2011. CDD: a Conserved Domain Database for the functional annotation of proteins. Nucleic Acids Research **39**: D225-D229.

Markell, S.G., and L.J. Francl. Fusarium Head Blight Inoculum: Species Prevalence and *Gibberella zeae* Spore Type. **7**: 814-820.

Marin, D.E., I. Taranu, R. Burlacu, and D.S. Tudor. Effects of zearalenone and its derivatives on the innate immune response of swine.Toxicon **56**: 956-963.

Maruoka, T., Y. Nagasoe, S. Inoue, Y. Mori, J. Goto, M. Ikeda, and H. Iida. 2002. Essential hydrophilic carboxyl-terminal regions including cysteine residues of the yeast stretch-activated calcium-permeable channel Mid1. The Journal of Biological Chemistry **277**: 11645-11652.

Matter, K., and M.S. Balda. 2003. Signalling to and from tight juctions. Nature Reviews Molecular Cell Biology **4**: 225-237.

Mattson, M.P., and S.L. Chan. 2003. Calcium orchestrates apoptosis. Nature Cell Biology **5**: 1041-1043.

McConnell, R., and M. Tyska. 2007. Myosin-1a powers the sliding of apical membrane along microvillar actin bundles. The Journal of Cell Biology **177**: 671-681.

McGoldrick, C., C. Gruver, and G. May. 1995. *myoA* of *Aspergillus nidulans* encodes an essential Myosin I required for secretion and polarized growth. The Journal of Cell Biology **128**: 577-587.

Metzenberg, R.L. and N.L. Glass. 1990. Mating type and mating strategies in Neurospora. BioEssays **12**:53-59.

Michalak, M., J.M.R Parker, and M. Opas. 2002. Ca2+ signaling and calcium binding chaperones of the endoplasmic reticulum. Cell Calcium **32**: 269-78.

Miller, J.D., J. Culley, K. Fraser, S. Hubbard, F. Meloche, T. Ouellet, W.L. Seaman, K.A. Seifert, K. Turkington, and H. Voldeng. 1998. Effect of tillage practice on Fusarium head blight of wheat. Revue Canadienne de Phytopathologie **20**: 95-103.

Minervini, F., and M.E. Dell'Aquila. 2008. Zearalenone and Reproductive Function in Farm Animals. International Journal of Molecular Sciences **9**: 2570-2584.

Mitter, V., L.J. Francl, S. Ali, S. Simpfendorfer, and S. Chakraborty. 2006. Ascosporic and conidial inoculum of *Gibberella zeae* play different roles in Fusarium head blight and crown rot of wheat in Australia and the USA. Australasian Plant Pathology **35**: 441-452.

Montagne, J.F.C. 1856. Sylloge generum specierumque plantarum cryptogamarum. Parisiis, sumptibus J.-B. Baillière.

Muller, E.M., E.G. Locke, and K.W. Cunnungham. 2001. Differential regulation of two Ca^{2+} influx systems by pheromone signaling in *Saccharomyces cerevisiae*. Genetics **159**: 1527-1538.

Muller, E., N. Mackin, S. Erdman, and K. Cunningham. 2003. Fig1p facilitates Ca^{2+} influx and cell fusion during mating of *Saccharomyces cerevisiae*. The Journal of Biological Chemistry **278**: 38461-38469.

Petch, T. 1936. *Gibberella Saubinetii* (Mont.) Sacc. Annals of Mycology **34**: 257-260.

Nganje, W., D. Johnson, W. Wilson, F. Leistritz, D. Bangsund, and N. Tiapo. 2001. Economic impacts of Fusarium Head Blight in wheat and barley: 1998-2000. Agribusiness and Applied Economics Report No. 464.

Nguyen, Q.B., N. Kadotani, s. Kasahara, Y. Tosa, S. Mayama, and H. Nakayahiki. 2008. Systematic functional analysis of calcium-signalling proteins in the genome of the rice-blast fungus, Magnaporthe oryzae, using a high-throughput RNA-silencing system. Molecular Microbiology **68**: 1348-1365.

Nyvall, R.F., and J.A. Percich. 1999. Fusarium Head Blight of Cultivated and Natural Wild Rice (Zizania palustris) in Minnesota Caused by Fusarium graminearum and Associated Fusarium spp. Plant Disease **83**: 159-164.

O'Donnell, K., Kistler, H.C., Tacke, B.K., Casper, H.H., 2000. Gene genealogies reveal global phylogeographic structure and reproductive isolation among lineages of Fusarium graminearum, the fungus causing wheat scab. Proc. Natl. Acad. Sci. USA **97**: 7905-7910.

O'Donnell, K., Ward, T.J., Geiser, D.M., Kistler, H.C., Aoki, T., 2004. Genealogical concordance between the mating type locus and seven other nuclear genes supports formal recognition of nine phylogenetically distinct species within the Fusarium graminearum clade. Fungal Genet. Biol. **41**: 600-623.

Odrinitz, F., and M. Kollmar. 2007. Drawing the tree of eukaryotic life based on the analysis of 2,269 manually annotated myosins from 328 species. Genome Biology **8**: R196.

Ozeki-Miyawaki, C., Y. Moriya, H. Tatsumi, H. Iida, and M. Sokabe. 2005. Identification of functional domains of Mid1, a stretch-activated channel component, necessary for localization to the plasma membrane and Ca^{2+} permeation. Experimental Cell Research **311**: 84-95.

Paidhungat, M., and S. Garrett. A homolog of mammalian, voltage-gated calcium channels mediates yeast pheromone-stimulated Ca2+ uptake and exacerbates the cdc1(Ts) growth defect. Molecular and Cell Biology **17**: 6339-6347.

Peiter, E., M. Fischer, K. Sidaway, S. Roberts, and D. Sanders. 2005. The *Saccharomyces cerevisiae* Ca^{2+} channel Cch1pMid1p is essential for tolerance to cold stress and iron toxicity. FEBS Letters **579**: 5697-5703.

Perraud, A., C. Schmiz, and A. Scharenberg. 2003. TRPM2 Ca^{2+} permeable cation channels: from gene to biological function. Cell Calcium **33**: 519-531.

Plowright, C.B. 1880. On spore diffusion in the larger Elvellacei. In Grevillea vol. ix, pp 47-51.

Pugh, W.G., and H. Johann. 1933. Factors affecting infection of wheat heads by *Gibberella saubinetti*. Journal of Agricultural Research **46**: 771-797.

R Development Core Team. 2010. R: A language and environment for statistical computing. R Foundation for Statistical Computing, Vienna, Austria. ISBN 3-900051-07-0, URL http://www.R-project.org.

Raghavender, C.R., and B.N. Reddy. 2008. Human and animal disease outbreaks in India due to mycotoxins other than aflatoxins. World Mycotoxin Journal **2**: 23-30.

Raju, N.B., 2008. Meiosis and ascospore development in *Cochliobolus heterostrophus*. Fungal Genetics and Biology **45**: 554-564.

Ramakrishna, Y., R.V. Bhat, and V. Ravindranath. 1989. Production of deoxynivalenol by Fusarium isolates from samples of wheat associated with a human mycotoxicosis outbreak and from sorghum cultivars. Applied and Environmental Microbiology **55**: 2619-2620.

Read, N.D., and A. Beckett. 1996. Ascus and ascospore morphogenesis. Mycological Research **100**: 1281-1314.

Richards, T.A., and T. Cavalier-Smith. 2005. Myosin domain evolution and the primary divergence of eukaryotes. Nature **436**: 1113-1118.

Ringer, S. 1883a. A further contribution regarding the influence of the different constituents of the blood on the contraction of the heart. The Journal of Physiology **4**: 29-42.

Ringer, S. 1883b. A third contribution regarding the influence of the inorganic constituents of the blood on the ventricular contraction. The Journal of Physiology **4**: 222-225.

Ringer, S. 1886. Further experiments regarding the influence of small quantities of lime potassium and other salts on muscular tissue. The Journal of Physiology **7**: 291-308.

Ringer, S. 1890. Concerning experiments to test the influence of lime, sodium and potassium salts on the development of ova and growth of tadpoles. The Journal of Physiology **11**: 79-84.

Ringer, S., and H. Sainsbury. 1894. The action of potassium, sodium and calcium salts on Tubifex rivulorum. The Journal of Physiology **16**: 1-9.

Robbana-Barnat, S., B. Loridon-Rosa, H. Cohen, C. Lafarge-Frayssinet, G.A. Neish, and C. Frayssinet. 1987. Protein synthesis inhibition and cardiac lesions associated with deoxynivalenol ingestion in mice. Food Addit Contam. **4**: 49-56.

Rosenfeld, S.S., and B. Rener. 1994. The GPQ-Rich segment of *Dictyostelium* myosin IB contains an actin binding site. Biochemistry **33**: 2322-2328.

Saccardo, P.A. 1879. Fungi Gallici lecti a cl. viris P. Brunaud, C.C. Gillet et Abb. Letendre. Michelia **1 5**: 500-538.

Sambrook, J., and D.W. Russell. 2001. Molecular cloning: a laboratory manual, 3rd ed. Cold Spring Harbor Laboratory Press, Cold Spring Harbor, NY.

Satoh, A.K., B.X. Li, H. Xia, and D.F. Ready. 2008. Calcium-Activated Myosin V Closes the *Drosophila* Pupil. Current Biology **18**: 951-955.

Schuchardt, I., D. Aßmann, E. Thines, C. Schuberth, and G. Steinberg. Myosin-V, Kinesin-1, and Kinesin-3 cooperate in hyphal growth of the fungus *Ustilago maydis*. Molecular Biology of the Cell **16**: 5191-5201.

Schwabe, S.H. 1839. Flora Anhaltina. Tomus 2. Berlin.

Schwartz, P., T.D. Bucheli, F.E. Wettstein, and P. Burkhardt-Holm. Short-term exposure to the environmentally relevant estrogenic mycotoxin zearalenone impairs reproduction in fish. Science of the Total Environment **409**: 326-333.

Schweinitz, L. D. de. 1822. Synopsis fungorum Carolinae superioris, secundum observationes. Johann Ambrosium Barth, Leipzig.

Schweinitz, L.D. de. 1832. Transactions of the American Philosophical Society **4**: 230.

Sellers, J.R. 2000. Myosins: a diverse superfamily. Biochimica et Biophysica Acta **1496**: 3-22.

Shear, C.L., and B.O. Dodge. 1927. Life histories and heterothallism of the red bread-mold fungi of the *Monilia sitophila* group. J. Agr. Res. **34**: 1019-1042.

Slayman, C.L., W.S. Long, and C.Y. Lu. 1973. The relationship between ATP and electrogenic pump in the plasma membrane of *Neurospora crassa*. J. Membr. Biol. **14**: 305-338.

Spanswick, R.M. 2006. Electrogenic pumps. p. 221-246. In A. G. Volkov (ed.), Plant electrophysiology—theory and methods. Springer, Berlin, Germany.

Starkey, D.E., Ward, T.J., Aoki, T., Gale, L.R., Kistler, H.C., Geiser, D.M., Suga, H., Toth, B., Varga, J., O'Donnell, K., 2007. Global molecular surveillance reveals novel Fusarium head blight species and trichothecene toxin diversity. Fungal Genet. Biol. **44**: 1191-1204.

Steinkellner, S., and I. Langer. 2004. Impact of tillage on the incidence of Fusarium spp. in soil. Plant and Soil **267**: 13-22.

Stępień, Ł, and J. Chełkowski. 2010. *Fusarium* head blight of wheat: pathogenic species and their mycotoxins. World Mycotoxin Journal **3**: 107-119.

Strickland, W.N., and D.D. Perkins. 1973. Rehydrating ascospores to improve germination. Neurospora Newsletter **20**: 34-35.

Stack, R.W. 2003. History of fusarium head blight with emphasis on North America. *In* Fusarium head blight of wheat and barley. Eds., K.J. Leonard and W.R. Bushnell. APS Press, St.Paul, MN.

Summerell, B.A., and J.F. Leslie. 2011. Fifty years of Fusarium: how could nine species have ever been enough?. Fungal Diversity **50**: 135-144.

Sutton, J.C. 1982. Epidemiology of wheat head blight and maize ear rot caused by *Fusarium graminearum*. Canadian Journal of Plant Pathology **4**: 195-209.

Tada, T., M. Ohmori, and H. Iida. 2003. Molecular Dissection of the Hydrophobic Segments H3 and H4 of the Yeast Ca^{2+} Channel Component Mid1. The Journal of Biological Chemistry **278**: 9647-9654.

Teich, A.M., and K. Nelson. 1984. Survey of Fusarium head blight and possible effects of cultural practices in wheat fields in Lambton County in 1983. Canadian Plant Disease Survey **64**: 11-13.

Thom, C., and M.B. Church. 1926. The Aspergilli. Williams and Wilkins Co., Baltimore, MD.

Thompson-Coffe, C., and D. Zickler. 1993. Cytoskeleton interactions in the ascus development and sporulation of *Sordaria macrospora*. Journal of Cell Science **104**: 883-898.

Tokes-Fuzesi, M., D. Bedwell, I. Repa, K. Sipos, B. Sumegi, A. Rab, and A. Miseta. 2002. Hexose phosphorylation and the putative calcium channel component Mid1p are required for the hexose-induced transient elevation of cytosolic calcium response in *Saccharomyces cerevisiae*. Molecular Microbiology **44**: 1299-1308.

Tóth, B., Mesterházy, Á., Horváth, Z., Bartók, T., Varga, M., Varga, J., 2005. Genetic variability of central European isolates of the Fusarium graminearum species complex. European Journal of Plant Pathology **113**: 35-45.

Trail, F. and R. Common. 2000. Perithecial development by *Gibberella zeae*: a light microscopy study. Mycologia **92**: 130-138.

Trail, F., H. Xu, R. Loranger, and D. Gadoury. 2002. Physiological and environmental aspects of ascospore discharge in *Gibberella zeae* (anamorph *Fusarium graminearum*). Mycologia **94**: 181-189.

Trail, F., I. Gaffoor, and S. Vogel, 2005. Ejection mechanics and trajectory of the ascospores of *Gibberella zeae* (anamorph *Fusarium graminearum*). Fungal Genetics and Biology **42**: 528-533.

Tschanz, A.T., and R.K. Horst. 1976. The effect of environment on sexual reproduction of *Gibberella zeae*. Mycologia **68**: 327-340.

Tsukita, S., M. Furuse, and M. Itoh. 1999. Structural and signalling molecules come together at tight junctions. Current Opinion in Cell Biology **11**: 628-633.

Ueno, Y., M. Hosoya, Y. Morita, I. Ueno, and T. Tatsuno. Inhibition of the Protein Synthesis in Rabbit Reticulocyte by Nivalenol, a Toxic Principle Isolated from *Fusarium nivale*-Growing Rice. The Journal of Biochemistry **64**: 479-485.

Uhlén, P., and N. Fritz. 2010. Biochemistry of calcium oscillations. Biochemical and Biophysical Research Communications **396**: 28-32.

Upadhyay, S. and B. Shaw. 2008. The role of actin, fimbrin and endocytosis in growth of hyphae in *Aspergillus nidulans*. Molecular Microbiology **68**: 690-705.

Walker, S. L., S. Leath, W.M. Hagler, Jr., and J.P. Murphy. 2001. Variation Among Isolates of *Fusarium graminearum* Associated with Fusarium Head Blight in North Carolina. Plant Disease **85**: 404-410.

Ward, T.J., R.M. Clear, A.P. Rooney, K. O'Donnell, D. Gaba, S. Patrick, D.E. Starkey, J. Gilbert, D.M. Geiser, and T.W. Nowicki. 2007. An adaptive evolutionary shift in Fusarium head blight pathogen populations is driving the rapid spread of more toxigenic *Fusarium graminearum* in North America. Fungal Genetics and Biology **45**: 473-484.

Watanabe, T., H. Hosoya, and S. Yonemura. 2007. Regulation of myosin II dynamics by phosphorylation and dephosphorylation of its light chain in epithelial cells. Molecular Biology of the Cell **18**: 605-616.

Waterhouse, A.M., J.B. Procter, D.M.A Martin, M. Clamp, and G.J. Barton. 2009. Jalview Version 2 - a multiple sequence alignment editor and analysis workbench. Bioinformatics **25**: 1189-1191.

Watts, H.J., A.-A. Very, T.H.S. Perera, J.M. Davies, and N.A.R. Gow. 1998. Thigmotropism and stretch-activated channels in the pathogenic fungus *Candida albicans*. Microbiology **144**: 689-695.

Wettstein, F.E., and T.D. Bucheli. 2010. Poor elimination rates in waste water treatment plants lead to continuous emission of deoxynivalenol into the aquatic environment. Water Research **44**: 4137-4142.

Williams, R.J.P. 2006. The evolution of calcium biochemistry. Biochimica et Biophysica Acta (BBA) - Molecular Cell Research **1763**: 1139-1146.

Williams, R.J.P. 2007. The evolution of the biochemistry of calcium. In Calcium: a Matter of Life or Death, Eds. J. Krebs and M. Michalak.Elsevier Science.

Windels C.E., and T. Kommedahl. 1984. Late-season colonization and survival of *Fusarium graminearum* group II in cornstalks in Minnesota. Plant Disease **68:** 791-793.

Wollenweber, H.W. 1914. Identification of species of Fusarium occurring on the sweet potato, *Ipomoea batatas*. Journal of Agricultural Research **2**: 251-286.

Woo, M., K. Lee, and K. Song. 2003. MYO2 is not essential for viability, but is required for polarized growth and dimorphic switches in *Candida albicans*. FEMS Microbiology Letters **218**: 195-202.

Wu, C.-G., and J.W. Kimbrough. 2001. Ascosporogenesis in *Tarzetta* (Otideaceae, Pezizales). International Journal of Plant Sciences **162**: 1075-1080.

Yafetto, L., L. Carroll, Y. Cui, D.J. Davis, M.W.F. Fischer, A.C. Henterly, J.D. Kessler, H.A. Kilroy, J.B. Shidler, J.L. Stolze-Rybczynski, Z. Sugawara, and N.P. Money. 2008. The Fastest Flights in Nature: High-Speed Spore Discharge Mechanisms among Fungi. PLoS ONE **3**: e3237. doi:10.1371/journal.pone.0003237.

Yang, M., A. Brand, T. Srikantha, K.J. Daniels, D.R. Soll, and N.A.R. Gow. 2011. Fig1 Facilitates Calcium Influx and Localizes to Membranes Destined To Undergo Fusion during Mating in *Candida albicans*. Eukaryotic Cell **10**: 435-444.

Yi, C., H.P. Kaul, E.Kubler, K. Schwadorf, and W. Aufhammer. 2001. Head blight (*Fusarium graminearum)* and deoxynivalenol concentration in winter wheat as affected by pre-crop, soil tillage and nitrogen fertilization. Zeitschrift für Pflanzenkrankheiten und Pflanzenschutz **108**: 217-230.

Yoshimura, H., T. Tada, and H. Iida. 2004. Subcellular localization and oligomeric structure of the yeast putative stretch-activated Ca^{2+} channel component Mid1. Experimental Cell Research **293**: 185-195.

Zeller, K.A., R.L. Bowden, and J.F. Leslie. 2003. Diversity of Epidemic Populations of *Gibberella zeae* from Small Quadrats in Kansas and North Dakota. Ecology and Population Biology **93**: 874-880.

Zerbino, D.R., and E. Birney. 2008. Velvet: Algorithms for de novo short read assembly using de Bruijn graphs. Genome Research **18**: 821-829.

Zerbino, D.R., G.K. McEwen, E.H. Margulies, and E. Birney. 2009. Pebble and Rock Band: Heuristic Resolution of Repeats and Scaffolding in the Velvet Short-Read *de Novo* Assembler. PLos ONE **4**: e8407. doi:10.1371/journal.pone.0008407.

Zhang, N.-N., D.D. Dudgeon, S. Paliwal, A. Levchenko, E. Grote, and K.W. Cunningham. 2006. Multiple Signaling Pathways Regulate Yeast Cell Death during the Response to Mating Pheromones. Molecular Biology of the Cell **17**: 3409-3422.

Zhou, X.L., M.A. Stumpf, C. Kung, and H.C. Hoch. 1991. A mechanosensitive channel in whole cells and in membrane patches of the fungus *Uromyces.* Science **253**: 1415-1417.